Comparative Study of Heel Movement and Foot Biomechanics in Aluminum Nail-On and Indirect Glue-On Fabric Cuff Shoes in Horses

Fabian Jimenez Roa

Thesis submitted to the faculty of the Virginia Polytechnic Institute and State University in partial fulfillment of the requirements for the degree of

Master of Science in Biomedical and Veterinary Sciences

Christopher R. Byron, Chair

Amy M. Santonastaso

Travis D. Burns

Rebecca A. Funk

Lauren Trager-Burns

Rafaella De Vita

July 30th 2025

Blacksburg VA

Keywords: equine biomechanics, hoof mechanism, heel expansion, shoeing techniques, glue-on shoes, nail-on shoes, barefoot horses, equine podiatry.

Comparative Study of Heel Movement and Foot Biomechanics in Aluminum Nail-On and Indirect Glue-On Fabric Cuff Shoes in Horses

Academic Abstract

Fabian J Roa

The equine hoof is a dynamic structure that undergoes deformation during locomotion, contributing to shock absorption and vascular perfusion. Traditional shoeing methods have been implicated in restricting natural hoof movement, potentially altering biomechanics and increasing the risk of hoof pathologies. This study aimed to compare the effects of two aluminum shoeing techniques—nail-on shoes and indirect glue-on fabric cuff shoes on heel movement in horses of various breeds and disciplines.

Fifteen healthy horses were evaluated under three conditions: barefoot, aluminum nail-on shoes, and indirect glue-on fabric cuff shoes. A displacement sensor was affixed to the heels of one forelimb to measure total heel displacement over 20 strides at both the walk and trot. Testing was conducted on both hard (asphalt) and soft (arena footing) surfaces. Mixed-model ANOVA was used to assess differences between shoeing conditions.

Results demonstrated significantly greater heel expansion in barefoot horses compared to both shoeing conditions ($P < 0.0001$). While indirect glue-on shoes allowed for more heel movement than nail-on shoes at the trot ($P = 0.0005$), no significant difference was observed between the two at the walk ($P = 0.1742$). These findings confirm that both shoe types restrict heel expansion, though to differing degrees.

Limitations of this study include the absence of an absolute zero baseline measurement, preventing differentiation between heel expansion and contraction, as well as data loss for some horses on soft footing due to low heel conformation.

This study contributes to the understanding of equine hoof biomechanics and the impact of shoeing techniques on heel movement. The findings support the need for further investigation into alternative materials and methods that optimize hoof function. Additionally, they have implications for therapeutic farriery, particularly in cases requiring hoof stabilization, such as coffin bone fractures.

Comparative Study of Heel Movement and Foot Biomechanics in Aluminum Nail-On and Indirect Glue-On Fabric Cuff Shoes in Horses

General Audience Abstract (Lay Summary)

Fabian J Roa

The equine hoof plays a crucial role in absorbing impact and maintaining blood flow as a horse moves. However, different types of horseshoes may influence this natural hoof movement. This study examined how two common types of aluminum horseshoes (traditional nail-on shoes and glue-on fabric cuff shoes) affect heel movement in horses of various breeds and disciplines.

Fifteen healthy horses were tested under three conditions: barefoot, wearing aluminum nail-on shoes, and wearing glue-on fabric cuff shoes. A specialized sensor measured heel expansion while the horses walked and trotted on both hard (asphalt) and soft (arena footing) surfaces.

The results showed that barefoot horses had the most heel movement, while both types of shoes restricted displacement. The glue-on shoes allowed for slightly more movement than nail-on shoes at the trot, but no significant difference was observed at the walk.

This study highlights the importance of understanding how different shoeing methods affect hoof function. While shoes are necessary for protection and performance, they can also impact natural hoof movement. The findings may help veterinarians and farriers make informed decisions when selecting shoes for different horses. Future research should explore additional shoe materials and designs that better preserve natural hoof function while meeting the demands of performance and therapeutic needs.

Acknowledgements

First and foremost, I would like to express my deepest gratitude to my family, especially my wife Gianina, whose unwavering support and love carried me through the most demanding stages of internship and residency. This journey has not been easy, but your belief in me has meant more than words can express. To my parents and sister, thank you for always standing by my side; to my mom in particular, thank you for putting me through veterinary school and constantly encouraging me to grow into the best version of myself.

To my friends from back home, thank you for your continued encouragement across the miles. I would also like to give special thanks to my brother, Dr. Umaña. Professionally, your guidance in navigating the statistics for this project (especially helping me make sense of the ANOVAs) was invaluable. But personally, your friendship has been a lifeline, especially during the toughest moments of my residency. Thank you for being both friend and unwavering support.

To my EFS family, thank you for shaping me into the clinician I am today. I am especially grateful to my supervisor, Dr. Amy Santonastaso, for her steady mentorship, calm leadership, and instrumental role in organizing and developing this project. Your optimism and encouraging words helped me stay grounded throughout the process. To Dr. Funk and Dr. Trager, your openness, availability, and willingness to teach were pivotal in advancing my clinical growth. Dr. De Vita and the Biomedical engineering and mechanics department for your support for the project. Will, Dr. De Vita's PhD student, who built the code to process the data was invaluable for the completion of this research project.

Travis, thank you for your dedication, mentorship, and essential contribution to this project. Your help during every data recording day made this work possible. To my fellow residents and my phenomenal technicians and friends, Morgan and Laney. Thank you for making every day smoother with your organization, support, and contagious sense of humor. You kept me on track and made the long days feel lighter.

This thesis stands on the shoulders of all of you. Thank you.

Attributions

Amy Santonastaso DVM MSc DABVP (Equine) Large Animal Clinical Sciences Equine Field Service Dept. Service Chief	Chair - Grant proposal writing - Subject lameness evaluations prior to inclusion in the study. - Data collection; sensor placement and recordings for all subjects in the study. - Manuscript and thesis writing and revision.
Christopher Byron, DVM, MSc, DACVS Large Animal Clinical Sciences Large Animal Surgery Dept. Department Head	Co-Chair - Grant proposal writing - Manuscript and thesis writing and revision.
Travis Burns, MSc, CJF, TE, EE, FWCF Large Animal Clinical Sciences Chief of farrier Services Hospital Administrator, VTH	- Responsible for shoeing and trimming for all 3 conditions for all the horses included in the study. - Data collection; sensor placement and recordings for all subjects in the study. - Manuscript and thesis writing and revision.
Raffaella De Vita, PhD Biomedical Engineering and Mechanics Associate Department Head	- Grant proposal writing. - Significant contribution to materials and methods; Displacement sensor calibration and recording software. - Assistance in creating Python/Jupyter code to process raw data (objective extraction of maximum and minimum displacements in recording over 20 strides). - Manuscript and thesis writing and revision.
Lauren Trager-Burns, DVM, MS, DACVSMR-Equine Large Animal Clinical Sciences Equine Field Service Dept. Assistant Clinical Professor	- Grant proposal writing - Subject lameness evaluations prior to inclusion in the study. - Manuscript and thesis writing and revision.
Rebecca Funk, DVM, MS, DACVIM Large Animal Clinical Sciences Equine Field Service Dept. Clinical Associate Professor.	- Grant proposal writing - Subject lameness evaluations prior to inclusion in the study. - Manuscript and thesis writing and revision.
Stephen R. Werre, PhD Department of Population Health Sciences Assistant Professor of Research	- All statistical analysis (3 Mixed model Anova's) - Manuscript and thesis writing and revision.

Contents

Table of Figures

1. Introduction

1.1 Background and significance

The equine hoof is a dynamic and complex structure that plays a fundamental role in locomotion, energy dissipation, and vascular perfusion (Dyhre-Poulsen et al., 1994; Floyd & Mansmann, 2007). During weight-bearing, the hoof undergoes expansion and contraction, a process commonly referred to as the hoof mechanism. This mechanism facilitates shock absorption and promotes circulation within the digital cushion, ensuring adequate perfusion to the distal limb (Shahkhosravi et al., 2023). Restriction of this natural movement has been implicated in various hoof pathologies, including heel contraction, decreased shock absorption, and reduced perfusion, potentially predisposing horses to lameness and degenerative joint conditions (Eliashar et al., 2004; Alves et al., 2023).

Shoeing is widely utilized in both performance and therapeutic farriery to enhance hoof protection, improve traction, and modify biomechanics (Aoun & Takawira, 2024; Parks, 2012). However, various studies have suggested that conventional shoeing techniques, particularly those utilizing metal shoes, may alter natural hoof function by restricting heel expansion and contraction. For instance, Roepstorff et al. (2001) used pressure mats and kinematic analysis on Standardbred trotters to demonstrate that metal shoes, particularly in shod vs. unshod comparisons, reduced medial-lateral heel expansion during stance phase. Similarly, Senderska-Płonowska et al. (2020) assessed hoof deformation using thermography and digital image analysis in Warmbloods fitted with steel shoes, reporting significantly reduced heel movement and increased asymmetry in the hoof capsule compared to barefoot conditions.

Research conducted by Reilly et al. (2024) employed force plate analysis and motion capture to evaluate the biomechanical effects of three different shoe types in jumping horses, concluding that shoe design significantly affected hoof orientation angles at mid-stance and altered vertical ground reaction forces, with glue-on composites producing the most uniform load distribution. Furthermore, comparative studies have indicated that certain glue-on applications may limit hoof deformation differently than traditional nail-on shoes. For example, Takahashi et al. (2022) analyzed the deformation patterns of the hoof capsule using 3D surface scanning in Japanese racehorses and found that indirect glue-on shoes maintained a more symmetrical hoof expansion compared to aluminum nail-on shoes. Similarly, Yoshihara et al. (2010) evaluated hoof wall mechanics under dynamic loading using finite element modeling, showing that nail placement in traditional shoeing created localized areas of high strain, which were absent in glue-on configurations.

While previous studies have primarily focused on the effects of shoeing in Thoroughbred racehorses, often tested in controlled environments such as high-speed treadmills with force plate integration (Horan et al., 2022; Bardin et al., 2022), there is a need to expand research to include diverse horse breeds, disciplines, and real-world surfaces. For example, Horan et al. (2022) investigated vertical force and breakover timing across four shoe types during gallop in treadmill trials, while Bardin et al. (2022) evaluated kinematic variability under synthetic and dirt surfaces. This study seeks to fill part of that gap by assessing hoof biomechanics in horses with varying conformations, using aluminum nail-on and indirect glue-on fabric cuff shoes in natural footing conditions.

1.2 Research objectives and hypothesis

The primary objective of this study is to quantify the effects of aluminum nail-on shoes and indirect glue-on fabric cuff shoes on heel movement across different breeds, disciplines, and ground surfaces. By using displacement sensors to objectively measure heel displacement, this research aims to enhance the understanding of how different shoeing methods impact equine biomechanics in vivo.

The study is based on the following hypotheses:

1. **Barefoot horses will exhibit greater heel movement** compared to those with shoes, supporting previous research that indicates unrestricted hoof expansion in unshod hooves (Aoun et al., 2023; Hampson & Pollitt, 2011).
2. **Indirect fabric cuff glue-on shoes will restrict heel movement to a greater degree than nail-on shoes**, due to the almost complete coverage of the entire hoof wall with the fabric cuff. Previous studies using conventional direct glue on shoes suggested that adhesive-based applications may allow more flexibility than metal nail-on shoes (Brunsting et al., 2019; Nicolai et al., 2017). Nevertheless, studies on fabric cuff indirect glue on shoes lack data to confirm similarities with other glue on shoes. It was our thought that the coverage of the entire hoof wall with hard materials would be more restrictive than a nail on shoe of the same material (aluminum). Burns et al. unpublished data suggested that the combination of the fabric cuff with the glue provides a very strong tension which may cause the heel contraction after the glue dries and prevent expansion to some degree. Additionally, shoes with nails are typically nailed from the widest part of the foot forward, which could potentially allow the heel to move more freely. In contrast, the fabric cuff from the indirect glue on shoes does cover the hoof wall entirely, including the lateral and medial aspect of the heels which leads us to hypothesize that this complete area coverage could potentially restrict heel movement to a greater degree than the nail on shoes.
3. **Both shoe types will significantly (statistically) restrict heel expansion compared to barefoot conditions**, consistent with research demonstrating that traditional and modern shoeing techniques alter the hoof's natural deformation (Moeller et al., 2019; Hagen et al., 2017).

1.3 Study Scope

Unlike previous investigations that predominantly focused on a single breed (Thoroughbreds) or controlled environments (treadmills and lab settings) (Horan et al., 2022; Yoshihara et al., 2010 Hampson & Pollitt, 2011; Reilly et al., 2024), this study evaluates a more diverse population of 15 horses across various breeds, sizes, and athletic disciplines. This broad selection provides a more representative sample of equine biomechanics across different conformations. Furthermore, testing was conducted in real-world conditions (including both hard ground/asphalt and soft footing/ arena surface) allowing for more applicable insights for veterinarians and farriers working in practical settings.

To quantify heel movement, displacement sensors were affixed to the heels of one forelimb (left), measuring total displacement over 20 strides on average at both the walk and trot. By employing a mixed-model ANOVA for statistical analysis, this study provides robust comparisons between shoeing conditions.

A key aspect of this study is its clinical relevance. The findings may inform farriers, veterinarians, and researchers about how different shoeing techniques impact hoof flexibility, shock absorption, and load distribution, contributing to the ongoing discussion of best practices for both performance and therapeutic shoeing.

However, certain limitations exist:

1. Lack of an absolute zero baseline. This study measured total displacement of the heels rather than distinguishing between heel expansion vs. contraction, making it difficult to determine how much of the total movement is due to each phase.
2. Data loss in horses with low heel conformation. Some recordings on soft ground were not obtained due to sensor placement limitations, particularly in horses with lower heels, which reduced statistical power for soft ground conditions.

Despite these limitations, this study provides clinically relevant data that extends beyond previous research, reinforcing the need for further investigation into alternative shoe materials and application techniques.

2. Literature Review

2.1Functional Anatomy of the equine digit

The equine digit is a highly specialized and biomechanically complex structure that serves as the primary weight-bearing component of the distal limb. It plays a critical role in shock absorption, locomotion, and proprioception, ensuring efficient and coordinated movement in both athletic and non-athletic horses. The digit comprises an intricate assembly of osseous, tendinous, ligamentous, vascular, and synovial components, which together form a dynamic system capable of withstanding substantial mechanical loads during the stance and propulsion phases of the stride (Floyd & Mansmann, 2007; Back & Clayton, 2013).

Central to the digit is the hoof capsule, a keratinized structure that encapsulates and protects the distal phalanx, or coffin bone, as well as associated soft tissue structures including the digital cushion, navicular apparatus, and laminar interface. The hoof acts as the primary interface between the limb and the ground and must accommodate variations in terrain and surface compliance while preserving internal structures from concussive forces (Parks, 2012; Hampson & Pollitt, 2011). The digital cushion, a fibro-fatty structure situated between the frog and the deep digital flexor tendon (DDFT), plays an essential role in dissipating energy and aiding in venous return from the distal limb, particularly under the compressive forces generated during impact (Aoun et al., 2023; Dyhre-Poulsen et al., 1994).

The synovial elements of the digit include the distal interphalangeal (coffin) joint, navicular bursa, and digital flexor tendon sheath, which collectively facilitate smooth articulation and reduce friction between moving structures. The navicular bursa, in particular, provides a protective buffer between the DDFT and the navicular bone, minimizing wear during locomotion (Shahkhosravi et al., 2023). Meanwhile, the vasculature of the digit, including the lateral and medial palmar digital arteries, ensures tissue perfusion and plays a significant role in thermoregulation and metabolic waste removal (Pietra et al., 2004).

The structural integrity and mechanical behavior of the digit are further influenced by the shape and conformation of the hoof. Variations in dorsal hoof wall angle, heel height, and mediolateral balance have been shown to affect the distribution of strain within the hoof capsule, loading of the distal phalanx, and the kinematics of the entire limb (Thomason et al., 2010; Alves et al., 2023). In their landmark study, Thomason et al. (2010) used strain gauges embedded within the hoof wall and sole of cadaver limbs subjected to controlled axial loading to simulate vertical forces during stance. They demonstrated that steeper dorsal hoof wall angles correlated with more uniform load transfer across the hoof capsule, whereas lower angles led to strain concentration in the toe region. Their finite element models also indicated that mediolateral imbalance (e.g., lateral wall longer than medial) produced asymmetric pressure distribution across the distal phalanx and navicular bone, with peak stress increases of up to 42% in the overloaded quarter.

More recently, Alves et al. (2023) conducted a dynamic kinematic and kinetic analysis of 24 live Warmbloods with varying hoof conformations using motion capture and force plate data. In this context, kinematic analysis refers to the measurement of motion parameters such as joint angles, stride length, and limb flight arc without regard to the forces causing the motion, while kinetic analysis involves quantifying the forces and moments that act on the limbs during locomotion, such as ground reaction forces and loading rates (Back & Clayton, 2013; Thomason et al., 2010). The study revealed that long toe–

low heel configurations resulted in delayed breakover timing ($p < 0.01$) and increased peak vertical force at the toe during stance phase. Additionally, horses with medial-lateral imbalance showed significant asymmetry in limb flight arc and fetlock hyperextension on the overloaded side ($p < 0.05$), supporting the idea that subtle hoof asymmetries can affect limb loading patterns and joint kinematics (Alves et al., 2023; Shahkhosravi et al., 2023).

Improper conformation, such as underrun heels or long toe–low heel alignment, has also been associated with increased risk of musculoskeletal disorders, including navicular syndrome and laminitis. Eliashar et al. (2004) performed radiographic and biomechanical assessments on horses with chronic navicular syndrome and compared them to control horses with ideal conformation. Their findings showed that affected horses had significantly lower heel angles (mean 23.4° vs. 29.7°, $p < 0.01$) and longer toe lengths, which altered the orientation of the distal phalanx and increased compressive forces on the navicular bone. The authors concluded that conformation-related biomechanical alterations likely play a critical role in the development and progression of the syndrome.

Similarly, Shahkhosravi et al. (2023) investigated the relationship between hoof morphology and the occurrence of laminitis in a cohort of 60 horses with varying degrees of hoof pathology. Using standardized lateral and dorsal radiographs along with 3D digital mapping of the hoof capsule, they found that horses with long toe–low heel configurations had a higher incidence of chronic laminitic changes, including dorsal capsular rotation and sole depth thinning ($p < 0.001$). Their regression analysis indicated that for every 5° decrease in heel angle, the risk of laminitis increased by a factor of 1.6, suggesting a strong predictive association between hoof geometry and laminar stress thresholds.

Furthermore, the mechanical properties of the digit are closely modulated by farriery practices. Different shoeing methods, such as the use of wedge shoes, glue-on cuffs, or heart-bar designs, can significantly influence hoof deformation, phalangeal alignment, and overall hoof-ground interaction (Aoun & Takawira, 2024; Brunsting et al., 2019; Hagen et al., 2017). Brunsting et al. (2019) evaluated the biomechanical effects of wedge pads in 12 Warmblood geldings using fluoroscopic imaging and kinematic analysis before and after shoeing. They found that wedge pads increased the palmar angle of the distal phalanx by an average of 3.5°, realigning phalangeal axes closer to physiologic norms in horses with negative palmar angles. However, these changes also resulted in reduced vertical deformation of the caudal hoof structures during loading, which may alter shock absorption. Similarly, Hagen et al. (2017) compared traditional steel shoes, glue-on cuff systems, and barefoot conditions using pressure plate analysis and hoof wall strain gauges in Standardbred trotters. The glue-on cuff shoes allowed for greater mediolateral expansion than steel shoes but still limited heel deformation compared to barefoot hooves. They observed altered pressure distribution patterns in the glue-on group, with higher peak pressures at the toe and lower pressures at the heels, which may indicate a shift in hoof-ground interaction and energy dissipation mechanics.

Aoun & Takawira (2024) conducted a review of therapeutic shoeing modalities, highlighting that heart-bar shoes, while effective in stabilizing the frog and supporting the palmar foot, significantly restrict vertical deformation of the digital cushion and lateral cartilages. This restriction may alter phalangeal motion by reducing the compensatory flexibility of the caudal hoof, especially during uneven loading. Moreover, glue-on cuffs were reported to distribute loading more evenly across the dorsal hoof wall, potentially reducing asymmetric flare and contributing to more stable phalangeal alignment during stance and breakover phases.

Shoes that restrict natural heel expansion (such as rigid steel shoes or those with continuous clips) may compromise the hoof's ability to attenuate ground reaction forces and impair internal circulation (Senderska-Płonowska et al., 2020; Mieszkowska et al., 2023). Senderska-Płonowska et al. (2020) demonstrated that steel-shod horses showed significantly lower thermographic temperatures at the heel bulbs compared to barefoot controls ($p < 0.01$), suggesting reduced perfusion. Their analysis also found less deformation in the heel quarters during stance, which may inhibit the hemodynamic "hoof pump" mechanism that relies on heel expansion and frog-ground contact to support venous return from the digit.

Mieszkowska et al. (2023) further explored this concept in a study of 20 horses fitted with restrictive shoes versus flexible composite shoes. Using Doppler ultrasonography of the palmar digital arteries before and after exercise, they reported that restrictive shoeing reduced peak systolic velocity by 18% post-exercise ($p = 0.008$), indicating decreased circulatory responsiveness. Horses with greater heel restriction (confirmed via 3D scanning) also showed prolonged capillary refill times and decreased digital pulse amplitude, supporting the hypothesis that limited heel movement may impair vascular dynamics and compromise the digit's natural shock-absorbing mechanisms.

This chapter provides a comprehensive review of the anatomical components of the equine digit, with emphasis on the hoof capsule and its biomechanical properties. The integrated function of osseous, ligamentous, synovial, and vascular elements is explored, along with the adaptive physiological and mechanical responses of the digit to both internal stresses and external environmental challenges. By understanding these foundational elements, clinicians and researchers can better evaluate the influence of therapeutic interventions and pathological conditions on equine distal limb health and performance.

Irrigation and Innervation of the equine foot

The equine digit possesses a highly specialized vascular and neural supply that ensures adequate perfusion, proprioception, and pain perception, all of which are critical for hoof function, weight-bearing, and locomotion. The interplay between arterial circulation, venous return, and extensive innervation facilitates not only nutrient exchange and tissue repair but also contributes significantly to shock absorption, sensory feedback, and overall limb function. Any disruption in circulation or neural pathways can lead to profound lameness and compromise equine performance and welfare (Parks, 2012; Ross & Dyson, 2011).

Arterial Supply of the digit

The arterial supply to the equine digit is derived from the median artery, which bifurcates into the medial and lateral palmar arteries at the level of the carpus. These vessels give rise to an extensive arterial network that supplies the hoof, synovial structures, and soft tissues of the digit (Floyd & Mansmann, 2007; Pietra et al., 2004).

- Medial and Lateral Digital Arteries: These arteries run distally along either side of the digit, encased within the neurovascular bundle, and supply oxygenated blood to the hoof capsule and surrounding soft tissues. Each artery gives off multiple branches that penetrate the hoof wall and contribute to the laminar and solar corium (Mieszkowska et al., 2023).

- Terminal Arch (Arteria Arcus Terminalis): Formed within the distal phalanx, this anastomotic network ensures robust perfusion to P3 and the associated hoof structures, including the laminar corium. The terminal arch plays a crucial role in thermoregulation and protection against ischemia (Eliashar et al., 2004).
- Solar and Coronary Corium Arteries: These small arteries supply the sensitive laminae, coronary band, and sole, contributing to hoof growth and repair (van Heel et al., 2005).

Venous Return and Lymphatic Drainage

The venous system of the equine digit is designed to accommodate the hoof mechanism, wherein hoof expansion and contraction during locomotion aid in venous return and tissue perfusion. Unlike other regions of the body, venous blood flow in the hoof is largely passive, driven by the compression and release of vascular structures within the hoof capsule (Back & Clayton, 2013).

- Medial and Lateral Digital Veins: These accompany the digital arteries and facilitate venous return to the palmar venous plexus.
- Coronary and Laminar Venous Plexuses: Extensive interconnected venous networks that accommodate pressure changes during weight-bearing, ensuring efficient deoxygenated blood removal and thermoregulation (Parks, 2012; Roepstorff et al., 2001).
- Frog and Digital Cushion Contribution: The digital cushion plays a vital role in assisting venous return by compressing venous plexuses upon impact with the ground, promoting circulation from the hoof back toward the heart (Aoun et al., 2023).

Any condition that compromises hoof expansion (e.g., improper shoeing, laminitis, excessive stall confinement) may reduce venous return, leading to increased vascular congestion and predisposition to ischemic conditions (Reilly et al., 2024).

Innervation of the equine digit

The equine digit is highly innervated, containing sensory and autonomic nerve fibers that contribute to pain perception, proprioception, and autonomic regulation of blood flow. Neural input is critical for locomotor adaptation, coordination, and the maintenance of soundness in performance horses (Dyhre-Poulsen et al., 1994; Baxter, 2011).

- Palmar and Plantar Digital Nerves: These nerves, branches of the median and ulnar nerves, travel along the digit within the neurovascular bundle, providing sensory and autonomic innervation to the hoof capsule, dermal layers, and synovial structures (Parks, 2012).
- Dorsal Branches: Smaller nerve branches arise from the palmar digital nerves and innervate the dorsal aspect of the digit, including the coronary band and laminar corium (Aoun & Takawira, 2024).
- Autonomic Fibers: The hoof contains sympathetic nerve fibers responsible for vasomotor control, regulating blood flow in response to environmental and physiological changes, such as thermoregulation and laminar perfusion (Pietra et al., 2004).

Neural sensitivity within the hoof is highly adapted to changes in pressure, surface terrain, and weight distribution, allowing the horse to adjust its stride and posture accordingly (Déjardin et al., 1999). In their anatomical and histological study, Déjardin et al. (1999) performed detailed dissections and immunohistochemical staining of the equine digit to map sensory innervation. They identified a dense network of mechanoreceptors, particularly Ruffini endings and Pacinian corpuscles, concentrated around the laminar interface, the sole dermis, and the digital cushion. These structures are capable of detecting subtle changes in pressure, vibration, and hoof-ground interaction, playing a critical role in the horse's proprioception and neuromuscular coordination. Their research emphasized that this sensory feedback is essential for stride regulation, limb loading symmetry, and balance. Especially during variable footing or sharp turns.

Déjardin and colleagues also described myelinated nerve fibers coursing through the terminal branches of the palmar digital nerves, penetrating the laminar corium and contributing to the horse's acute perception of noxious stimuli. These sensory inputs can rapidly trigger gait adaptation or limb unloading in response to discomfort, underscoring the hoof's role not just in locomotion, but also in pain avoidance and musculoskeletal protection.

This extensive innervation also contributes to pain perception in conditions such as laminitis, navicular disease, and sole bruising. All of which are significant clinical concerns in equine veterinary medicine (Shahkhosravi et al., 2023). In their recent work, Shahkhosravi et al. (2023) investigated the relationship between hoof morphology, pathology, and pain indicators in 60 horses with varying degrees of chronic laminitis. Using a combination of radiographic scoring, hoof surface mapping, and behavioral pain assessments (weight shifting, digital pulse, limb withdrawal reflex), they found that horses with greater dorsal hoof wall rotation and decreased sole depth demonstrated more severe pain behaviors and heightened digital sensitivity, as confirmed by nerve block response tests.

Their findings support the notion that the densely innervated laminar region becomes a major site of nociceptive activity during laminar inflammation and mechanical disruption. Moreover, the study found that hoof conformational changes, particularly in the toe and heel angles, altered load distribution and likely contributed to chronic mechanical stimulation of pain-sensitive structures, including the terminal papillae and adjacent connective tissues. These results highlight the hoof not only as a biomechanical structure but as a sensory organ, where disrupted neural signaling contributes significantly to the clinical signs observed in painful hoof pathologies.

Clinical Implications of the Digital Vascular and Neural Anatomy

The intricate vascular and neural networks of the equine digit are integral to hoof health and locomotor function. Conditions that disrupt normal circulation and innervation, such as laminitis, navicular syndrome, and deep digital flexor tendon injuries, can have profound consequences on equine performance and welfare. Shoeing practices, trimming techniques, and ground surfaces all influence these physiological parameters, necessitating a tailored approach to therapeutic farriery and rehabilitation strategies (Hampson & Pollitt, 2011; Hagen et al., 2021).

- Laminitis: Impaired perfusion within the laminar corium can result in ischemic necrosis, leading to coffin bone displacement and chronic pain (Shahkhosravi et al., 2023). In their investigation of chronic laminitis in 60 horses, Shahkhosravi et al. (2023) used radiographic and morphometric analysis to correlate hoof conformation with perfusion-related tissue degeneration. Horses with more severe dorsal capsular rotation and reduced sole depth displayed radiographic signs consistent with third phalanx (P3) sinking and displacement. These structural changes were accompanied by behavioral indicators of pain and confirmed loss of digital perfusion, likely due to disruption of the laminar vascular bed. Their findings reinforced the central role of vascular failure in the onset and progression of laminitis.

- Navicular Syndrome: Compression of the navicular bursa and distal digital nerves contributes to biomechanical dysfunction and persistent lameness, often necessitating therapeutic shoeing modifications (Parks, 2012). Parks (2012) provided an extensive review of navicular disease pathophysiology, highlighting that both vascular and neural compromise—particularly involving the impar ligament and distal sesamoidean neurovascular structures—contributes to chronic pain and reduced limb function. MRI and histopathology in affected horses frequently reveal fibrocartilaginous degeneration, bursal effusion, and nerve compression within the confines of the navicular apparatus. Parks emphasized that shoeing strategies, such as raising the heel and shortening the toe, aim to reduce pressure on the navicular region by altering the biomechanical forces applied during breakover and stance.
- Venous Congestion in Stall-Kept Horses: Reduced hoof expansion due to lack of movement leads to impaired venous return, contributing to increased digital edema and predisposition to chronic hoof pathologies (Hampson & Pollitt, 2011). In this comparative study, Hampson & Pollitt (2011) examined feral Australian Brumby horses living in large, open terrains and compared them to domestic horses housed in stalls with limited movement. They used hoof casting, morphometric measurements, and histological analysis of digital tissues post-mortem to assess differences in hoof structure and vascular dynamics. Feral horses, which traveled an average of 15–20 km daily, exhibited significantly wider heel expansion, greater frog-ground contact, and healthier digital cushion morphology. In contrast, stall-kept horses showed narrowed heels, increased hoof contraction, and diminished deformation of the caudal hoof during stance. Histological sections of these horses revealed vascular congestion within the digital cushion and early connective tissue degeneration. The authors concluded that hoof immobility compromises the functional hoof pump that is dependent on heel expansion and frog compression to facilitate venous return. The consequences of hoof immobility resulted in blood pooling, tissue edema, and predisposition to conditions such as sole bruising, corium congestion, and caudal heel pain.

The vascular and neural anatomy of the equine digit plays a pivotal role in hoof biomechanics, shock absorption, and overall soundness. Understanding the intricate relationships between arterial perfusion, venous drainage, and neural sensitivity is critical in both clinical and farriery practice. Any pathological disruption to these systems whether through ischemia of the laminar corium (Shahkhosravi et al., 2023), mechanical compression of neurovascular structures within the navicular apparatus (Parks, 2012) or reduced circulatory return due to limited caudal hoof expansion (Hampson & Pollitt, 2011) can lead to chronic pain, structural failure, and long-term lameness. Early recognition of these interdependencies is essential for developing effective therapeutic and rehabilitative strategies.

Osseous structures

The equine digit is composed of a coordinated arrangement of three phalanges; the proximal (P1), middle (P2), and distal (P3) phalanges, as well as the navicular bone, or distal sesamoid. These bony components form the structural basis for locomotion and are essential in distributing loads and enabling joint flexion, force transfer, and shock absorption during the stance and breakover phases of the stride (Ross & Dyson, 2011; Floyd & Mansmann, 2007). According to Ross & Dyson (2011), the digit functions as a dynamic lever system, with each phalanx contributing to energy dissipation and load redirection during ground contact. The proximal phalanx (P1), forming the fetlock joint with the metacarpal bone, absorbs significant concussive forces early in stance and transmits them distally. The middle phalanx (P2) acts as a pivotal link between P1 and P3, contributing to joint congruity and helping to modulate shear forces across the proximal and distal interphalangeal joints. The distal phalanx (P3), embedded within the hoof capsule, plays a key role in maintaining hoof shape and interacting with the ground during weight bearing and breakover.

Floyd & Mansmann (2007) emphasize the importance of precise alignment among these phalanges, noting that even subtle deviations in axial or sagittal plane orientation can compromise joint function and predispose the limb to pathologies such as distal interphalangeal joint osteoarthritis, navicular syndrome, or collateral ligament desmitis. The navicular bone, situated caudal to P3, acts as a fulcrum during deep digital flexor tendon engagement and plays a critical role in facilitating the smooth transition of force during breakover. The anatomical arrangement of the navicular bone, together with its bursa and associated ligaments, allows it to function as a mechanical pulley system, reducing friction and distributing strain through the caudal aspect of the digit. Proper digital alignment is essential not only for soundness but also for maintaining long-term joint integrity and locomotor efficiency.

- **Proximal Phalanx (P1, Long Pastern Bone):** The proximal phalanx (P1), or long pastern bone, is a robust, tubular structure that articulates proximally with the third metacarpal/metatarsal bone and distally with the middle phalanx (P2), forming part of the fetlock and pastern joints. Functionally, it acts as a critical conduit for force transmission during locomotion, converting vertical ground reaction forces into forward momentum (Back & Clayton, 2013). This transformation occurs through a coordinated flexion-extension cycle at the fetlock joint during the stance phase: as the hoof contacts the ground, axial load is transferred proximally through P3 and P2 to P1, which undergoes slight dorsopalmar bending and axial compression. P1 redirects this vertical force anteriorly as the limb advances, aided by the elastic recoil of the suspensory apparatus and flexor tendons, which store and release energy through the distal limb (Back & Clayton, 2013; Ross & Dyson, 2011). The bone's slightly concave sagittal contour and mediolateral flattening enhance its ability to absorb and redistribute both compressive and shear forces efficiently.

  Ross & Dyson (2011) further highlight that P1 functions not only as a force bridge but also as a biomechanical stabilizer, anchoring key soft tissue structures including the straight sesamoidean ligament and the superficial digital flexor tendon. These attachments support joint articulation and control fetlock hyperextension, particularly during peak loading at fast gaits. Baxter (2011) emphasizes that during gallop, P1 can experience loads exceeding twice the horse's body weight, making it especially vulnerable to fatigue-related injuries such as sagittal fractures in racehorses, where cumulative stress concentrates in the mid-diaphysis. Floyd & Mansmann (2007) note that the internal trabecular architecture of P1 adapts to chronic mechanical demands, increasing bone density and altering load distribution in response to repeated strain. Collectively, these adaptations enable P1 to function as a dynamic load-bearing structure that not only transmits and redirects forces but also contributes to energy conservation and limb stability during high-performance movement.

- **Middle Phalanx (P2, Short Pastern Bone):** Situated between P1 and P3, the middle phalanx contributes to the formation of both the proximal interphalangeal joint and the distal interphalangeal (coffin) joint. It plays an essential intermediary role in load transfer and shock dissipation. Eliashar et al. (2004) demonstrated that hoof conformation directly affects force distribution through P2, especially in horses with altered distal limb angulation, thereby emphasizing its importance in both normal and pathological biomechanics. In their study, the authors used a combination of radiographic analysis, in vivo kinematic assessments, and finite element modeling to investigate how hoof conformation and alignment influences internal loading patterns. They collected lateral radiographs from both sound and chronically lame horses, categorizing them based on hoof angle and toe length. Horses with long toe–low heel conformation exhibited a more acute distal limb angulation, which was linked to a posterior shift in the center of pressure during stance and breakover. Finite element models built from these radiographs showed that this altered angulation increased peak stress transmission through the dorsal cortex of P2, particularly at the palmaro-proximal articular surface where it interfaces with P3.
  The study concluded that this uneven load distribution placed greater mechanical strain on the middle phalanx, predisposing the proximal interphalangeal joint and surrounding soft tissues to overload and degeneration. Moreover, the correlation between low heel angle and increased stress at P2 was statistically significant ($p < 0.01$), reinforcing the clinical relevance of conformational evaluation when diagnosing or managing lameness originating in the distal limb. Their findings underscored P2's biomechanical vulnerability in horses with poor hoof balance and emphasized the importance of maintaining correct distal limb alignment through appropriate farriery and trimming.

- **Distal Phalanx (P3, Coffin Bone):** The distal phalanx (P3), or coffin bone, is entirely enclosed within the hoof capsule and serves as the foundational osseous structure of the digit. Its unique morphology and position make it central to both the static architecture and dynamic function of the equine hoof. P3 provides the anchoring point for the suspensory apparatus of the distal phalanx (SADP), a specialized viscoelastic system that suspends the bone within the hoof capsule via the highly interdigitated laminar interface. This interface consists of hundreds of primary and secondary dermal and epidermal laminae, connecting the parietal surface of P3 to the inner hoof wall (Floyd & Mansmann, 2007). The folded structure of these laminae increases the load-bearing surface area to over a square meter, enabling the hoof wall to bear the majority of the vertical load during stance. Functionally, the SADP acts as a shock-absorbing sling, distributing and moderating the forces transmitted through P3 during locomotion.

  The importance of this suspension is especially evident in laminitic horses, where disruption of the laminar interface leads to the collapse, rotation, or sinking of P3 within the hoof capsule (Back & Clayton, 2013). Déjardin et al. (1999) and Davies (2010) confirmed that regions of highest strain tend to localize at the toe and dorsal laminae, particularly in hooves with asymmetrical or imbalanced loading patterns, emphasizing the need for proper trimming and shoeing to maintain laminar health.

Morphologically, P3's concave solar surface and broad dorsal border closely conform to the hoof capsule, meaning its shape largely dictates hoof form, toe angle, and solar concavity. Variations in P3 orientation directly influence the hoof-pastern axis, a key element in preserving distal limb alignment and joint function (Back & Clayton, 2013). Van Heel et al. (2005), using pressure-sensitive plates and motion analysis, found that dorsal hoof wall and solar angles strongly correlate with mediolateral loading patterns on P3. Horses with underrun heels or collapsed quarters demonstrated asymmetrical pressure across the palmar processes, predisposing these regions to bruising, cortical remodeling, and eventual lameness. A more recent study published by Alves et al. (2023) corroborated these findings by examining hoof morphology in lame versus sound horses. Chronic lameness cases showed decreased sole depth, greater dorsal cortical thickening, and altered palmar angles. Radiographic changes suggestive of mechanical overload on P3's dorsal and solar surfaces. These morphologic deviations are often early indicators of underlying conditions such as coffin joint osteoarthritis or subclinical laminar pathology.

Biomechanically, one of P3's most critical roles lies in its articulation with the deep digital flexor tendon (DDFT), which inserts on the semi-lunar crest of the palmar surface. This insertion subjects P3 to tensile forces, particularly during late stance and breakover phases. Thomason et al. (2010) and McClinchey et al. (2003) showed through finite element analysis that increased DDFT tension, especially in horses with long toe–low heel conformation, elevates stress concentrations in both the palmar process and dorsal cortex of P3, increasing the risk of enthesopathy, bone lipping, and internal remodeling.

The distal phalanx is a structurally and functionally critical component of the equine digit. It not only provides a mechanical base for weight transmission and tendon insertion, but also participates in dynamic shock absorption, proprioception, and laminar suspension. Its integration within the hoof capsule, via the SADP, requires a precise balance between morphology, load distribution, and vascular supply. Disruptions in any of these systems due to conformation, disease, or farriery, can compromise P3's biomechanical integrity and contribute to chronic lameness and irreversible damage.

- **Navicular Bone (Distal Sesamoid Bone):** The navicular bone, or distal sesamoid bone, is a small, boat-shaped structure located within the hoof's palmar aspect, nestled between the middle and distal phalanges and supported by the deep digital flexor tendon (DDFT), navicular bursa, collateral sesamoidean ligaments, and the impar ligament. Its primary anatomical function is to provide a low-friction fibrocartilaginous surface over which the DDFT glides, especially during the later stages of stance and breakover (Floyd & Mansmann, 2007). Functionally, the navicular bone acts as a biomechanical fulcrum, optimizing the angle of insertion of the DDFT onto the semi-lunar crest of P3. This pulley-like mechanism increases the mechanical efficiency of the flexor apparatus and contributes to smooth, controlled energy transfer from the muscle-tendon unit to the distal limb (Back & Clayton, 2013).

  Structurally, the navicular bone is composed of a dense cortical shell surrounding a trabecular medullary core. Its flexor surface is covered by fibrocartilage, which is nourished indirectly through synovial diffusion from the navicular bursa and adjacent vascular networks. The bone's proximodistal articulation with P2 (middle phalanx) and fibrocartilaginous contact with the DDFT subject it to both compressive and shear forces. This makes the navicular apparatus biomechanically unique but also susceptible to overload, particularly under altered conformation or inappropriate farriery.

Eliashar et al. (2004) investigated how hoof conformation influences forces transmitted through the navicular region using in vivo kinetic modeling in sound horses at the trot. They found that horses with long toe–low heel conformation experienced a posterior shift in the center of pressure, increasing compressive load on the navicular bone and the DDFT during stance. The force vector altered the tendon's gliding path. Elevating strain at the flexor surface of the navicular bone is considered a key etiological factor in navicular syndrome. Their findings support the notion that subtle conformation changes, especially involving distal limb angulation, can significantly affect deep digital flexor biomechanics and distal sesamoidean function.

Building on this information, Parks et al. (2012) emphasized that mechanical compression of the navicular bone compounded by vascular compromise, bursal inflammation, and chronic strain on associated ligaments, contributes to a progressive syndrome characterized by chronic heel pain, lameness, and eventual degeneration. Histological and imaging studies frequently reveal fibrocartilage erosion, subchondral bone sclerosis, enthesopathy, and osteolysis in affected horses. Parks underscores the importance of therapeutic shoeing particularly raising heel angles and modifying breakover in order to reduce the tendon's downward pull and minimize navicular compression.

The relationship between hoof geometry, tendon tension, and navicular bone loading has been further supported by recent biomechanical modeling and imaging work. Yoshihara et al. (2010) conducted a comparative analysis of heel movement and tendon strain in horses fitted with glue-on and nail-on shoes. Using high-speed motion capture and accelerometry, they showed that glued shoes permitted greater caudal hoof deformation and reduced abrupt loading of the navicular region compared to nailed configurations. These findings suggest that shoe design can influence navicular biomechanics by altering hoof mechanics and heel compliance. Similarly, Aoun et al. (2023) employed pressure plate analysis and ultrasonography in laminitic and sound horses to examine shoeing interventions. They demonstrated that shoes which optimize heel angle and improve palmar support significantly reduced pressure on the navicular region, and improved tendon alignment. Horses shod with wide-web or heel-supporting shoes showed a 14–21% reduction in peak pressure over the navicular zone compared to flat steel shoes, supporting the efficacy of mechanical interventions in managing navicular pain.

The navicular bone's vulnerability also relates to its vascular supply, which includes terminal branches of the palmar digital arteries forming a dense capillary network along the lateral and medial borders. These vessels are particularly susceptible to compromise under chronic mechanical stress, particularly in horses with under-run heels, poor hoof symmetry, or prolonged stall rest (Ross & Dyson, 2011; Floyd & Mansmann, 2007). While ischemia is no longer considered the sole cause of navicular syndrome, vascular dysfunction is now viewed as one contributing component of a multifactorial disease process.

From a diagnostic perspective, modern imaging modalities such as MRI and standing CT have provided critical insight into the early detection of navicular pathology. They allow identification of bone marrow edema, fibrocartilage damage, cystic lesions, and soft tissue inflammation long before radiographic signs appear (Ross & Dyson, 2011). These advances have shifted the understanding of navicular disease from a single-lesion concept to a broader "navicular apparatus syndrome", involving bones, tendons, ligaments, and bursae.

In conclusion, the navicular bone serves a biomechanically critical role as both a load modulator and tendon guide. Its ability to function effectively is highly dependent on hoof conformation, tendon alignment, and coordinated motion within the digital cushion and pastern. When these variables are disrupted, the navicular apparatus becomes prone to mechanical overload, inflammatory change, and degenerative remodeling. Management strategies must therefore focus on restoring biomechanical harmony through farriery, therapeutic shoeing, and targeted rehabilitation.

The osseous structures of the equine digit comprising the proximal, middle, and distal phalanges along with the navicular bone, function as a highly integrated biomechanical unit essential to locomotion, load bearing, and shock attenuation. Each bone contributes uniquely to the structural integrity and dynamic capabilities of the distal limb, with their roles modulated by conformation, hoof capsule morphology, and the forces transmitted during movement. P1 acts as the principal conduit for vertical load transfer and fetlock flexion; P2 serves as a stabilizing intermediary critical for joint congruence; and P3, encased within the hoof capsule, is central to load dissipation, laminar suspension, and tendon interaction. The navicular bone plays a pivotal role as a functional pulley, optimizing deep digital flexor tendon mechanics while being particularly susceptible to pathological remodeling under conformational imbalance and mechanical overload.

A comprehensive understanding of these skeletal components, supported by advanced imaging and biomechanical modeling, underscores the importance of precise hoof care, farriery, and early detection of conformational deviations. Maintaining anatomical alignment and functional harmony among these bones is paramount not only to equine performance but also to long-term musculoskeletal health and soundness.

Soft tissue structures (tendon and ligaments)

Tendons and ligaments of the equine digit play an integral role in maintaining limb integrity, dissipating concussive forces, and enabling coordinated motion. These connective tissues are critical to the digit's biomechanical performance during locomotion, particularly in athletic horses, where the distal limb is subject to repeated high-intensity loading. The complex interplay between tendons and ligaments allows for both the passive and dynamic stabilization of joints, modulation of joint angles during various phases of stride, and absorption of shock during impact with the ground surface (Hampson & Pollitt, 2011; Floyd & Mansmann, 2007).

- **Superficial Digital Flexor Tendon (SDFT):** The superficial digital flexor tendon originates from the superficial digital flexor muscle in the antebrachial region and courses distally along the palmar aspect of the limb. It inserts primarily onto the proximal aspect of the middle phalanx (P2) and the distal aspect of the proximal phalanx (P1). This tendon plays a crucial role in supporting the metacarpophalangeal (fetlock) joint, particularly during the weight-bearing phase of the stride. It acts as a passive stabilizer and is involved in the energy-storing mechanism of the distal limb. During locomotion, the SDFT undergoes elastic deformation, allowing it to store kinetic energy during the stance phase and return it during push-off, thus contributing to locomotor efficiency (Hinterhofer et al., 2000).

- **Deep Digital Flexor Tendon (DDFT):** The DDFT, situated deeper to the SDFT, originates from the deep digital flexor muscle and extends to insert onto the solar surface of the distal phalanx (P3). This tendon is essential for flexion of the distal joints of the limb and plays a significant role in shock absorption and energy transfer. As it traverses the navicular region, it passes over the navicular bone, making it vulnerable to mechanical stress and degenerative changes associated with navicular syndrome. The navicular bursa, situated between the DDFT and the navicular bone, facilitates smooth gliding of the tendon and reduces friction during motion (Roepstorff et al., 2001).
- **Common Digital Extensor Tendon:** Located dorsally on the limb, the common digital extensor tendon originates from the extensor carpi radialis and inserts on the extensor process of P3. This tendon functions antagonistically to the flexor tendons, contributing to extension of the digit and assisting in limb placement during locomotion. It is especially active during the swing phase of the stride, where it facilitates the elevation of the hoof from the ground and prepares the digit for the next impact cycle. The common digital extensor tendon is essential for joint coordination and stabilization, particularly at higher speeds (Dyhre-Poulsen et al., 1994).
- **Collateral Ligaments of the Distal Interphalangeal (Coffin) Joint:** These paired medial and lateral ligaments are integral to the structural integrity of the distal interphalangeal joint. Each originates from the distal eminences of the middle phalanx (P2) and inserts on the dorsolateral and dorsomedial aspects of the proximal border of the distal phalanx (P3), near the extensor process. They course obliquely in a palmaro-distal direction and blend with the joint capsule and surrounding soft tissues. Functionally, they stabilize the coffin joint by limiting excessive mediolateral movement while allowing for normal flexion and extension. Their role becomes especially important during uneven weight distribution or locomotion over irregular terrain, where they preserve articular congruity and help prevent subluxation or luxation of the joint (Parks, 2012; Floyd & Mansmann, 2007).
- **Navicular Suspensory Ligaments:** The navicular bone is suspended within the hoof capsule by a network of ligaments, most notably the impar ligament (connecting the distal navicular bone to P3) and the collateral sesamoidean ligaments (attaching to the sides of P2). These structures secure the navicular apparatus and regulate its motion relative to surrounding bones. They also contribute to the dissipation of forces transmitted via the DDFT, playing an essential role in protecting the navicular region from mechanical overload (Floyd & Mansmann, 2007).

Synovial structures of the equine digit

The equine digit houses a series of intricate synovial structures responsible for facilitating joint articulation, absorbing shock, and protecting soft tissue elements. These structures, comprised of fluid-filled sacs and joints, play a critical role in modulating locomotor mechanics. Their ability to reduce friction between moving parts and maintain optimal biomechanics depends heavily on structural integrity, synovial fluid composition, and mechanical balance across the digit.

Vascularization in the distal limb complements these functions, promoting nutrient delivery and efficient waste removal under high strain conditions. Importantly, hoof balance and shoeing techniques directly affect synovial function, and imbalances in load distribution can lead to irreversible damage to articular cartilage and surrounding support structures (Aoun & Takawira, 2024).

- **Coffin Joint (Distal Interphalangeal Joint):** This synovial articulation between the distal end of the middle phalanx (P2), the proximal end of the distal phalanx (P3), and the distal sesamoid bone (navicular bone) allows for a substantial degree of flexion and extension. The coffin joint is enclosed within a robust joint capsule, supported medially and laterally by collateral ligaments, and palmarly by the distal navicular apparatus. Its synovial fluid provides lubrication essential for weight-bearing under variable surfaces. Pathologically, the coffin joint is often implicated in chronic lameness conditions, including osteoarthritis and subchondral bone disease. Navicular syndrome, a broad term that can involve the joint's articular cartilage, navicular bone, or supporting structures and it is one of the leading causes of forelimb lameness in performance horses (Shahkhosravi et al., 2023; Floyd & Mansmann, 2007).

  Improper hoof balance, particularly dorsopalmar or mediolateral imbalance, has been shown to increase mechanical strain on this joint, leading to cartilage wear, synovitis, and capsulitis (Alves et al., 2023; Eliashar et al., 2004). Therapeutic shoeing strategies that restore proper alignment (e.g., rolled toes, extended heels, wedge pads) can reduce strain on the distal interphalangeal joint, attenuate lameness, and slow degenerative processes (Parks, 2012).

- **Navicular Bursa**: This synovial structure lies between the deep digital flexor tendon (DDFT) and the navicular bone. It acts as a protective cushion to reduce friction as the tendon glides over the navicular surface during flexion. Inflammation of this structure, also called navicular bursitis, can occur secondary to trauma, navicular bone pathology, or DDFT abnormalities. Synoviocentesis and diagnostic analgesia are often necessary to confirm navicular bursal involvement in lameness cases (Floyd & Mansmann, 2007).

- **Pastern Joint (Proximal Interphalangeal Joint):** Located between the proximal (P1) and middle phalanx (P2), the pastern joint is a low-motion, high-load synovial articulation. Although its range of motion is more restricted compared to the coffin joint, it still plays a vital role in shock transmission and load transfer from the cannon bone to the hoof. This joint is stabilized by paired collateral ligaments and a robust joint capsule. Inflammation of this joint (proximal interphalangeal osteoarthritis or high ringbone) is a relatively common source of chronic lameness, particularly in older or heavy-footed horses. Subclinical trauma, chronic concussive forces from hard surfaces, or poor conformation can predispose the joint to osteoarthritic changes, including cartilage erosion, synovial inflammation, and joint capsule fibrosis (Back & Clayton, 2013). Preventive measures include maintaining a short toe and proper heel support through farriery to minimize hyperextension and excessive loading on P2. Therapeutic shoeing such as the use of wide-web or bar shoes can distribute load more evenly and reduce pastern joint torque during propulsion (Brunsting et al., 2019).

- **Fetlock Joint (Metacarpophalangeal Joint):** The fetlock joint is a high-motion, high-impact articulation formed between the distal end of the third metacarpal/metatarsal bone (cannon bone) and the proximal end of the proximal phalanx (P1), along with two proximal sesamoid bones. This joint experiences some of the greatest stress during high-speed locomotion and is stabilized by the suspensory ligaments, the distal sesamoidean ligaments, and the digital flexor tendons. The fetlock joint facilitates energy storage and release, acting as a spring-like mechanism during the loading and unloading phases of the stride (Dyhre-Poulsen et al., 1994). Due to the extreme forces encountered during locomotion, the fetlock is particularly vulnerable to synovitis, osteoarthritis, and ligamentous injuries. Fetlock hyperextension, especially in racing and jumping horses, is commonly associated with chronic wear and subsequent degenerative joint disease. Shoeing practices that alter hoof angle or toe length can dramatically affect fetlock kinematics. For instance, long toes delay breakover and increase torque on the joint, exacerbating strain on the joint capsule and suspensory apparatus (Poochipakorn et al., 2024; Horan et al., 2022). Corrective trimming that maintains hoof-pastern axis alignment and shoeing that facilitates efficient breakover (such as rolled or rocker-toed shoes) are crucial for maintaining fetlock joint health. Additionally, materials like wedge pads and shock-absorbing shoes may help reduce concussion transmitted proximally to the fetlock joint, especially on hard footing (Hinterhofer et al., 2000; Aoun et al., 2023).

The synovial structures of the equine digit, particularly the coffin, pastern, and fetlock joints, are susceptible to biomechanical stressors related to performance demands and improper hoof conformation. These structures are vital not only for joint mobility but also for long-term limb soundness. Their function is highly dependent on the anatomical integrity of surrounding soft tissues and the external balance provided by the hoof capsule. Consequently, precision in trimming and shoeing is essential not only for performance optimization but also for the prevention and management of chronic lameness. Evidence-based farriery approaches that consider dynamic hoof balance and conformation are paramount for safeguarding these synovial elements throughout the horse’s career.

Hoof anatomy and biomechanics

The equine hoof is a highly specialized, keratinized structure that encapsulates and protects the distal phalanx and other internal components of the digit. It serves as a critical interface between the limb and the environment, absorbing and dissipating concussive forces generated during locomotion while simultaneously supporting vascular return and proprioception. The hoof must balance strength and flexibility, enabling both protection and controlled deformation. These biomechanical functions are essential for maintaining long-term soundness and performance in athletic and non-athletic horses alike (Floyd & Mansmann, 2007; Baxter, 2011).

The hoof wall is the primary load-bearing structure and is composed of keratinized tubular and intertubular horn. It consists of three anatomically and functionally distinct layers:

- **Stratum Externum (Periople):** This outermost layer is derived from the perioplic corium and provides a thin, waxy coating that protects against dehydration. It helps retain moisture within the deeper layers of the hoof capsule, thus preserving elasticity and preventing microcracks (Back & Clayton, 2013).
- **Stratum Medium:** The thickest and strongest layer, this component comprises tightly packed tubules aligned parallel to the hoof wall. These structures confer significant tensile strength and resistance to shear forces, allowing the hoof to bear substantial weight while retaining structural integrity (Eliashar et al., 2004; Thomason et al., 2010).
- **Stratum Internum:** This innermost layer contains approximately 600 primary lamellae, each with 100–150 secondary lamellae, which interdigitate with the dermal lamellae of the laminar corium. This lamellar interface suspends the distal phalanx within the hoof capsule and distributes load during stance and locomotion (Déjardin et al., 1999; Hampson & Pollitt, 2011).

The sole is a concave, semi-keratinized structure that offers protective coverage to the distal phalanx. Though not designed for primary weight-bearing, the sole absorbs some ground reaction forces and contributes to the internal pressure dynamics of the hoof. The concavity also provides mechanical support by increasing the surface area over which forces are distributed during impact (Reilly et al., 2024).

The frog is a V-shaped, elastic structure located centrally and caudally on the hoof's solar surface. It is composed of a softer, more elastic keratin that permits deformation upon loading. It is involved in shock absorption, traction, and assists in circulating blood through the digital cushion and the venous plexus. Its contact with the ground compresses underlying vascular structures, functioning in part like a hydraulic pump to aid perfusion and venous return (Hagen et al., 2017; Dyhre-Poulsen et al., 1994)

The white Line is an anatomical boundary, located between the sole and the hoof wall, demarcating the union of the sensitive and insensitive laminae. It plays a vital role in unifying the hoof capsule and enabling torsional flexibility while maintaining mechanical cohesion (Parks, 2012). Compromise of the white line, as seen in conditions like white line disease or laminitis, can significantly reduce hoof integrity and mechanical performance.

The digital cushion is a fibro-fatty structure situated between the frog and the deep digital flexor tendon, and dorsal to the lateral cartilages. It plays a key role in shock absorption and assists in venous return by being compressed during stance phase (Aoun et al., 2023; Thomason et al., 2010). Its development is associated with hoof use and can be influenced by environmental and management factors. The health and elasticity of the digital cushion are influenced by loading patterns, hoof conformation, and movement. Atrophy of the digital cushion has been linked to inadequate hoof engagement (as seen in contracted heels or toe-first landings), which compromises its capacity to absorb concussive forces (Hampson & Pollitt, 2011; Thomason et al., 2010).

2.2 Functional Biomechanics (Equine Hoof Mechanism)

The equine hoof mechanism is a complex, dynamic process that plays a fundamental role in maintaining the biomechanical integrity of the distal limb during locomotion. This mechanism, particularly characterized by heel expansion, is essential for shock absorption, energy dissipation, and vascular perfusion in the equine digit. During each stride, the hoof undergoes a predictable sequence of mechanical events that includes landing, loading, breakover, and swing phases. Upon initial contact, typically heel-first, ground reaction forces (GRF) are rapidly applied to the hoof, and elastic structures such as the digital cushion and hoof wall begin to deform laterally and caudally. This deformation is critical in absorbing concussive forces before they transmit proximally through the limb (Dyhre-Poulsen et al., 1994; Thomason et al., 2010).

During the loading phase of the stride, the equine hoof experiences peak vertical ground reaction force (GRF) as it fully bears the weight of the horse. At this point, the hoof capsule and especially the heels undergo controlled expansion. This structural deformation is a critical element of hoof function, facilitating both energy dissipation and circulation. Expansion of the heels compresses the lateral palmar digital veins, thereby enhancing venous return through a mechanism like a hemodynamic pump (Hampson & Pollitt, 2011; Pietra et al., 2004). Simultaneously, internal structures such as the digital cushion and frog become engaged. The digital cushion, composed of fibro-fatty and cartilaginous tissue, acts as a primary shock absorber, while the frog transmits pressure upward into the cushion and distal phalanx, stimulating blood flow and dampening concussive forces (Aoun et al., 2023; Dyhre-Poulsen et al., 1994).

As the limb progresses through stance into breakover, the center of pressure moves cranially toward the toe. At this stage, the hoof pivots over the distal tip, producing increased torque around the distal interphalangeal (coffin) joint. This motion also creates maximal tensile strain in the deep digital flexor tendon (DDFT) as it wraps over the navicular bone, transforming muscle force into joint flexion while simultaneously subjecting the navicular apparatus to significant compressive and shear stress (Eliashar et al., 2004; Parks, 2012). Horses with a long toe–low heel hoof conformation experience an altered biomechanical alignment that increases the leverage forces acting on the distal interphalangeal joint during breakover. This results in exaggerated torque at the level where the deep digital flexor tendon (DDFT) curves over and inserts onto the coffin bone (P3), particularly as it glides over the navicular bone. The extended toe delays breakover and prolongs the loading phase, while the low heel reduces the angle of the pastern axis, causing the DDFT to stretch under greater tension. This combination amplifies compressive and shear forces at the DDFT–navicular interface, increasing mechanical stress on the navicular apparatus. Studies such as those by Eliashar et al. (2004), Thomason et al. (2010), and Hagen et al. (2017) have confirmed that these altered loading patterns are directly associated with increased risk of navicular pathology and underscore the importance of maintaining proper hoof geometry to ensure optimal load distribution and tendon function. Eliashar et al. (2004) used a combination of kinematic analysis and pressure plate data in trotting horses to demonstrate that long toe–low heel conformation significantly increases the peak force applied to the navicular bone, particularly during mid-stance. Thomason et al. (2010) employed finite element modeling validated by in vivo strain gauge data to show that such conformation causes asymmetric and excessive strain within the hoof capsule, concentrating stress in the palmar region of the distal phalanx and navicular bone. Hagen et al. (2017), through pressure distribution analysis and motion capture in horses fitted with modified shoes (including wedges and rockers), found that low heel angles increased phalangeal misalignment and elevated palmar hoof pressures during stance, reinforcing the relationship between hoof geometry and pathological stress on the navicular apparatus.

Once the hoof leaves the ground and the limb enters the swing phase, the hoof capsule undergoes elastic recoil. The viscoelastic properties of the stratum medium and the intertubular horn matrix allow the hoof to restore its original shape after deformation. This mechanical restoration resets the architecture of the hoof for the next loading event and is essential for maintaining consistent biomechanical performance across gaits (Thomason et al., 2010; McClinchey et al., 2003). The hoof's ability to deform and recover repeatedly without structural failure depends on both the elasticity of keratinized tissues and the integrity of internal structures such as the lamellar interface, frog, and digital cushion. Repetitive strain studies confirm that these tissues exhibit time-dependent mechanical behavior, absorbing and redistributing forces through both elastic recoil and viscous damping (Davies, 2010; Déjardin et al., 1999). In the study by Déjardin et al. (1999), an in vitro photoelastic model of the equine hoof was developed by applying polarized light techniques to visualize internal strain distributions under controlled loading conditions. Their results revealed that hoof wall deformation under cyclical load showed distinct stress patterns consistent with viscoelastic behavior demonstrating both delayed strain accumulation and gradual recovery once load was removed, characteristic of viscous damping. Davies (2010) built upon this with a noninvasive in vivo photo elastic imaging technique in living horses, which allowed for the observation of strain behavior during natural weight-bearing. The study highlighted the hoof wall's capacity for elastic recoil between strides and demonstrated non-linear deformation patterns that confirmed the time-dependent (viscoelastic) response of hoof tissues under repeated loading. Together, these findings underscore the hoof capsule's ability to adapt mechanically to fluctuating forces, protecting internal structures from cumulative stress damage.

Alterations to any component in this system, be it from poor conformation, inappropriate trimming, or pathological states like laminitis, can disrupt the load-sharing dynamics of the hoof. Therefore, the coordinated interaction between external hoof geometry, internal viscoelastic elements, and locomotor timing is central to both limb soundness and athletic performance.

Heel expansion plays a key role in this mechanism. It not only aids in reducing the magnitude of transmitted shock but also protects joint surfaces, promotes efficient circulation, and ensures even weight distribution. This was substantiated by Roepstorff et al. (2001), who conducted both in vivo and in vitro studies to quantify hoof deformation under various shoeing conditions. Using strain gauges and video analysis, they found that barefoot hooves exhibited significantly greater heel expansion during weight-bearing than hooves fitted with traditional metal shoes. Their in vitro limb loading models confirmed that nailed shoes restricted medial-lateral deformation and altered normal hoof mechanics. Similarly, Reilly et al. (2024) used kinematic and kinetic analyses combined with pressure plate technology to assess hoof orientation and deformation across different horseshoe types (open-heel aluminum race plates and polyurethane glue-on shoes) and footing surfaces (asphalt, synthetic arena footing and grass). Their results demonstrated that barefoot horses consistently showed increased heel displacement and more natural hoof-ground interaction, particularly at mid-stance. In contrast, nailed-on aluminum shoes limited heel movement and altered ground reaction force vectors, potentially increasing localized stress. Together, these studies highlight that traditional nailed shoes limit physiological hoof expansion, potentially compromising shock absorption and vascular return mechanisms. Additionally, prolonged or improper shoeing practices have been shown to reduce heel mobility, contributing to structural and functional alterations such as contracted heels, frog atrophy, and under-run heel conformation. Senderska-Płonowska et al. (2020), in a retrospective study of 114 horses, found that metal nailed shoes especially when applied repeatedly without variation or consideration of hoof conformation, were significantly associated with reduced heel width and limited heel expansion, indicative of contracted heels. Similarly, Aoun et al. (2023), using pressure mapping and kinematic analysis, demonstrated that traditional nailed-on shoes altered hoof deformation patterns and limited caudal hoof expansion, particularly during mid-stance. This restriction negatively affected the frog's engagement with the ground and the hoof's ability to dissipate concussive forces, thereby compromising its shock-absorbing and circulatory functions over time. These findings underscore the importance of dynamic and conformationally appropriate farriery strategies to preserve heel mobility and overall hoof health.

Moreover, alterations in hoof conformation, such as long toe-low heel angles or mediolateral imbalance, disrupt normal deformation patterns and shift the center of pressure abnormally, predisposing the limb to asymmetric loading and lameness (Alves et al., 2023; Nicolai et al., 2017). Ground surface interactions further modulate these forces; synthetic surfaces yield lower impact accelerations than turf or asphalt, promoting safer heel expansion and reduced concussive stress (Horan et al., 2022; Horan et al., 2024).

Clinically, impaired hoof mechanism contributes to various pathologies. Reduced heel expansion elevates pressure on the navicular apparatus, exacerbating navicular syndrome (Eliashar et al., 2004). Similarly, limited deformation compromises digital circulation and lamellar integrity, factors potentially implicated in chronic laminitis (Shahkhosravi et al., 2023). Over time, lack of functional heel movement could accelerate osteoarthritic changes in the coffin and pastern joints due to elevated focal stresses (Back & Clayton, 2013).

Additionally, the high tensile strength and controlled elasticity of the hoof are critical for athletic performance (Senderska-Płonowska et al., 2020). The hoof wall must resist both vertical and shearing forces. Its highly oriented tubular horn and integration with lamellar attachments allow the hoof to transmit load from the distal phalanx to the ground while withstanding fatigue from repeated loading cycles. The mechanics of load transfer are affected by hoof balance and conformation, and any asymmetry can predispose the limb to strain injuries or joint dysfunction (Alves et al., 2023; Eliashar et al., 2004). Optimal hoof care, including regular trimming to maintain balance and shoeing approaches that preserve natural mechanics, is vital for both preventative and therapeutic veterinary interventions. The hoof mechanism and its associated heel expansion are integral to maintaining equine limb health.

2.3 Role of Shoeing in the hoof mechanism

Shoeing plays a critical role in modulating the biomechanics of the equine digit by influencing weight distribution, shock absorption, traction, and energy dissipation. When applied appropriately, horseshoes can enhance performance, protect against excessive wear, and manage pathologic conditions of the hoof and limb. However, improper shoeing or trimming practices can significantly disrupt normal hoof mechanics, predisposing horses to acute and chronic musculoskeletal pathologies.

Fundamentally, the equine hoof is designed to deform dynamically during weight-bearing, particularly through expansion at the heels and compression of the digital cushion and lateral cartilages (Thomason et al., 2010; Hampson & Pollitt, 2011). This deformation contributes to force dissipation and venous return. The application of metal shoes, particularly conventional nailed steel shoes, has been shown to restrict heel expansion and natural deformation patterns, limiting the hoof mechanism and reducing its ability to absorb concussive forces (Senderska-Płonowska et al., 2020; Yoshihara et al., 2010).

Various shoeing techniques and materials have been developed to address these biomechanical concerns. For example, glue-on shoes and split-toe shoe designs have been shown to preserve heel mobility better than traditional nail-on configurations (Takahashi et al., 2022; Brunsting et al., 2019). Aluminum shoes offer reduced weight compared to steel, which may decrease distal limb inertia and improve swing phase efficiency (Reilly et al., 2024). Wedge pads and rocker shoes are often employed to alter the phalangeal alignment and breakover point, but improper application can cause abnormal pressure distribution and increased strain on flexor tendons or the suspensory apparatus (Hagen et al., 2017; Hinterhofer et al., 2000).

Improper trimming practices, such as leaving long toes or underrun heels, shift the center of pressure cranially, leading to increased tension on the deep digital flexor tendon and navicular bone (Eliashar et al., 2004; Alves et al., 2023). This compensatory biomechanical loading has been implicated in the development of navicular syndrome, toe cracks, and other chronic lameness conditions (Parks, 2012). Moreover, when medial-lateral balance is not maintained through balanced trimming, horses often exhibit uneven hoof loading and abnormal ground reaction forces, which predispose them to soft tissue injuries and joint disease (van Heel et al., 2005; Nicolai et al., 2017).

In performance horses, shoe selection must also consider ground surface interactions. Horan et al. (2024) demonstrated that certain shoe and surface combinations can either excessively increase or insufficiently dampen hoof impact acceleration, altering gait kinematics and increasing the risk of injury. Composite shoes, which offer more flexibility than steel, may reduce impact concussions while allowing partial heel deformation, making them suitable for horses with sensitive feet or recovering from injury (Burns, 2020).

In Summary, shoeing profoundly influences hoof biomechanics, and the selection of shoe type, material, and trimming technique must be tailored to the horse's conformation, discipline, and medical history. Veterinary-farrier collaboration, guided by contemporary evidence and clinical findings, remains essential in optimizing hoof function and preventing lameness.

2.4 Previous Research on Nail-On vs. Glue-On Shoes

A growing body of literature has evaluated the biomechanical consequences of different shoeing methods, particularly focusing on traditional nail-on versus glue-on horseshoes. Nail-on shoes, while offering reliable fixation and longevity, have been consistently associated with reduced heel expansion and restricted hoof deformation compared to unshod or minimally shod hooves (Yoshihara et al., 2010; Roepstorff et al., 2001). In contrast, glue-on shoes, particularly those with flexible cuff or composite bases, have shown the potential to preserve more natural hoof movement by reducing mechanical restriction of the hoof capsule.

In a comparative kinematic study, Yoshihara et al. (2010) investigated the effects of shoe type on heel expansion in Thoroughbred horses using a within-subject crossover design. Each horse underwent gait analysis under three different conditions: barefoot, shod with standard nailed-on aluminum racing plates, and shod with glue-on aluminum shoes. While the specific brand of glue-on shoes was not disclosed, they were fabricated with similar aluminum alloy dimensions as the nailed-on variants and affixed using acrylic adhesive compounds common in racetrack practice.

The horses were trotted and walked over a flat asphalt surface, and high-speed digital video recording (250 frames per second) captured motion data from reflective markers placed on the heels. The researchers measured maximum heel expansion during stance phase by comparing the mediolateral displacement between markers at the time of maximum loading. The barefoot condition demonstrated the highest degree of heel expansion, followed by the glue-on shoe condition, while nailed-on shoes significantly restricted caudal hoof deformation. The disparity was most evident at the trot, correlating with higher peak ground reaction forces. The study concluded that traditional nailed-on shoes reduce natural heel mobility, which may alter internal hoof mechanics and impact vascular and shock-absorbing function over time.

Expanding on this work, Takahashi et al. (2022) evaluated two commercially available glue-on horseshoes—Siga Polyflex® and Shufit®—in comparison to nailed-on aluminum shoes in Thoroughbreds at walk and trot. The shoes were applied according to manufacturer guidelines: Polyflex shoes were heat-molded and applied with urethane-based adhesives, while Shufit shoes used a pre-molded design fixed with two-part epoxy. Digital motion capture and pressure mat systems recorded heel displacement and surface pressures during midstance and propulsion.

The results showed that both glue-on shoes allowed for significantly greater heel expansion than nailed shoes, particularly at trot, with Polyflex shoes demonstrating the most favorable deformation profile, closely mimicking barefoot hoof behavior. The nailed-on shoes once again exhibited the most restrictive effect on heel movement, confirming previous findings. Furthermore, the authors highlighted that heel displacement was more symmetric in glue-on groups, which may enhance load distribution and proprioceptive feedback during motion.

These studies underscore the importance of shoe type and application technique in preserving natural hoof mechanics. Glue-on shoes, by reducing mechanical restriction at the heel quarters, support physiological expansion, which is critical for circulation, shock absorption, and laminar health. The implications are especially relevant in horses predisposed to underrun heels, digital cushion atrophy, or chronic caudal hoof pathologies

In a controlled biomechanical study, Brunsting et al. (2019) investigated the effects of shoe design on heel expansion and hoof deformation by comparing traditional open-heel nailed steel shoes, a novel split-toe shoe, and barefoot conditions in sound Warmblood horses. The split-toe shoe featured a sagittal cut at the toe, allowing for independent movement of the medial and lateral branches at the heels. Using high-resolution motion capture systems and a pressure plate (Footscan® RSscan International), the researchers evaluated heel expansion, mediolateral independence, stance duration, and breakover symmetry during walk and trot on a flat asphalt surface. The findings demonstrated that barefoot horses exhibited the greatest heel expansion, serving as the physiological benchmark. However, the split-toe shoe preserved significantly more heel movement than conventional nailed shoes ($p < 0.05$), particularly in the lateral quarters, and more closely mimicked natural hoof deformation patterns. In contrast, traditional open-heel shoes substantially restricted mediolateral deformation, limiting the hoof's adaptive response to ground contact. Importantly, the split-toe shoe allowed for improved mediolateral independence and more symmetric breakover patterns, features believed to support natural shock absorption and circulation within the hoof capsule. While the study did not directly assess long-term clinical outcomes, the authors highlighted the clinical relevance of maintaining heel mobility, particularly in horses prone to caudal heel pain, frog atrophy, or underrun heels. The findings support the use of alternative shoeing designs that emulate barefoot mechanics and suggest that shoe architecture plays a pivotal role in preserving biomechanical function and preventing hoof pathology.

Glue-on shoes, especially those made from flexible or polymer-based materials, offer notable biomechanical benefits. Aoun et al. (2023) studied the effects of different shoe configurations (open-heel, egg-bar, and heart-bar heart-bar included) on the motion of the third phalanx (P3) and hoof capsule deformation using cadaveric forelimbs from normal and laminitic horses. Limbs were compressed in situ (up to 5.5 kN), and motion-capture markers on P3 and the hoof wall tracked displacement. Results showed that egg-bar and heart-bar shoes significantly reduced P3 motion and hoof wall deformation compared to open-heel and barefoot conditions, restoring internal architecture—particularly in laminitic hooves. This finding highlights the clinical utility of glue-on polymer shoes in stabilizing P3 and reducing stress on lamellar structures.

In a performance-focused study, Horan et al. (2022) assessed hoof impact and foot-off accelerations in retired Thoroughbred racehorses under four shoe conditions—aluminum racing plates, steel shoes, GluShu® (aluminum–rubber composite glued on), and barefoot—across turf and artificial (Martin Collins Activ-Track) surfaces. Using tri-axial hoof-mounted accelerometers (5,000 Hz sampling), they analyzed over 40,000 strides per hoof. Data showed that GluShu® shoes reduced peak impact accelerations compared to steel and aluminum, while barefoot conditions yielded the lowest accelerations. Impact forces were highest on turf. The GluShu® condition offered a middle ground, providing protection with improved shock mitigation. Particularly valuable for racing safety and musculoskeletal health.

The clinical implications are significant: polymer glue-on shoes protect lame or compromised hooves while reducing focal pressure peaks and absorbed vibrational energy, which can contribute to repetitive strain injuries. Furthermore, as note, the glue-on method minimizes nail-induced trauma to the hoof wall which is essential in managing thin-walled, flare-prone, or white-line disease cases. (Floyd & Mansmann 2007)

Further biomechanical investigations by Thomason et al. (2010) and McClinchey et al. (2003) have demonstrated how the type and material of shoeing significantly influence the mechanical behavior of the equine hoof. Using finite element modeling, McClinchey and colleagues simulated the effects of various hoof shape measurements such as hoof wall angle and heel height on capsule strain. Their results indicated that variations in hoof geometry alone could cause substantial changes in the stress distribution across the hoof capsule, even before shoeing was considered. This foundational work set the stage for deeper inquiry into the effects of external modifications like shoes.

Building upon this, Thomason et al. (2010) employed a combined in vivo and modeling approach, integrating real-time strain gauge data with finite element analysis to assess the stress and strain profiles of the hoof under load. Their work specifically compared shod versus unshod hooves and showed that conventional nailed metal shoes constrained the natural expansion of the heel and shifted strain concentrations toward the quarters and heels. This mechanical constraint was associated with increased risk of chronic stress injuries and diminished shock absorption capability, particularly during high-impact locomotion.

Moreover, both studies emphasized that materials with higher stiffness such as steel or aluminum, disrupted the hoof's natural viscoelastic deformation, reducing its ability to dissipate concussive forces. These findings collectively underscore the critical need to consider not only the protective role of horseshoes but also their influence on internal biomechanical behavior. Modern therapeutic and performance-oriented shoeing techniques should therefore aim to preserve or mimic natural hoof deformation as much as possible while delivering traction and protection, especially in athletic horses.

2.5 Limitations of Previous Studies and the Justification for This Research

Despite the valuable insights gained from these previous investigations, several methodological limitations persist across studies comparing nail-on and glue-on shoeing systems. Many of these trials have small sample sizes, often involving fewer than 20 horses, which limits statistical power and generalizability. For instance, the Yoshihara et al. (2010) and Takahashi et al. (2022) studies each included 10–15 horses, all Thoroughbreds, which narrows applicability to other breeds or disciplines.

Another notable limitation is the lack of long-term follow-up. Most studies assess hoof mechanics over short timeframes (single sessions or a few weeks), without evaluating chronic effects on hoof health, structural remodeling, or incidence of lameness. Furthermore, data are frequently collected under controlled laboratory conditions or limited to walk and trot speeds, thereby excluding the dynamic impact of higher-intensity exercise (Horan et al., 2024).

Few studies incorporate objective kinetic and kinematic analyses such as pressure plate data, accelerometry, or high-speed motion capture which could be essential for understanding subtle biomechanical changes. Additionally, the role of individual hoof conformation, age, work type, and terrain is often underreported or not controlled for, despite being critical confounders in hoof-related studies (Back & Clayton, 2013; Alves et al., 2023).

There is also a significant gap in evaluating the physiological implications of shoeing methods, including perfusion metrics (as explored by Mieszkowska et al., 2023) and laminar stress under load (Senderska-

Płonowska et al., 2020). The biomechanical efficacy of shoe types in pathologic conditions such as laminitis or navicular disease has only recently begun to be explored (Aoun et al., 2023).

The present study aimed to address some of these limitations. Specifically, our study included a broader breed representation, used a consistent experimental model across variable surfaces, and used a modern sensor technology capable of providing a quantifiable comparison of heel movement between shoeing methods. This work contributes meaningfully to the optimization of evidence-based farriery practices by addressing critical gaps in the current literature and emphasizing the biomechanical relevance of shoe design in maintaining hoof health and long-term performance. By comparing the effects of different shoeing techniques on hoof deformation and expansion, the study enhances our understanding of how various materials and methods can either support or compromise the natural hoof mechanism.

Additionallly, this research establishes a foundational reference for the validation of the sensor technology employed, serving as a pilot study for more comprehensive investigations. Future directions include expanding shoe type comparisons and exploring how shoeing interventions influence hoof biomechanics in horses with underlying pathologic conditions, such as laminitis, navicular syndrome, or underrun heels as well as potential differences in weight bearing and heel expansion in horses that present more proximal sources of lameness. These findings may ultimately support the development of therapeutic farriery protocols tailored to individual biomechanical and clinical needs.

Chapter 3: Manuscript/ Research project

Title: Comparative Study of Heel Movement and Foot Biomechanics in Aluminum Nail-On and Indirect Glue-On Fabric Cuff Shoes in Horses

Background: Heel movement is a critical component of the equine hoof mechanism, contributing to shock absorption and vascular perfusion. Conventional horseshoeing techniques, particularly metal shoes, have been suspected to restrict natural hoof deformation, potentially affecting hoof biomechanics and soundness. While several studies have explored the effects of shoeing on hoof function, many have been limited to treadmill conditions, cadaver limbs, or homogenous populations such as racing Thoroughbreds.

Objective: This study aimed to compare the effects of two aluminum shoeing techniques (nail-on shoes versus indirect glue-on fabric cuff shoes) on heel movement in horses of various breeds and disciplines. The objective was to determine which shoeing technique allowed greater heel movement and how both methods compare to barefoot conditions in both hard footing (asphalt) as well as soft footing (arena).

Study design: A controlled experimental study using a repeated-measures design to assess heel movement across three conditions (indirect fabric cuff aluminum glue-on shoe/ barefoot/ nail on aluminum open heel shoe.)

Methods: Fifteen healthy horses underwent three conditions: barefoot, aluminum nail-on shoes, and indirect glue-on fabric cuff shoes. A displacement sensor (Linear displacement sensors LDR-25-SA Inductive displacement sensor Micro-Epsilon, USA) was affixed to the heels of one forelimb to measure total heel displacement during locomotion. Measurements were taken over 20 strides at both walk and trot across all conditions. Data was analyzed using mixed-model ANOVA to determine differences in heel movement among the three groups.

Results: Heel movement was significantly greater in barefoot horses compared to both shoeing conditions ($P < 0.0001$). Glue-on shoes restricted heel movement less than nail-on shoes at the trot, but no significant difference was found between the two shoe types at the walk These findings confirm that both shoeing techniques reduce natural heel movement, with glue-on shoes allowing slightly more movement than nail-on shoes.

Main Limitations: One limitation was the lack of an absolute zero baseline measurement, preventing differentiation between heel expansion and contraction during locomotion. Additionally, due to low heel conformation in some horses, recordings on soft arena footing could not be obtained for all subjects, reducing the statistical power for that condition.

Conclusions: This study reinforces previous findings that shoeing restricts heel movement compared to barefoot conditions. While indirect glue-on shoes allow for more heel movement than traditional nail-on shoes at the trot, both techniques limit the hoof mechanism to some extent. Further research is needed to explore additional materials and techniques that could better preserve natural hoof biomechanics, as well as to evaluate therapeutic applications where restricting hoof deformation may be beneficial.

Keywords: equine biomechanics, hoof mechanism, heel expansion, shoeing techniques, glue-on shoes, nail-on shoes, barefoot horses, equine podiatry.

3.1 Introduction

Equine hoof deformation during locomotion is a critical component of the hoof mechanism, significantly contributing to shock absorption, vascular perfusion, and overall limb health (Dyhre-Poulsen et al., 1994; Floyd & Mansmann, 2007; Back & Clayton, 2013). Heel expansion and contraction, a key aspect of this mechanism, facilitates energy dissipation and circulation within the hoof, thus playing an essential role in maintaining soundness and performance in horses (Eliashar et al., 2004; Shahkhosravi et al., 2023; van Heel et al., 2005). However, concerns persist within the veterinary and farrier communities regarding the potential restriction of natural hoof deformation caused by conventional shoeing techniques, particularly those employing metal shoes (Roepstorff et al., 2001; Senderska-Płonowska et al., 2020; Aoun & Takawira, 2024).

Previous research has investigated the biomechanical implications of various shoeing methods, including aluminum nail-on and indirect glue-on shoes. These studies have produced mixed findings and have often been limited by methodological constraints, such as the exclusive use of cadaver limbs (Déjardin et al., 1999; Thomason et al., 2010; McClinchey et al., 2003), evaluations conducted solely on treadmill surfaces (Yoshihara et al., 2010; Takahashi et al., 2022), or studies restricted to specific breeds and disciplines, predominantly Thoroughbreds (Horan et al., 2022; Bardin et al., 2022; Hampson & Pollitt, 2011).

Heel movement is influenced significantly by hoof conformation and trimming practices (Poochipakorn et al., 2024; Hagen et al., 2017), as well as the choice of shoeing materials and techniques (Brunsting et al., 2019; Moeller et al., 2019). For instance, aluminum nail-on shoes, despite their widespread use due to ease of application and durability, have been associated with restricted heel movement when compared to barefoot conditions (Hinterhofer et al., 2000; Nicolai et al., 2017). Similarly, indirect glue-on shoes, although developed to minimize interference with natural hoof biomechanics, have shown variable effects on hoof deformation in preliminary studies (Takahashi et al., 2022; Burns, 2020).

This study aimed to address some of these methodological limitations and gaps in existing literature by comparatively evaluating the effects of aluminum nail-on shoes and commercial fabric-cuff indirect glue-on shoes on heel movement and overall hoof biomechanics in realistic conditions. Using in vivo displacement sensor technology (Davies, 2010; Pietra et al., 2004), this research objectively measures heel movement across different conditions (barefoot, aluminum nail-on shoes, and indirect glue-on shoes) on soft arena footing typical of equine performance environments as well as asphalt for a hard ground which is typical for lameness examinations under usual clinical circumstances. (Reilly et al., 2024; Alves et al., 2023). The standing hypothesis was that both shoeing techniques would restrict heel movement compared to barefoot conditions. Additionally, because of the rigid fabric cuff/glue combination that covers the entire hoof wall, we hypothesize that these shoes would restrict movement to a greater degree than the open heel aluminum nail on shoe.

Findings from this comparative study will provide practical, evidence-based guidance for veterinarians and farriers (Parks, 2012; Ross & Dyson, 2011), assisting in informed decision-making regarding shoeing techniques for both performance horses and therapeutic applications. Ultimately, these insights will contribute to improved equine limb health and optimal athletic performance, as well as support the development of shoeing techniques designed to enhance or strategically limit hoof movement based on specific therapeutic needs.

3.2 Materials and Methods

Fifteen healthy adult horses currently engaged in regular work were included in this study. The horses represented various breeds and disciplines to ensure a diverse and broadly applicable sample population (Table 1). Prior to inclusion, all horses underwent comprehensive physical, orthopedic, and lameness examinations performed by experienced veterinarians, including specialists board-certified by the American College of Veterinary Sports Medicine and Rehabilitation, the American College of Veterinary Surgeons, or the American Board of Veterinary Practitioners (Equine Specialty). These examinations included hoof tester evaluations and subjective gait assessments. Hoof trimming was performed based on visual assessment from the farrier to balance the hoof in a medial-lateral plane as well as the dorso-palmar plane. This procedure was performed in all 15 subjects by the same experienced farrier who has Certified Journeyman Farrier and Fellow of the Worshipful Company of Farriers qualifications. Exclusion criteria included horses with systemic illness, significant forelimb lameness (greater than grade 2/5 on the AAEP scale), notable hoof or limb abnormalities, or positive hoof tester responses. One horse that presented for the study was excluded due to a baseline 3/5 fore limb lameness.

Animals	Breed	Age	Discipline
Subject #1	American Paint Horse	20	Trail riding
Subject #2	American Quarter Horse	24	Trail riding
Subject #3	Holsteiner	14	Hunter jumper/ lesson horse
Subject #4	American sport pony	20	Hunter jumper/ lesson horse
Subject #5	Thoroughbred	17	Eventing/ Dressage
Subject #6	American Quarter Horse	12	Trail riding
Subject # 7	American Quarter Horse	25	Western pleasure/ lesson horse.
Subject#8	Mixed breed sport horse	20	Hunter jumper/ lesson horse
Subject #9	Mixed breed	10	Dressage
Subject #10	American Paint horse	19	Lesson horse (flat small jumps)
Subject # 11	Foreign Warmblood	20	Hunter jumper/ lesson horse
Subject #12	American Quarter Horse	13	Western Pleasure horse
Subject #13	American Quarter Horse	9	Lesson horse
Subject #14	Foreign Warmblood	16	Hunter jumper/ lesson horse
Subject # 15	Thoroughbred	15	Hunter jumper/ lesson horse

Table 1: List of subjects by age, breed and discipline

Study Design and Experimental Approach

Each horse was evaluated under three shoeing conditions: barefoot (unshod), aluminum open-heel nail-on shoes (Kerckhaert Aluminum Comfort Horseshoes from Kerckhaert Horseshoe Royal Horseshoe Factroy Rapenburg 76 4581 AE Vogelwaarde Nederland), and commercial indirect glue-on shoes with a fabric cuff (SoundHorse Technologies Series 1™, SoundHorse Technologies, Lexington Kentucky, USA) attached using polymethyl-methacrylate acrylic adhesive (Equilox I™, Equilox International, USA). An LDR-25-SA Inductive displacement sensor (Micro-Epsilon, Raleigh, North Carolina, USA) was secured at the base of the heel bulbs on the left forelimb for all the horses using urethane adhesive (SuperFast™, Vettec Animal Health, USA), and the associated transmitter was securely attached to the horse by placing a surcingle/saddle pad with 2 side pockets that carried both the transmitter as well as the windows tablet (Vanquisher 8-Inch Industrial Rugged Tablet PC, Windows 10 Pro 64-bit | 7800mAH Battery | GPS GNSS | 4G LTE| Drop Resistant, for Enterprise Field Mobility) containing Indu sensor software (included with Micro-Epsilon displacement sensor) as the horse was walked and trotted on hand under the different conditions. (Picture 1: Equipment setup).

Picture group 1: Equipment setup

The displacement sensor measured heel movement in millimeters across 20 strides at both the walk and trot. Measurements were taken under each shoeing condition and on both hard ground (asphalt) and soft ground (arena footing.) Due to potential interference with the sensor from the glue on shoe application process, the indirect glue-on shoes were applied before the displacement sensor. The order of treatments was glue on shoes, barefoot, then nail on shoes. No additional trimming or farrier work was done between treatments. Each horse underwent testing sequentially in the same order of conditions to maintain sensor integrity and measurement consistency.

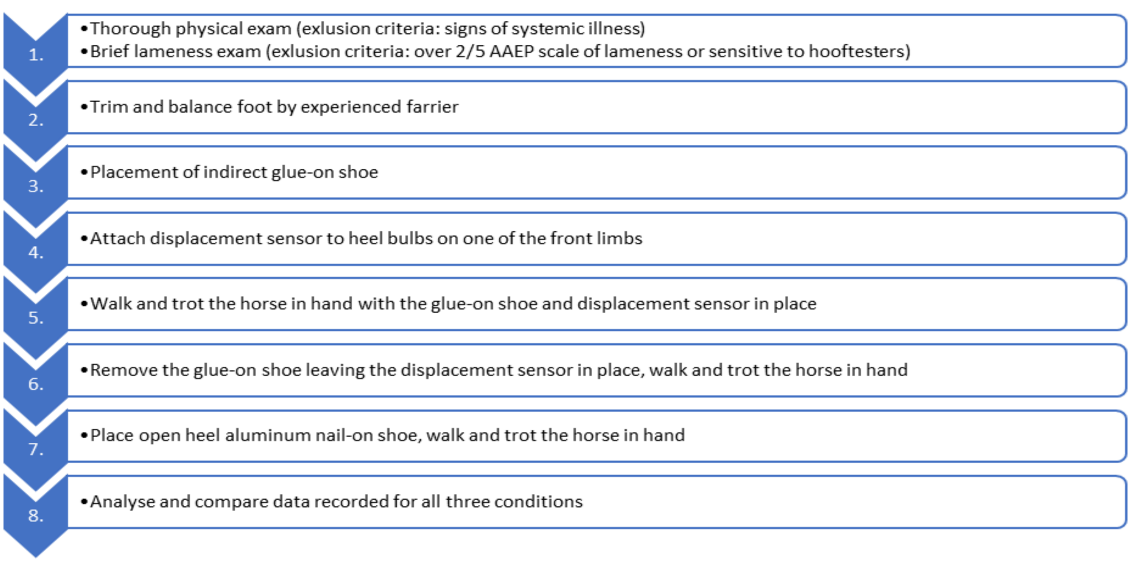

Figure 1: Illustrated methodology showing step by set experimental design.

Data Analysis

Data from the displacement sensor were transmitted to a tablet and analyzed using specialized software (Indu sensor tool that was included with the Micro-Epsilon displacement sensor purchase) to determine heel movement. A Python/Jupiter code was written by the department of biomedical sciences in order to clean the raw data and extract key values for statistical analysis. (Key values= maximum/ minimum measurements in mm to obtain total displacement per condition over the 20 plus-stride recording.) Normal probability plots showed that all outcomes followed an approximately normal distribution. Subsequently, data were summarized as mean ± standard deviation. Heel movement data across the three shoeing conditions (barefoot, aluminum nail-on shoes, indirect glue-on shoes) were compared statistically using mixed-model ANOVA followed by Tukey's procedure for multiple comparisons. Statistical significance was set at $P<0.05$. Normal probability plots and ANOVA analyses were performed using SAS version 9.4 (Cary, NC, USA).

3.3 Results

Heel movement varied significantly on the asphalt across the three conditions: barefoot, aluminum nail-on shoes, and indirect glue-on shoes. The mixed-model ANOVA showed a significant effect of shoeing condition on total heel displacement ($P < 0.0001$). Horses in barefoot conditions exhibited the greatest heel movement at both the walk and trot, whereas horses wearing aluminum nail-on and glue-on shoes had less movement compared to barefoot conditions. (Figure 2). Mean heel displacement (±SD) for the walk phase on hard ground (asphalt); was highest in barefoot horses (3.03 ± 0.67 mm), followed by glue-on shoes (2.23 ± 0.58 mm), and was lowest in aluminum nail-on shoes (1.96 ± 0.48 mm). Similarly, at the trot, mean heel movement was greatest in barefoot horses (3.29 ± 0.62 mm), followed by glue-on shoes (2.56 ± 0.55 mm), with the lowest displacement observed in aluminum nail-on shoes (2.12 ± 0.47 mm).

Pairwise comparisons (Tukey-Kramer adjustment) demonstrated significant differences between barefoot and both shoeing conditions ($P < 0.0001$). Glue-on shoes also restricted heel movement significantly more than barefoot conditions ($P < 0.0001$), but less than aluminum nail-on shoes ($P = 0.0005$).

On soft arena footing (Figure 3), heel movement followed a similar trend to the asphalt surface, with the greatest displacement observed in the barefoot condition and the least movement observed with glue-on shoes. However, the mixed-model ANOVA did not detect a statistically significant effect of shoeing condition on total heel displacement.

A separate mixed-model ANOVA (Figure 4) evaluating the effect of surface type (asphalt vs arena footing) revealed a statistically significant difference in heel movement across all conditions ($P = 0.0099$), with greater displacement observed on asphalt.

On average, horses exhibited more heel movement on asphalt at both the walk (4.03 ± 1.27 mm) and trot (3.87 ± 1.68 mm) compared to soft footing surface (walk: 2.71 ± 1.26 mm; trot: 2.66 ± 1.56 mm). While post-hoc comparisons between surfaces at each gait did not reach statistical significance after adjustment (adjusted $P > 0.05$), the asphalt condition was associated with numerically greater heel expansion than the arena footing across both gaits.

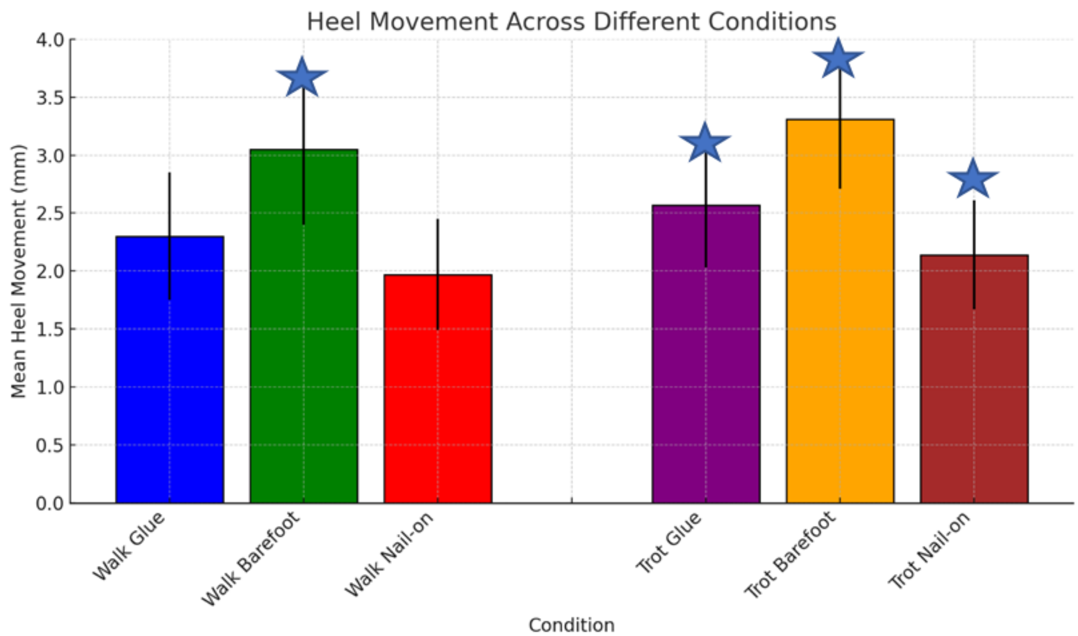

Figure 2: Asphalt ANOVA results: The Y Axis shows the distance of heel movement in mm. The first 3 columns represent walking conditions on asphalt and the last 3 columns represent trotting conditions on asphalt. The only comparison that did not reach statistical significant difference was the walk on glue vs the walk on nail-on. All other mixed comparisons within the mixed Anova were statistically significant.

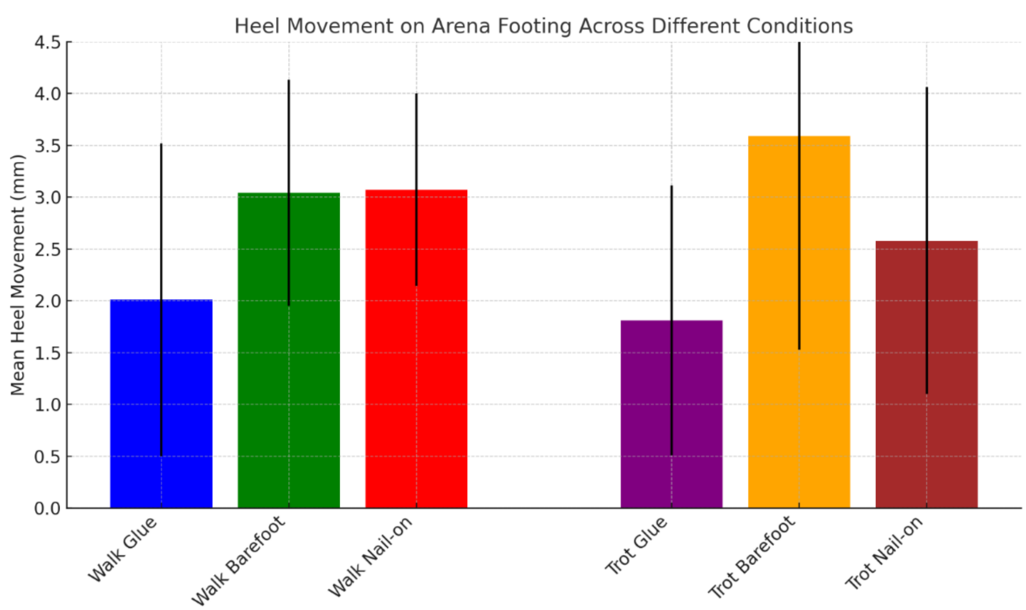

Figure 3: Footing ANOVA results: These findings show a similar trend to the asphalt regarding heel movement (barefoot>Glue>Nail-on) yet none reached statistical significance on the soft footing.

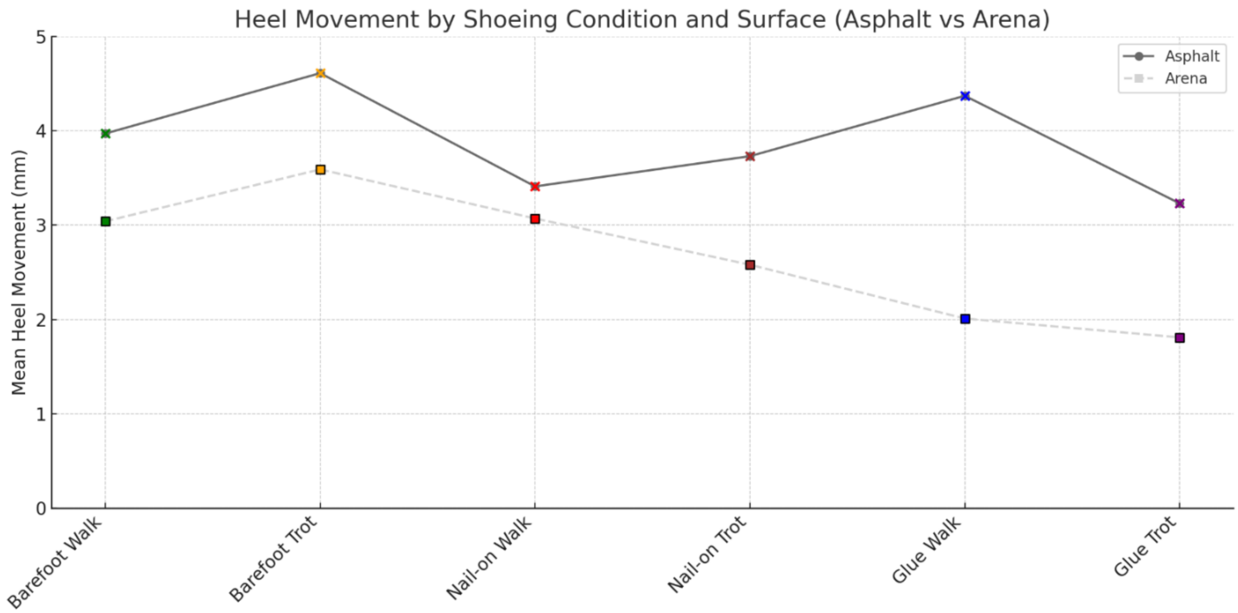

Figure 4: Asphalt vs Footing comparative results show a greater heel movement on asphalt vs soft footing.

3.4 Discussion

The findings of this study contribute to the growing body of literature investigating the biomechanical effects of shoeing on equine heel movement and hoof deformation. Previous studies have demonstrated that shoeing alters hoof expansion and contraction, potentially impacting shock absorption and vascular perfusion (Dyhre-Poulsen et al., 1994; Eliashar et al., 2004; Hampson & Pollitt, 2011). Consistent with existing research, our data confirmed that both aluminum nail-on and indirect glue-on shoes significantly restricted heel movement compared to barefoot conditions (Roepstorff et al., 2001; Senderska-Płonowska et al., 2020; Aoun & Takawira, 2024). However, a clear gradient in restriction was observed: barefoot horses exhibited the greatest displacement, followed by glue-on shoes, with nail-on shoes producing the most limited movement, particularly on hard ground and at the trot. These results suggest that while all forms of shoeing reduce heel expansion to some degree, the method of application exerts a meaningful influence on hoof biomechanics, independent of shoe material.

One possible explanation for the greater movement permitted by glue-on shoes lies in the nature of their attachment. Unlike nail-on shoes, which rigidly affix the shoe to the hoof wall via direct penetration, the indirect glue-on system used in this study adhered a fabric cuff to the dorsal and lateral hoof wall without mechanically anchoring the quarters or heels. This design may allow for more flexibility in the caudal hoof region, preserving a degree of natural movement (Takahashi et al., 2022; Senderska-Płonowska et al., 2020).

Interestingly, although glue-on shoes allowed significantly more heel movement than nail-on shoes at the trot, this difference was not statistically significant at the walk, suggesting a potential interaction between gait dynamics and shoe application method. At slower speeds, passive deformation may play a more prominent role, rendering the adhesive interface less restrictive; in contrast, the increased ground reaction forces and shorter stance duration at the trot may amplify the mechanical constraints imposed by shoe type (Dyhre-Poulsen et al., 1994; Yoshihara et al., 2010; Back & Clayton, 2013). Gait consistently influenced heel displacement across all shoeing conditions, with greater expansion observed at the trot. This supports earlier findings that dynamic loading increases strain within the hoof capsule (Thomason et al., 2010). However, the absolute heel movement values observed in our study were slightly lower than those reported using radiographic or in vivo strain mapping techniques (Brunsting et al., 2019; Déjardin et al., 1999), likely due to methodological differences; our external digital tracking system may have underestimated subtle internal deformations. Additional variability in trimming, breed, conformation and speed may also contribute to differences in baseline movement thresholds (Poochipakorn et al., 2024; Shahkhosravi et al., 2023).

In addition to shoeing type, this study evaluated the influence of ground surface on heel mechanics. While surface was not a statistically significant main effect in the arena setting, a consistent trend was observed across both gaits: horses exhibited greater heel displacement on asphalt compared to arena footing, with this difference reaching statistical significance when data from both gaits and all shoeing types were combined. This supports previous findings that firmer substrates produce greater hoof deformation due to higher peak ground reaction forces and reduced energy absorption by the surface (Reilly et al., 2024; Bardin et al., 2022; Horan et al., 2024). On arena footing, glue-on shoes resulted in numerically lower heel displacement than nail-on shoes at both gaits, reversing the pattern seen on asphalt. This could suggest that the adhesive interface of glue-on shoes interacts differently with softer ground, potentially altering stress distribution or the timing of deformation (Hagen et al., 2017; van Heel et al., 2005). Another possible explanation for this phenomenon could be that the soft footing may not cause enough ground force reaction to cause a significant heel expansion and therefore the overall movement appreciated under this condition could potentially be just the contraction that happens during breakover and flight phase of the stride. Nevertheless, is important to highlight that one of the limitations of this study was a significant loss in statistical power regarding the footing data due to the inability to obtain measurements for all 15 horses in arena footing due to low heel conformation and disruption of sensor placement in the soft ground. Though speculative, these findings highlight the importance of context-specific interpretation when selecting shoeing techniques for horses in different environments.

The variability observed across gaits and surfaces reinforces the clinical relevance of shoeing decisions in sport and rehabilitation contexts. For example, in horses predisposed to heel collapse or chronic underrun heels, even small restrictions in movement—such as those imposed by rigid nail-on shoes—may compound over time and exacerbate existing conformational challenges (Poochipakorn et al., 2024; Shahkhosravi et al., 2023). Conversely, therapeutic scenarios such as laminitis, quarter cracks, or coffin bone instability may benefit from reduced deformation and increased mechanical stabilization (Parks, 2012; Ross & Dyson, 2011).

This study is further strengthened by its inclusion of a diverse population of horses representing multiple breeds, conformational types, and disciplines. This enhances the external validity of our findings, in contrast to many prior studies focused narrowly on Thoroughbreds or racing stock (Horan et al., 2022;

Bardin et al., 2022). Such diversity introduces real-world variability but also allows for broader clinical application in sport and leisure horses, many of which present with distinct biomechanical and conformational profiles (Alves et al., 2023; Hagen et al., 2017).

Finally, by comparing two aluminum shoe types rather than contrasting metal versus non-metal shoes, this study isolates the biomechanical impact of application method. Our findings suggest that glue-on shoes may offer a biomechanically favorable compromise by reducing hoof deformation less than traditional nail-on shoes while still offering mechanical protection. Although, it is also important to highlight the fact that by not being able to obtain a baseline measurement during this study, we were unable to differentiate between heel contraction and heel expansion. This leaves the question of how much of the total heel movement in each condition is due to contraction of the heels with the different shoeing techniques. Future work should explore additional shoe configurations, including composite materials, hybrid techniques, or more flexible adhesives, to determine whether these alternatives can better replicate barefoot biomechanics while meeting therapeutic or performance demands (Brunsting et al., 2019; Aoun et al., 2023; Takahashi et al., 2022).

Taken together, these results underscore the multifactorial nature of hoof biomechanics, highlighting how shoe application method, gait, and surface interact to influence heel deformation. The observed difference between glue-on and nail-on shoes—despite identical material composition—emphasizes that the mechanical interface between shoe and hoof wall can significantly alter hoof mechanics. Specifically, the more flexible, non-penetrative nature of glue-on cuffs may preserve partial expansion, particularly during slower gaits where passive deformation dominates. At the trot, where stance duration is shorter and ground reaction forces increase, these mechanical differences become more pronounced resulting in statistically significant reductions in heel movement under nail-on shoes. Notably, the absolute values of heel expansion in this study were lower than those reported in fluoroscopic or in vivo strain-based studies (e.g., Brunsting et al., 2019; Thomason et al., 2010), which likely reflects differences in measurement technique (external digital markers vs. internal strain mapping), hoof conformation, or surface compliance. Additionally, most previous in vivo studies have been done on thoroughbred racehorses at full speed which could potentially explain the significant difference in displacement compared to our study where horses were only trotted in hand and the gallop was not included in our results. These comparisons emphasize the importance of methodological transparency and caution against overgeneralizing displacement thresholds across studies. Ultimately, the nuanced differences observed here reinforce the need for individualized farriery strategies tailored not only to pathology and conformation, but also to workload, gait demands, and environmental footing.

Clinical and therapeutic implications

While maximizing heel movement is often desirable for shock absorption and circulation, there are clinical situations where limiting natural hoof expansion may be beneficial. Therapeutic shoeing aims to provide mechanical stabilization for certain conditions, such as coffin bone fractures, severe hoof cracks, and laminitis, where excessive hoof deformation could exacerbate the pathology (Parks, 2012; Ross & Dyson, 2011). In these cases, materials and techniques that restrict heel movement may play a vital role in pain management and rehabilitation. Future studies should investigate which combinations of materials and applications offer the optimal balance between hoof stability and function, particularly in therapeutic settings (Aoun et al., 2023; Hagen et al., 2021).

Study limitations and future directions

One major limitation is the inability to establish an absolute zero or baseline measurement of heel movement. Our methodology allowed us to measure total heel displacement but did not differentiate between heel expansion and contraction during locomotion. This limitation has been highlighted in previous research, where measurement techniques such as optical tracking and Doppler ultrasound have struggled to capture absolute baseline hoof movement (Mieszkowska et al., 2023; Alves et al., 2023). Future studies may incorporate high-speed motion analysis or pressure plate technology to address this gap (Hinterhofer et al., 2000; Hagen et al., 2021).

Another limitation of our study was the inability to obtain recordings on soft arena footing for some horses due to low heel conformation, which placed the displacement sensor in close proximity to the ground resulting in interference with the sensor. This issue reduced the statistical power for measurements taken on soft footing, as certain datasets could not be included in the final analysis. Previous studies have encountered similar challenges when measuring hoof deformation in horses with low heel conformation (McClinchey et al., 2003; Nicolai et al., 2017), suggesting that additional adaptations to sensor placement or alternative measurement techniques may be necessary. As the interaction between shoe type and surface becomes increasingly relevant in both sport and clinical settings, more refined techniques for accurately capturing deformation under variable ground conditions are warranted (Chateau et al., 2013; Hagen et al., 2021).

4. Conclusion and future directions

Overall, our findings support the current understanding of hoof biomechanics and effects of shoeing while also emphasizing the need for further research to refine measurement methodologies and explore alternative shoeing techniques that better preserve natural hoof function (Parks, 2012; Ross & Dyson, 2011). The first hypothesis, that the barefoot condition would result in the greatest heel movement, was confirmed by the data. However, the second hypothesis in which we expected the fabric cuff glue on to be more restrictive of heel movement than the nail on shoeing technique was not supported. It was initially expected that the glue-on shoe would allow less heel movement than the nail-on shoe due to the increased area coverage of the hoof wall in addition to the adhesive and fabric. Contrary to this expectation, the results showed a significant difference in movement between the nail-on and glue-on conditions on the asphalt, with the glue-on shoe being less restrictive to heel movement overall. This suggests that the method of attachment, rather than just the area of coverage, plays a more critical role in restricting heel movement. Nevertheless, it is also important to reiterate the limitations of the study and clarify that we were unable to differentiate between heel expansion vs contraction which leaves the question open. Do indirect glue-on shoes potentially allow more heel contraction while limiting expansion? Is that greater overall movement due to contracting effect on the heel bulbs rather than allowing more expansion like the unshod horse hoof mechanism?

Future studies should aim to answer these remaining questions by incorporating larger sample sizes, alternative measurement tools, and expanded testing across different surfaces to enhance the applicability of findings to diverse equine disciplines and clinical settings. Further research comparing additional materials and shoeing techniques will be essential in determining the most biomechanically favorable methods for both performance optimization and therapeutic intervention.

This thesis consolidates current knowledge on equine hoof anatomy and biomechanics, with an emphasis on how hoof conformation, shoeing techniques, and materials affect the functional integrity of the digit. Across the reviewed literature, there is overwhelming evidence that preserving the natural hoof mechanism, particularly heel expansion, sole deformation, and frog-ground contact, is fundamental to maintaining soundness and promoting long-term performance in horses. Multiple studies highlighted throughout the writing of this project have demonstrated how different horseshoe types and applications distinctly alter biomechanical parameters such as ground reaction forces, digital cushion compression, and navicular apparatus strain. Some materials like flexible polymers and glue-on shoes have been shown to better preserve heel expansion and reduce concussive loads when compared to traditional nailed metal shoes. These findings contribute valuable guidance to evidence-based farriery and raise critical questions regarding the long-term impact of restricting hoof dynamics.

While this research supports the broader effort to optimize hoof management through objective analysis, our pilot study was limited by a small sample size and methodological constraints inherent to the displacement sensor employed. Most notably, we were unable to definitively distinguish between heel expansion and contraction and instead measured heel movement in general terms. The sensor lacked the capacity to establish a clear zero-reference point, preventing accurate classification of the directionality of displacement. Nonetheless, this project represents a crucial first step in validating the potential of displacement sensors in live horses, and it lays the groundwork for more robust experimental designs in future work.

Going forward, future studies should not only incorporate larger and more diverse equine populations but also explore the use of therapeutic shoeing in conjunction with real-time biomechanical monitoring. For example, the same sensor system could be used to evaluate stabilization techniques in horses with pathological conditions such as coffin bone fractures, where restriction of natural hoof motion is intentionally sought. In this context, being able to measure displacement with high fidelity would help clinicians determine which methods best preserve hoof stability without compromising adjacent structures.

The scientific contributions gathered through this thesis, spanning decades of foundational and emerging research, serve to enrich the growing body of literature surrounding equine podiatry and biomechanics. However, continued investigation is necessary. Longitudinal retrospective studies examining heel movement and hoof conformation changes over time may offer meaningful insights into the long-term outcomes associated with specific shoeing techniques or materials. Such data could lead to stronger correlations between biomechanical dysfunction and the onset of pathology, ultimately improving our ability to match therapeutic and preventive shoeing strategies to individual equine patients. The goal is not only to optimize performance in elite athletes, but to enhance the welfare, longevity, and comfort of horses across all sectors of the industry. This thesis contributes a meaningful step in that direction. But it is only the beginning.

5. References

1. Shahkhosravi, N. A., Kakavand, R., Davies, H. M. S., & Komeili, A. (2023). The influence of equine hoof conformation on the initiation and progression of laminitis. Equine Veterinary Journal, 55(5), 862–871. https://doi.org/10.1111/evj.13887
2. Aoun, R., & Takawira, C. (2024). Horseshoe effects on equine gait. A systematic scoping review. Veterinary Surgery, 54(1). https://doi.org/10.1111/vsu.14162
3. Poochipakorn, K., Meesuk, S., & Viriyarampa, S. (2024). Effects of palmar hoof wall trimming on heel angles and hoof conformation in horses with underrun heels. Veterinary Sciences, 11(1). https://doi.org/10.3390/vetsci11010012
4. Reilly, P. T., Dyson, S. J., & van Heel, M. C. V. (2024). Influence of horseshoe design and ground surface on hoof orientation at mid-stance. Equine Veterinary Journal. https://doi.org/10.1111/evj.13950
5. Mieszkowska, M., Zabielski, R., & Davies, H. M. S. (2023). Doppler ultrasound evaluation of circulatory effects of egg-bar versus wedge-pad horseshoes in horses. Polish Journal of Veterinary Sciences. https://doi.org/10.24425/pjvs.2023.141234
6. Aoun, R., Stewart, S., & Takawira, C. (2023). Biomechanical efficacy of horseshoe types on normal and laminitic hooves under load. PLoS ONE, 18(7), e0287654. https://doi.org/10.1371/journal.pone.0287654
7. Horan, K., Roepstorff, L., Clayton, H., & Hobbs, S. (2024). Hoof-surface traction characteristics in galloping Thoroughbreds across shoe and track surface combinations. Veterinary Sciences, 11(2), 45. https://doi.org/10.3390/vetsci11020045
8. Horan, K., Coburn, A., Roepstorff, L., & Hobbs, S. J. (2022). Impact and toe-off accelerations in horses across various shoe–surface combinations. Animals, 12(10), 1266. https://doi.org/10.3390/ani12101266
9. Alves, E. G. L., Sampaio, R. C. L., Silva, R. A. G., & Dias, D. P. M. (2023). Hoof morphological parameters associated with lameness in riding horses. Animals, 13(3), 451. https://doi.org/10.3390/ani13030451
10. Eliashar, E., McGuigan, M. P., & Wilson, A. M. (2004). Relationship of foot conformation and force applied to the navicular bone of sound horses at the trot. Equine Veterinary Journal, 36(5), 431–435. https://doi.org/10.2746/0425164044877281
11. van Heel, M. C. V., Barneveld, A., van Weeren, P. R., & Back, W. (2005). Dynamic pressure measurements for the detailed study of hoof balance: The effect of trimming. Equine Veterinary Journal, 37(8), 778–782. https://doi.org/10.2746/042516405775314808
12. Hampson, B. A., & Pollitt, C. C. (2011). Comparison of the morphology of feral and domestic horse hooves. American Journal of Veterinary Research, 72(6), 648–655. https://doi.org/10.2460/ajvr.72.6.648
13. Parks, A. H. (2012). Therapeutic shoeing for horses: A veterinary perspective. Veterinary Clinics of North America: Equine Practice, 28(2), 333–350. https://doi.org/10.1016/j.cveq.2012.05.001
14. Roepstorff, L., Johnston, C., & Drevemo, S. (2001). The influence of shoeing on hoof deformation in horses. Equine Veterinary Journal Supplement, (33), 49–54. https://doi.org/10.1111/j.2042-3306.2001.tb05368.x
15. Dyhre-Poulsen, P., Smedegaard, H. H., Roed, J., & Korsgaard, E. (1994). Equine hoof function investigated by pressure transducers inside the hoof and accelerometers mounted on the first phalanx. Journal of Experimental Biology, 197(1), 189–209. https://doi.org/10.1242/jeb.197.1.189

16. Hinterhofer, C., Stanek, C., & Haider, H. (2000). The effect of flat horseshoes, raised heels, and lowered heels on hoof deformation. Journal of Veterinary Medicine Series A, 47(2), 73–82. https://doi.org/10.1046/j.1439-0442.2000.00270.x
17. Floyd, A. E., & Mansmann, R. A. (2007). Equine podiatry. Saunders Elsevier.
18. Yoshihara, E., Takahashi, T., Otsuka, N., Isayama, T., Tomiyama, T., Higara, A., & Wada, S. (2010). Heel movement in horses: Comparison between glued and nailed horse shoes at different speeds. Equine Veterinary Journal, 42, 431–435. https://doi.org/10.1111/j.2042-3306.2010.00243.x
19. Brunsting, J., Dumoulin, M., Oosterlinck, M., Haspeslagh, M., Lefère, L., & Pille, F. (2019). Can the hoof be shod without limiting the heel movement? A comparative study between barefoot, shoeing with conventional shoes and a split-toe shoe. The Veterinary Journal, 246, 7–11. https://doi.org/10.1016/j.tvjl.2019.01.012
20. Bardin, A. L., Taylor, N. C., & Robert Colborne, G. (2022). Response of the Thoroughbred forelimb to perturbations caused by a change in ground surface. Journal of Equine Veterinary Science, 112, 103897. https://doi.org/10.1016/j.jevs.2022.103897
21. Thomason, J. J., McClinchey, H. L., & Jofriet, J. C. (2010). Analysis of strain and stress in the equine hoof capsule using finite element methods: Comparison with principal strains recorded in vivo. Equine Veterinary Journal, 34(7), 719–725. https://doi.org/10.2746/042516402776250388
22. Senderska-Płonowska, M., Zielińska, P., Żak, A., & Stefaniak, T. (2020). Do metal shoes contract heels? A retrospective study on 114 horses. Journal of Equine Veterinary Science, 95, 103293. https://doi.org/10.1016/j.jevs.2020.103293
23. McClinchey, H. L., Jofriet, J. C., & Thomason, J. J. (2003). Isolating the effects of equine hoof shape measurements on capsule strain with finite element analysis. Veterinary and Comparative Orthopaedics and Traumatology, 16(2), 67–75. https://doi.org/10.1055/s-0038-1632762
24. Davies, H. M. S. (2010). Noninvasive photoelastic method to show distribution of strain in the hoof wall of a living horse. Equine Veterinary Journal, 29(S23), 13–15. https://doi.org/10.1111/j.2042-3306.1997.tb05043.x
25. Déjardin, L. M., Arnoczky, S. P., & Cloud, G. L. (1999). A method for determination of equine hoof strain patterns using photoelasticity: An in vitro study. Equine Veterinary Journal, 31(3), 232–237. https://doi.org/10.1111/j.2042-3306.1999.tb03178.x
26. Pietra, M., Guglielmini, C., Nardi, S., Gandini, G., & Cipone, M. (2004). Influence of weight bearing and hoof position on Doppler evaluation of lateral palmar digital arteries in healthy horses. American Journal of Veterinary Research, 65(9), 1211–1215. https://doi.org/10.2460/ajvr.2004.65.1211
27. Takahashi, Y., Yoshihara, E., & Takahashi, T. (2022). Comparison of heel movement between two different glue-on type shoes and nailed shoes in Thoroughbreds. Journal of Equine Veterinary Science, 113, 103939. https://doi.org/10.1016/j.jevs.2022.103939
28. Burns, T.D. (2020). Mechanical evaluation of composites used to treat hoof wall cracks/fractures [Conference presentation]. American Farrier's Association Annual Convention, Chattanooga Tennessee.
29. Moeller, S., Patan-Zugaj, B., Däullary, T., Tichy, A., & Licka, T. (2019). The influence of trimming of the hoof wall on the damage of laminar tissue after loading: An in vitro study. The Veterinary Journal, 250, 63–70. https://doi.org/10.1016/j.tvjl.2019.07
30. Nicolai, R. P., Van Den Belt, A. J. M., Bakker, J., De Heer, N., Ter Braake, F., Meeus, P., Hofland, L. J., & Back, W. (2017). Radiographic differences between uneven feet in horses with foot lameness and admitted for MRI examination. Journal of Equine Veterinary Science, 54, 50–53. https://doi.org/10.1016/j.jevs.2017.03.001

31. Hagen, J., Hüppler, M., Geiger, S. M., Mäder, D., & Häfner, F. S. (2017). Modifying the height of horseshoes: Effects of wedge shoes, studs, and rocker shoes on the phalangeal alignment, pressure distribution, and hoof-ground contact during motion. Journal of Equine Veterinary Science, 53, 8–18. https://doi.org/10.1016/j.jevs.2017.01.014
32. Roepstorff, L., Johnston, C., & Drevemo, S. (2001). In vivo and in vitro heel expansion in relation to shoeing and frog pressure. Equine Veterinary Journal, 33(S33), 54–57. https://doi.org/10.1111/j.2042-3306.2001.tb05359.x
33. Hagen, J., Geburek, F., Kathrinaki, V., Naem, M. A., Roecken, M., & Hoffmann, J. (2021). Effect of perineural anesthesia on the centre of pressure (COP) path during stance phase at trot in sound horses. Journal of Equine Veterinary Science, 101, 103429. https://doi.org/10.1016/j.jevs.2021.103429
34. Yoshihara, E., Takahashi, T., Otsuka, N., Isayama, T., Tomiyama, T., Higara, A., & Wada, S. (2010). Heel movement in horses: Comparison between glued and nailed horse shoes at different speeds. Equine Veterinary Journal, 42, 431–435. https://doi.org/10.1111/j.2042-3306.2010.00243.x
35. Brunsting, J., Dumoulin, M., Oosterlinck, M., Haspeslagh, M., Lefère, L., & Pille, F. (2019). Can the hoof be shod without limiting the heel movement? A comparative study between barefoot, shoeing with conventional shoes and a split-toe shoe. The Veterinary Journal, 246, 7–11. https://doi.org/10.1016/j.tvjl.2019.01.012
36. Bardin, A. L., Taylor, N. C., & Robert Colborne, G. (2022). Response of the Thoroughbred forelimb to perturbations caused by a change in ground surface. Journal of Equine Veterinary Science, 112, 103897. https://doi.org/10.1016/j.jevs.2022.103897
37. Thomason, J. J., McClinchey, H. L., & Jofriet, J. C. (2010). Analysis of strain and stress in the equine hoof capsule using finite element methods: Comparison with principal strains recorded in vivo. Equine Veterinary Journal, 34(7), 719–725. https://doi.org/10.2746/042516402776250388
38. Senderska-Płonowska, M., Zielińska, P., Żak, A., & Stefaniak, T. (2020). Do metal shoes contract heels?—A retrospective study on 114 horses. Journal of Equine Veterinary Science, 95, 103293. https://doi.org/10.1016/j.jevs.2020.103293
39. McClinchey, H. L., Jofriet, J. C., & Thomason, J. J. (2003). Isolating the effects of equine hoof shape measurements on capsule strain with finite element analysis. Veterinary and Comparative Orthopaedics and Traumatology, 16(2), 67–75. https://doi.org/10.1055/s-0038-1632762
40. Davies, H. M. S. (2010). Noninvasive photoelastic method to show distribution of strain in the hoof wall of a living horse. Equine Veterinary Journal, 29(S23), 13–15. https://doi.org/10.1111/j.2042-3306.1997.tb05043.x
41. Déjardin, L. M., Arnoczky, S. P., & Cloud, G. L. (1999). A method for determination of equine hoof strain patterns using photoelasticity: An in vitro study. Equine Veterinary Journal, 31(3), 232–237. https://doi.org/10.1111/j.2042-3306.1999.tb03178.x
42. Pietra, M., Guglielmini, C., Nardi, S., Gandini, G., & Cipone, M. (2004). Influence of weight bearing and hoof position on Doppler evaluation of lateral palmar digital arteries in healthy horses. American Journal of Veterinary Research, 65(9), 1211–1215. https://doi.org/10.2460/ajvr.2004.65.1211
43. Takahashi, Y., Yoshihara, E., & Takahashi, T. (2022). Comparison of heel movement between two different glue-on type shoes and nailed shoes in Thoroughbreds. Journal of Equine Veterinary Science, 113, 103939. https://doi.org/10.1016/j.jevs.2022.103939
44. Moeller, S., Patan-Zugaj, B., Däullary, T., Tichy, A., & Licka, T. (2019). The influence of trimming of the hoof wall on the damage of laminar tissue after loading: An in vitro study. The Veterinary Journal, 250, 63–70. https://doi.org/10.1016/j.tvjl.2019.07

45. Nicolai, R. P., Van Den Belt, A. J. M., Bakker, J., De Heer, N., Ter Braake, F., Meeus, P., Hofland, L. J., & Back, W. (2017). Radiographic differences between uneven feet in horses with foot lameness admitted for MRI examination. Journal of Equine Veterinary Science, 54, 50–53. https://doi.org/10.1016/j.jevs.2017.03.001
46. Hagen, J., Hüppler, M., Geiger, S. M., Mäder, D., & Häfner, F. S. (2017). Modifying the height of horseshoes: Effects of wedge shoes, studs, and rocker shoes on the phalangeal alignment, pressure distribution, and hoof-ground contact during motion. Journal of Equine Veterinary Science, 53, 8–18. https://doi.org/10.1016/j.jevs.2017.01.014
47. Roepstorff, L., Johnston, C., & Drevemo, S. (2001). In vivo and in vitro heel expansion in relation to shoeing and frog pressure. Equine Veterinary Journal, 33(S33), 54–57. https://doi.org/10.1111/j.2042-3306.2001.tb05359.x
48. Hagen, J., Geburek, F., Kathrinaki, V., Naem, M. A., Roecken, M., & Hoffmann, J. (2021). Effect of perineural anesthesia on the centre of pressure (COP) path during stance phase at trot in sound horses. Journal of Equine Veterinary Science, 101, 103429. https://doi.org/10.1016/j.jevs.2021.103429
49. Baxter, G. M. (Ed.). (2011). Adams and Stashak's lameness in horses (6th ed.). Wiley-Blackwell.
50. Back, W., & Clayton, H. M. (2013). Equine locomotion (2nd ed.). Saunders Elsevier.
51. Ross, M. W., & Dyson, S. J. (2011). Diagnosis and management of lameness in the horse (2nd ed.). Saunders Elsevier.

6 . Addendums

5.1 Raw data

HorseNo	Condition	total displacement	min	max
Subject #1	walk glue asphalt	1.96	18.98	20.94
Subject #2	walk glue asphalt	1.7	15.89	17.59
Subject #3	walk glue asphalt	2.66	14.48	17.14
Subject #4	walk glue asphalt	3.06	15.74	18.8
Subject #5	walk glue asphalt	1.68	14.03	15.71
Subject #6	walk glue asphalt	2.39	18.23	20.62
Subject #7	walk glue asphalt	2.64	19.11	21.75
Subject #8	walk glue asphalt	2.46	15.42	17.88
Subject #9	walk glue asphalt	2.72	13.25	15.97
Subject #10	walk glue asphalt	2.46	8.55	11.01
Subject #11	walk glue asphalt	2.07	19.2	21.27
Subject #12	walk glue asphalt	1.85	15.07	16.92
Subject #13	walk glue asphalt	0.8	18.76	19.56
Subject #14	walk glue asphalt	2.2	22.16	24.36
Subject #15	walk glue asphalt	2.84	25.4	28.24
Subject #1	walk barefoot asphalt	2.35	18.99	21.34
Subject #2	walk barefoot asphalt	2.61	14.96	17.57
Subject #3	walk barefoot asphalt	2.93	13.32	16.25
Subject #4	walk barefoot asphalt	4.41	14.88	19.29
Subject #5	walk barefoot asphalt	2.6	14.23	16.83
Subject #6	walk barefoot asphalt	2.87	17.92	20.79
Subject #7	walk barefoot asphalt	3.29	17.98	21.27
Subject #8	walk barefoot asphalt	2.84	14.64	17.48
Subject #9	walk barefoot asphalt	3.65	12.39	16.04
Subject #10	walk barefoot asphalt	3.31	8.33	11.64
Subject #11	walk barefoot asphalt	3.41	18.85	22.26
Subject #12	walk barefoot asphalt	2.61	14.73	17.34
Subject #13	walk barefoot asphalt	1.58	18.4	19.98
Subject #14	walk barefoot asphalt	3.16	21.82	24.98
Subject #15	walk barefoot asphalt	3.78	25.52	29.3
Subject #1	walk aluminum asphalt	1.54	19.37	20.91
Subject #2	walk aluminum asphalt	1.26	15.1	16.36
Subject #3	walk aluminum asphalt	2.62	13.16	15.78
Subject #4	walk aluminum asphalt	2.67	15.28	17.95
Subject #5	walk aluminum asphalt	1.59	13.63	15.22
Subject #6	walk aluminum asphalt	1.75	18.96	20.71
Subject #7	walk aluminum asphalt	1.83	18.01	19.84

Subject #8	walk aluminum asphalt	1.97	15.16	17.13
Subject #9	walk aluminum asphalt	2.52	12.54	15.06
Subject #10	walk aluminum asphalt	2.21	8.78	10.99
Subject #11	walk aluminum asphalt	1.55	20.3	21.85
Subject #12	walk aluminum asphalt	2.16	15.09	17.25
Subject #13	walk aluminum asphalt	1.18	18.75	19.93
Subject #14	walk aluminum asphalt	2.25	21.89	24.14
Subject #15	walk aluminum asphalt	2.35	25.87	28.22
Subject #1	trot glue asphalt	2.63	19.12	21.75
Subject #2	trot glue asphalt	2.39	16.06	18.45
Subject #3	trot glue asphalt	2.96	13.89	16.85
Subject #4	trot glue asphalt	3.32	15.86	19.18
Subject #5	trot glue asphalt	2.58	14.17	16.75
Subject #6	trot glue asphalt	1.83	18.14	19.97
Subject #7	trot glue asphalt	2.8	18.31	21.11
Subject #8	trot glue asphalt	3.06	14.89	17.95
Subject #9	trot glue asphalt	3.45	12.98	16.43
Subject #10	trot glue asphalt	2.5	8.55	11.05
Subject #11	trot glue asphalt	1.69	19.74	21.43
Subject #12	trot glue asphalt	2.39	15.56	17.95
Subject #13	trot glue asphalt	1.61	18.83	20.44
Subject #14	trot glue asphalt	2.85	22.42	25.27
Subject #15	trot glue asphalt	2.29	25.94	28.23
Subject #1	trot barefoot asphalt	2.89	19.24	22.13
Subject #2	trot barefoot asphalt	3.48	15.23	18.71
Subject #3	trot barefoot asphalt	3.29	13.5	16.79
Subject #4	trot barefoot asphalt	4.22	15.28	19.5
Subject #5	trot barefoot asphalt	2.74	13.43	16.17
Subject #6	trot barefoot asphalt	2.57	18.35	20.92
Subject #7	trot barefoot asphalt	3.46	18.16	21.62
Subject #8	trot barefoot asphalt	3.75	15.57	19.32
Subject #9	trot barefoot asphalt	4.35	12.73	17.08
Subject #10	trot barefoot asphalt	3.15	7.79	10.94
Subject #11	trot barefoot asphalt	2.57	19.94	22.51
Subject #12	trot barefoot asphalt	3.37	15.31	18.68
Subject #13	trot barefoot asphalt	2.17	18.49	20.66
Subject #14	trot barefoot asphalt	3.72	21.96	25.68
Subject #15	trot barefoot asphalt	3.6	26.12	29.72
Subject #1	trot aluminum asphalt	2.06	19.69	21.75
Subject #2	trot aluminum asphalt	2.24	15.41	17.65
Subject #3	trot aluminum asphalt	1.38	14.35	15.73

Subject #4	trot aluminum asphalt	2.81	15.51	18.32
Subject #5	trot aluminum asphalt	1.65	13.88	15.53
Subject #6	trot aluminum asphalt	2.06	18.21	20.27
Subject #7	trot aluminum asphalt	2.41	18.53	20.94
Subject #8	trot aluminum asphalt	2.36	15.49	17.85
Subject #9	trot aluminum asphalt	3.01	13.02	16.03
Subject #10	trot aluminum asphalt	2.03	7.9	9.93
Subject #11	trot aluminum asphalt	1.95	19.9	21.85
Subject #12	trot aluminum asphalt	2.16	14.96	17.12
Subject #13	trot aluminum asphalt	1.33	18.82	20.15
Subject #14	trot aluminum asphalt	2.49	22.55	25.04
Subject #15	trot aluminum asphalt	1.93	26.22	28.15
Subject #1	walk glue footing	no data	no data	no data
Subject #2	walk glue footing	1.40	16.09	17.49
Subject #3	walk glue footing	3.22	14.69	17.91
Subject #4	walk glue footing	2.23	15.91	18.14
Subject #5	walk glue footing	0.634	13.972	14.606
Subject #6	walk glue footing	0.1352	19.3583	19.4935
Subject #7	walk glue footing	4.501	18.419	22.92
Subject #8	walk glue footing	no data	no data	no data
Subject #9	walk glue footing	4.38	12.4	16.78
Subject #10	walk glue footing	0.694266667	8.840133	9.5344
Subject #11	walk glue footing	2.423	19.336	21.759
Subject #12	walk glue footing	1.8647	15.0819	16.9466
Subject #13	walk glue footing	0.6466	18.8141	19.4607
Subject #14	walk glue footing	no data	no data	no data
Subject #15	walk glue footing	no data	no data	no data
Subject #1	trot glue footing	no data	no data	no data
Subject #2	trot glue footing	2.832	15.869	18.701
Subject #3	trot glue footing	0.707	14.666	15.373
Subject #4	trot glue footing	3.875	16.014	19.889
Subject #5	trot glue footing	0.799	13.953	14.752
Subject #6	trot glue footing	1.05	19.179	20.229
Subject #7	trot glue footing	0.6851	18.9814	19.6665
Subject #8	trot glue footing	no data	no data	no data
Subject #9	trot glue footing	0.263	14.41	14.673
Subject #10	trot glue footing	2.8996	8.875	11.7746
Subject #11	trot glue footing	no data	no data	no data
Subject #12	trot glue footing	3.322	15.059	18.381
Subject #13	trot glue footing	1.674	18.825	20.499
Subject #14	trot glue footing	no data	no data	no data

Subject #15	trot glue footing	no data	no data	no data
Subject #1	walk barefoot footing	no data	no data	no data
Subject #2	walk barefoot footing	no data	no data	no data
Subject #3	walk barefoot footing	2.6394	14.2584	16.8978
Subject #4	walk barefoot footing	no data	no data	no data
Subject #5	walk barefoot footing	1.0899	14.5092	15.5991
Subject #6	walk barefoot footing	no data	no data	no data
Subject #7	walk barefoot footing	no data	no data	no data
Subject #8	walk barefoot footing	no data	no data	no data
Subject #9	walk barefoot footing	no data	no data	no data
Subject #10	walk barefoot footing	2.953	8.037	10.99
Subject #11	walk barefoot footing	4.35	18.91	23.26
Subject #12	walk barefoot footing	2.75	15.17	17.92
Subject #13	walk barefoot footing	2.45	18.72	21.17
Subject #14	walk barefoot footing	4.33	21.62	25.95
Subject #15	walk barefoot footing	3.72	25.27	28.99
Subject #1	trot barefoot footing	no data	no data	no data
Subject #2	trot barefoot footing	no data	no data	no data
Subject #3	trot barefoot footing	4.39	14.55	18.94
Subject #4	trot barefoot footing	no data	no data	no data
Subject #5	trot barefoot footing	4.04	12.62	16.66
Subject #6	trot barefoot footing	no data	no data	no data
Subject #7	trot barefoot footing	no data	no data	no data
Subject #8	trot barefoot footing	no data	no data	no data
Subject #9	trot barefoot footing	no data	no dat a	no data
Subject #10	trot barefoot footing	0.85	8.63	9.48
Subject #11	trot barefoot footing	5.9	19.23	25.13
Subject #12	trot barefoot footing	4.4	15.53	19.93
Subject #13	trot barefoot footing	4.97	19.02	23.99
Subject #14	trot barefoot footing	0.55	22.96	23.51
Subject #15	trot barefoot footing	no data	no data	no data
Subject #1	walk footing aluminum	no data	no data	no data
Subject #2	walk footing aluminum	3.59	14.99	18.58
Subject #3	walk footing aluminum	3.11	13.04	16.15
Subject #4	walk footing aluminum	2.54	15.28	17.82
Subject #5	walk footing aluminum	no data	no data	no data
Subject #6	walk footing aluminum	2.84	18.31	21.15
Subject #7	walk footing aluminum	2.02	18.07	20.09
Subject #8	walk footing aluminum	no data	no data	no data
Subject #9	walk footing aluminum	4.48	11.8	16.28
Subject #10	walk footing aluminum	3.86	7.92	11.78

Subject #11	walk footing aluminum	3.97	19.88	23.85
Subject #12	walk footing aluminum	2.37	14.95	17.32
Subject #13	walk footing aluminum	1.42	18.75	20.17
Subject #14	walk footing aluminum	3.56	22.25	25.81
Subject #15	walk footing aluminum	no data	no data	no data
Subject #1	trot footing aluminum	no data	no data	no data
Subject #2	trot footing aluminum	2.35	14.97	17.32
Subject #3	trot footing aluminum	4.85	13.37	18.22
Subject #4	trot footing aluminum	3.72	15.45	19.17
Subject #5	trot footing aluminum	0.91	18.9	19.81
Subject #6	trot footing aluminum	0.67	8.78	9.45
Subject #7	trot footing aluminum	4.35	18.34	22.69
Subject #8	trot footing aluminum	no data	no data	no data
Subject #9	trot footing aluminum	3.08	15.27	18.35
Subject #10	trot footing aluminum	0.92	14.91	15.83
Subject #11	trot footing aluminum	0.67	16.04	16.71
Subject #12	trot footing aluminum	3.07	15.31	18.38
Subject #13	trot footing aluminum	2.82	18.79	21.61
Subject #14	trot footing aluminum	3.57	24.78	28.35
Subject #15	trot footing aluminum	no data	no data	no data

5.2 Mixed model ANOVA for Ashalt

Total displacement: Overall Summary Statistics

Condition	SampleSize	Means	Medians	SD	SEM	Minimum	Maximum	FirstQuartile	ThirdQuartile	IQR
walk glue	15	2.23267	2.39	0.57678	0.14892	0.80	3.06	1.85	2.66	0.81
walk barefoot	15	3.02667	2.93	0.67256	0.17365	1.58	4.41	2.61	3.41	0.80
walk aluminum	15	1.96333	1.97	0.48053	0.12407	1.18	2.67	1.55	2.35	0.80
trot glue	15	2.55667	2.58	0.55118	0.14231	1.61	3.45	2.29	2.96	0.67
trot barefoot	15	3.28867	3.37	0.61678	0.15925	2.17	4.35	2.74	3.72	0.98
trot aluminum	15	2.12467	2.06	0.46563	0.12023	1.33	3.01	1.93	2.41	0.48

Totaldisplacement: Mixed Model Anova to assess the effects of Condition

The Mixed Procedure

Model Information	
Data Set	WORK.SDATA1
Dependent Variable	totaldisplacement
Covariance Structure	Variance Components
Estimation Method	REML
Residual Variance Method	Profile
Fixed Effects SE Method	Kenward-Roger
Degrees of Freedom Method	Kenward-Roger

Class Level Information		
Class	**Levels**	**Values**
HorseNo	15	Subject #1 Subject #10 Subject #11 Subject #12 Subject #13 Subject #14 Subject #15 Subject #2 Subject #3 Subject #4 Subject #5 Subject #6 Subject #7 Subject #8 Subject #9
Condition	6	trot aluminum trot barefoot trot glue walk aluminum walk barefoot walk glue

Covariance Parameter Estimates	
Cov Parm	**Estimate**
HorseNo	0.2159
Residual	0.1036

Type 3 Tests of Fixed Effects				
Effect	**Num DF**	**Den DF**	**F Value**	**Pr > F**
Condition	5	70	40.45	<.0001

Least Squares Means									
Effect	**Condition**	**Estimate**	**Standard Error**	**DF**	**t Value**	**Pr > |t|**	**Alpha**	**Lower**	**Upper**
Condition	trot aluminum	2.1247	0.1459	25.6	14.56	<.0001	0.05	1.8244	2.4249
Condition	trot barefoot	3.2887	0.1459	25.6	22.53	<.0001	0.05	2.9884	3.5889
Condition	trot glue	2.5567	0.1459	25.6	17.52	<.0001	0.05	2.2564	2.8569
Condition	walk aluminum	1.9633	0.1459	25.6	13.45	<.0001	0.05	1.6631	2.2636
	walk barefoot	3.0267	0.1459	25.6	20.74	<.0001 **Condition**	0.05	2.7264	3.3269
Condition	walk glue	2.2327	0.1459	25.6	15.30	<.0001	0.05	1.9324	2.5329

Differences of Least Squares Means

Effect	**Condition**	**Condition**	**Estimate**	**Standard Error**	**DF**	**t Value**	**Pr > |t|**	**Adjustment**	**Adj P**	**Alpha**
Condition	trot aluminum	trot barefoot	-1.1640	0.1175	70	-9.90	<.0001	Tukey-Kramer	<.0001	0.05
Condition	trot aluminum	trot glue	-0.4320	0.1175	70	-3.68	0.0005	Tukey-Kramer	0.0059	0.05
Condition	trot aluminum	walk aluminum	0.1613	0.1175	70	1.37	0.1742	Tukey-Kramer	0.7429	0.05
Condition	trot aluminum	walk barefoot	-0.9020	0.1175	70	-7.68	<.0001	Tukey-Kramer	<.0001	0.05

Condition	trot aluminum	walk glue	-0.1080	0.1175	70	-0.92	0.3613	Tukey-Kramer	0.9404	0.05
Condition	trot barefoot	trot glue	0.7320	0.1175	70	6.23	<.0001	Tukey-Kramer	<.0001	0.05
Condition	trot barefoot	walk aluminum	1.3253	0.1175	70	11.28	<.0001	Tukey-Kramer	<.0001	0.05
Condition	trot barefoot	walk barefoot	0.2620	0.1175	70	2.23	0.0290	Tukey-Kramer	0.2377	0.05
Condition	trot barefoot	walk glue	1.0560	0.1175	70	8.99	<.0001	Tukey-Kramer	<.0001	0.05
Condition	trot glue	walk aluminum	0.5933	0.1175	70	5.05	<.0001	Tukey-Kramer	<.0001	0.05
Condition	trot glue	walk barefoot	-0.4700	0.1175	70	-4.00	0.0002	Tukey-Kramer	0.0021	0.05
Condition	trot glue	walk glue	0.3240	0.1175	70	2.76	0.0074	Tukey-Kramer	0.0769	0.05
Condition	walk aluminum	walk barefoot	-1.0633	0.1175	70	-9.05	<.0001	Tukey-Kramer	<.0001	0.05
Condition	walk aluminum	walk glue	-0.2693	0.1175	70	-2.29	0.0249	Tukey-Kramer	0.2113	0.05
Condition	walk barefoot	walk glue	0.7940	0.1175	70	6.76	<.0001	Tukey-Kramer	<.0001	0.05

Differences of Least Squares Means						
Effect	**Condition**	**Condition**	**Lower**	**Upper**	**Adj Lower**	**Adj Upper**
Condition	trot aluminum	trot barefoot	-1.3984	-0.9296	-1.5084	-0.8196
Condition	trot aluminum	trot glue	-0.6664	-0.1976	-0.7764	-0.08765
Condition	trot aluminum	walk aluminum	-0.07306	0.3957	-0.1830	0.5057
Condition	trot aluminum	walk barefoot	-1.1364	-0.6676	-1.2464	-0.5576

Differences of Least Squares Means						
Effect	Condition	Condition	Lower	Upper	Adj Lower	Adj Upper
Condition	trot aluminum	walk glue	-0.3424	0.1264	-0.4524	0.2364
Condition	trot barefoot	trot glue	0.4976	0.9664	0.3876	1.0764
Condition	trot barefoot	walk aluminum	1.0909	1.5597	0.9810	1.6697
Condition	trot barefoot	walk barefoot	0.02761	0.4964	-0.08235	0.6064
Condition	trot barefoot	walk glue	0.8216	1.2904	0.7116	1.4004
Condition	trot glue	walk aluminum	0.3589	0.8277	0.2490	0.9377
Condition	trot glue	walk barefoot	-0.7044	-0.2356	-0.8144	-0.1256
Condition	trot glue	walk glue	0.08961	0.5584	-0.02035	0.6684
Condition	walk aluminum	walk barefoot	-1.2977	-0.8289	-1.4077	-0.7190
Condition	walk aluminum	walk glue	-0.5037	-0.03494	-0.6137	0.07502
Condition	walk barefoot	walk glue	0.5596	1.0284	0.4496	1.1384

min: Overall Summary Statistics

Condition	SampleSize	Means	Medians	SD	SEM	Minimum	Maximum	FirstQuartile	ThirdQuartile	IQR
walk glue	15	16.9513	15.89	4.00580	1.03429	8.55	25.40	14.48	19.11	4.63
walk barefoot	15	16.4640	14.96	4.13761	1.06833	8.33	25.52	14.23	18.85	4.62
walk aluminum	15	16.7927	15.28	4.25558	1.09879	8.78	25.87	13.63	19.37	5.74
trot glue	15	16.9640	16.06	4.15417	1.07260	8.55	25.94	14.17	19.12	4.95

Condition	SampleSize	Means	Medians	SD	SEM	Minimum	Maximum	FirstQuartile	ThirdQuartile	IQR
trot barefoot	15	16.7400	15.57	4.34951	1.12304	7.79	26.12	13.50	19.24	5.74
trot aluminum	15	16.9627	15.51	4.35193	1.12366	7.90	26.22	14.35	19.69	5.34

min: Mixed Model Anova to assess the effects of Condition

The Mixed Procedure

Model Information

Data Set	WORK.SDATA1
Dependent Variable	min
Covariance Structure	Variance Components
Estimation Method	REML
Residual Variance Method	Profile
Fixed Effects SE Method	Kenward-Roger
Degrees of Freedom Method	Kenward-Roger

Class Level Information		
Class	**Levels**	**Values**
HorseNo	15	Subject #1 Subject #10 Subject #11 Subject #12 Subject #13 Subject #14 Subject #15 Subject #2 Subject #3 Subject #4 Subject #5 Subject #6 Subject #7 Subject #8 Subject #9
Condition	6	trot aluminum trot barefoot trot glue walk aluminum walk barefoot walk glue

Covariance Parameter Estimates	
Cov Parm	**Estimate**
HorseNo	17.6238
Residual	0.1080

Type 3 Tests of Fixed Effects				
Effect	**Num DF**	**Den DF**	**F Value**	**Pr > F**
Condition	5	70	5.33	0.0003

Least Squares Means									
Effect	**Condition**	**Estimate**	**Standard Error**	**DF**	**t Value**	**Pr > |t|**	**Alpha**	**Lower**	**Upper**
Condition	trot aluminum	16.9627	1.0873	14.1	15.60	<.0001	0.05	14.6330	19.2924
Condition	trot barefoot	16.7400	1.0873	14.1	15.40	<.0001	0.05	14.4103	19.0697
Condition	trot glue	16.9640	1.0873	14.1	15.60	<.0001	0.05	14.6343	19.2937
Condition	walk aluminum	16.7927	1.0873	14.1	15.45	<.0001	0.05	14.4630	19.1224
Condition	walk barefoot	16.4640	1.0873	14.1	15.14	<.0001	0.05	14.1343	18.7937
Condition	walk glue	16.9513	1.0873	14.1	15.59	<.0001	0.05	14.6216	19.2810

Differences of Least Squares Means										
Effect	**Condition**	**Condition**	**Estimate**	**Standard Error**	**DF**	**t Value**	**Pr > |t|**	**Adjustment**	**Adj P**	**Alpha**
Condition	trot aluminum	trot barefoot	0.2227	0.1200	70	1.86	0.0678	Tukey-Kramer	0.4380	0.05
Condition	trot aluminum	trot glue	-0.00133	0.1200	70	-0.01	0.9912	Tukey-Kramer	1.0000	0.05
Condition	trot aluminum	walk aluminum	0.1700	0.1200	70	1.42	0.1611	Tukey-Kramer	0.7170	0.05
Condition	trot aluminum	walk barefoot	0.4987	0.1200	70	4.15	<.0001	Tukey-Kramer	0.0012	0.05
Condition	trot aluminum	walk glue	0.01133	0.1200	70	0.09	0.9250	Tukey-Kramer	1.0000	0.05
Condition	trot barefoot	trot glue	-0.2240	0.1200	70	-1.87	0.0662	Tukey-Kramer	0.4312	0.05
Condition	trot barefoot	walk aluminum	-0.05267	0.1200	70	-0.44	0.6621	Tukey-Kramer	0.9979	0.05
Condition	trot barefoot	walk barefoot	0.2760	0.1200	70	2.30	0.0245	Tukey-Kramer	0.2081	0.05
Condition	trot barefoot	walk glue	-0.2113	0.1200	70	-1.76	0.0826	Tukey-Kramer	0.4973	0.05
Condition	trot glue	walk aluminum	0.1713	0.1200	70	1.43	0.1579	Tukey-Kramer	0.7103	0.05
Condition	trot glue	walk barefoot	0.5000	0.1200	70	4.17	<.0001	Tukey-Kramer	0.0012	0.05
Condition	trot glue	walk glue	0.01267	0.1200	70	0.11	0.9162	Tukey-Kramer	1.0000	0.05
Condition	walk aluminum	walk barefoot	0.3287	0.1200	70	2.74	0.0078	Tukey-Kramer	0.0804	0.05
Condition	walk aluminum	walk glue	-0.1587	0.1200	70	-1.32	0.1905	Tukey-Kramer	0.7719	0.05
Condition	walk barefoot	walk glue	-0.4873	0.1200	70	-4.06	0.0001	Tukey-Kramer	0.0017	0.05

Differences of Least Squares Means						
Effect	**Condition**	**Condition**	**Lower**	**Upper**	**Adj Lower**	**Adj Upper**
Condition	trot aluminum	trot barefoot	-0.01670	0.4620	-0.1290	0.5743
Condition	trot aluminum	trot glue	-0.2407	0.2380	-0.3530	0.3503
Condition	trot aluminum	walk aluminum	-0.06936	0.4094	-0.1817	0.5217
Condition	trot aluminum	walk barefoot	0.2593	0.7380	0.1470	0.8503
Condition	trot aluminum	walk glue	-0.2280	0.2507	-0.3403	0.3630
Condition	trot barefoot	trot glue	-0.4634	0.01536	-0.5757	0.1277
Condition	trot barefoot	walk aluminum	-0.2920	0.1867	-0.4043	0.2990
Condition	trot barefoot	walk barefoot	0.03664	0.5154	-0.07566	0.6277
Condition	trot barefoot	walk glue	-0.4507	0.02803	-0.5630	0.1403
Condition	trot glue	walk aluminum	-0.06803	0.4107	-0.1803	0.5230
Condition	trot glue	walk barefoot	0.2606	0.7394	0.1483	0.8517
Condition	trot glue	walk glue	-0.2267	0.2520	-0.3390	0.3643
Condition	walk aluminum	walk barefoot	0.08930	0.5680	-0.02300	0.6803
Condition	walk aluminum	walk glue	-0.3980	0.08070	-0.5103	0.1930
Condition	walk barefoot	walk glue	-0.7267	-0.2480	-0.8390	-0.1357

max: Overall Summary Statistics

Condition	SampleSize	Means	Medians	SD	SEM	Minimum	Maximum	FirstQuartile	ThirdQuartile	IQR
walk glue	15	19.1840	18.80	4.03494	1.04182	11.01	28.24	16.92	21.27	4.35
walk barefoot	15	19.4907	19.29	4.19232	1.08245	11.64	29.30	16.83	21.34	4.51
walk aluminum	15	18.7560	17.95	4.18989	1.08182	10.99	28.22	15.78	20.91	5.13
trot glue	15	19.5207	19.18	3.99469	1.03142	11.05	28.23	16.85	21.43	4.58
trot barefoot	15	20.0287	19.50	4.31917	1.11521	10.94	29.72	17.08	22.13	5.05
trot aluminum	15	19.0873	18.32	4.33783	1.12002	9.93	28.15	16.03	21.75	5.72

max: Mixed Model Anova to assess the effects of Condition

The Mixed Procedure

Model Information	
Data Set	WORK.SDATA1
Dependent Variable	max
Covariance Structure	Variance Components
Estimation Method	REML
Residual Variance Method	Profile
Fixed Effects SE Method	Kenward-Roger
Degrees of Freedom Method	Kenward-Roger

Class Level Information		
Class	**Levels**	**Values**
HorseNo	15	Subject #1 Subject #10 Subject #11 Subject #12 Subject #13 Subject #14 Subject #15 Subject #2 Subject #3 Subject #4 Subject #5 Subject #6 Subject #7 Subject #8 Subject #9
Condition	6	trot aluminum trot barefoot trot glue walk aluminum walk barefoot walk glue

Covariance Parameter Estimates	
Cov Parm	**Estimate**
HorseNo	17.2811
Residual	0.1924

Type 3 Tests of Fixed Effects				
Effect	**Num DF**	**Den DF**	**F Value**	**Pr > F**
Condition	5	70	14.95	<.0001

Least Squares Means									
Effect	**Condition**	**Estimate**	**Standard Error**	**DF**	**t Value**	**Pr > |t|**	**Alpha**	**Lower**	**Upper**
Condition	trot aluminum	19.0873	1.0793	14.3	17.68	<.0001	0.05	16.7764	21.3983
Condition	trot barefoot	20.0287	1.0793	14.3	18.56	<.0001	0.05	17.7177	22.3396
Condition	trot glue	19.5207	1.0793	14.3	18.09	<.0001	0.05	17.2097	21.8316
Condition	walk aluminum	18.7560	1.0793	14.3	17.38	<.0001	0.05	16.4451	21.0669

Least Squares Means									
Effect	**Condition**	**Estimate**	**Standard Error**	**DF**	**t Value**	**Pr > |t|**	**Alpha**	**Lower**	**Upper**
Condition	walk barefoot	19.4907	1.0793	14.3	18.06	<.0001	0.05	17.1797	21.8016
Condition	walk glue	19.1840	1.0793	14.3	17.77	<.0001	0.05	16.8731	21.4949

Differences of Least Squares Means

Effect	**Condition**	**Condition**	**Estimate**	**Standard Error**	**DF**	**t Value**	**Pr > |t|**	**Adjustment**	**Adj P**	**Alpha**
Condition	trot aluminum	trot barefoot	-0.9413	0.1602	70	-5.88	<.0001	Tukey-Kramer	<.0001	0.05
Condition	trot aluminum	trot glue	-0.4333	0.1602	70	-2.71	0.0086	Tukey-Kramer	0.0870	0.05
Condition	trot aluminum	walk aluminum	0.3313	0.1602	70	2.07	0.0423	Tukey-Kramer	0.3156	0.05
Condition	trot aluminum	walk barefoot	-0.4033	0.1602	70	-2.52	0.0141	Tukey-Kramer	0.1329	0.05
Condition	trot aluminum	walk glue	-0.09667	0.1602	70	-0.60	0.5481	Tukey-Kramer	0.9905	0.05
Condition	trot barefoot	trot glue	0.5080	0.1602	70	3.17	0.0023	Tukey-Kramer	0.0263	0.05
Condition	trot barefoot	walk aluminum	1.2727	0.1602	70	7.95	<.0001	Tukey-Kramer	<.0001	0.05
Condition	trot barefoot	walk barefoot	0.5380	0.1602	70	3.36	0.0013	Tukey-Kramer	0.0154	0.05
Condition	trot barefoot	walk glue	0.8447	0.1602	70	5.27	<.0001	Tukey-Kramer	<.0001	0.05
Condition	trot glue	walk aluminum	0.7647	0.1602	70	4.77	<.0001	Tukey-Kramer	0.0001	0.05
Condition	trot glue	walk barefoot	0.03000	0.1602	70	0.19	0.8520	Tukey-Kramer	1.0000	0.05
Condition	trot glue	walk glue	0.3367	0.1602	70	2.10	0.0392	Tukey-Kramer	0.2984	0.05

Condition	walk aluminum	walk barefoot	-0.7347	0.1602	70	-4.59	<.0001	Tukey-Kramer	0.0003	0.05
Condition	walk aluminum	walk glue	-0.4280	0.1602	70	-2.67	0.0094	Tukey-Kramer	0.0940	0.05
Condition	walk barefoot	walk glue	0.3067	0.1602	70	1.91	0.0596	Tukey-Kramer	0.4022	0.05

max: Mixed Model Anova to assess the effects of Condition

The Mixed Procedure
Differences of Least Squares Means

Effect	Condition	Condition	Lower	Upper	Adj Lower	Adj Upper
Condition	trot aluminum	trot barefoot	-1.2608	-0.6219	-1.4107	-0.4720
Condition	trot aluminum	trot glue	-0.7528	-0.1139	-0.9027	0.03601
Condition	trot aluminum	walk aluminum	0.01187	0.6508	-0.1380	0.8007
Condition	trot aluminum	walk barefoot	-0.7228	-0.08387	-0.8727	0.06601
Condition	trot aluminum	walk glue	-0.4161	0.2228	-0.5660	0.3727
Condition	trot barefoot	trot glue	0.1885	0.8275	0.03865	0.9773
Condition	trot barefoot	walk aluminum	0.9532	1.5921	0.8033	1.7420
Condition	trot barefoot	walk barefoot	0.2185	0.8575	0.06865	1.0073
Condition	trot barefoot	walk glue	0.5252	1.1641	0.3753	1.3140
Condition	trot glue	walk aluminum	0.4452	1.0841	0.2953	1.2340
Condition	trot glue	walk barefoot	-0.2895	0.3495	-0.4393	0.4993

Condition	trot glue	walk glue	0.01720	0.6561	-0.1327	0.8060
Condition	walk aluminum	walk barefoot	-1.0541	-0.4152	-1.2040	-0.2653
Condition	walk aluminum	walk glue	-0.7475	-0.1085	-0.8973	0.04135
Condition	walk barefoot	walk glue	-0.01280	0.6261	-0.1627	0.7760

5.3 Mixed model ANOVA for footing

Total_displacement: Overall Summary Statistics

Condition	SampleSize	Means	Medians	SD	SEM	Minimum	Maximum	FirstQuartile	ThirdQuartile	IQR
walk glue footing	11	2.01150	1.8647	1.51325	0.45626	0.1352	4.501	0.6466	3.2200	2.5734
trot glue footing	10	1.81067	1.3620	1.30280	0.41198	0.2630	3.875	0.7070	2.8996	2.1926
walk barefoot footing	8	3.03529	2.8515	1.08533	0.38372	1.0899	4.350	2.5447	4.0250	1.4803
trot barefoot footing	7	3.58571	4.3900	2.06107	0.77901	0.5500	5.900	0.8500	4.9700	4.1200
walk aluminum footing	11	3.06909	3.1100	0.92645	0.27934	1.4200	4.480	2.3700	3.8600	1.4900
trot aluminum footing	12	2.58167	2.9450	1.47731	0.42646	0.6700	4.850	0.9150	3.6450	2.7300

total_displacement: Mixed Model Anova to assess the effects of Condition

The Mixed Procedure

Model Information	
Data Set	WORK.SDATA2
Dependent Variable	total_displacement
Covariance Structure	Variance Components
Estimation Method	REML
Residual Variance Method	Profile
Fixed Effects SE Method	Kenward-Roger
Degrees of Freedom Method	Kenward-Roger

Class Level Information		
Class	**Levels**	**Values**
HorseNo	15	Subject #1 Subject #10 Subject #11 Subject #12 Subject #13 Subject #14 Subject #15 Subject #2 Subject #3 Subject #4 Subject #5 Subject #6 Subject #7 Subject #8 Subject #9
Condition	6	trot aluminum footing trot barefoot footing trot glue footing walk aluminum footing walk barefoot footing walk glue footing

Covariance Parameter Estimates	
Cov Parm	**Estimate**
HorseNo	0.05097
Residual	1.9208

Type 3 Tests of Fixed Effects				
Effect	**Num DF**	**Den DF**	**F Value**	**Pr > F**
Condition	5	44.9	2.07	0.0870

Least Squares Means									
Effect	**Condition**	**Estimate**	**Standard Error**	**DF**	**t Value**	**Pr > |t|**	**Alpha**	**Lower**	**Upper**
Condition	trot aluminum footing	2.5831	0.4057	52.9	6.37	<.0001	0.05	1.7694	3.3969
Condition	trot barefoot footing	3.6006	0.5387	53	6.68	<.0001	0.05	2.5200	4.6812
Condition	trot glue footing	1.8188	0.4470	52.9	4.07	0.0002	0.05	0.9222	2.7154
Condition	walk aluminum footing	3.0588	0.4251	52.9	7.20	<.0001	0.05	2.2061	3.9114
Condition	walk barefoot footing	3.0462	0.5025	53	6.06	<.0001	0.05	2.0382	4.0541
Condition	walk glue footing	2.0125	0.4249	52.9	4.74	<.0001	0.05	1.1602	2.8647

Differences of Least Squares Means										
Effect	**Condition**	**Condition**	**Estimate**	**Standard Error**	**DF**	**t Value**	**Pr > |t|**	**Adjustment**	**Adj P**	**Alpha**
Condition	trot aluminum footing	trot barefoot footing	-1.0175	0.6675	46	-1.52	0.1343	Tukey-Kramer	0.6507	0.05
Condition	trot aluminum footing	trot glue footing	0.7643	0.5962	43.3	1.28	0.2067	Tukey-Kramer	0.7931	0.05
Condition	trot aluminum footing	walk aluminum footing	-0.4757	0.5799	42.5	-0.82	0.4167	Tukey-Kramer	0.9622	0.05
Condition	trot aluminum footing	walk barefoot footing	-0.4630	0.6401	46.7	-0.72	0.4731	Tukey-Kramer	0.9780	0.05
Condition	trot aluminum footing	walk glue footing	0.5706	0.5797	42.5	0.98	0.3305	Tukey-Kramer	0.9206	0.05
Condition	trot barefoot footing	trot glue footing	1.7818	0.6961	48.1	2.56	0.0137	Tukey-Kramer	0.1289	0.05

Differences of Least Squares Means										
Effect	**Condition**	**Condition**	**Estimate**	**Standard Error**	**DF**	**t Value**	**Pr > |t|**	**Adjustment**	**Adj P**	**Alpha**
Condition	trot barefoot footing	walk aluminum footing	0.5418	0.6809	47	0.80	0.4301	Tukey-Kramer	0.9668	0.05
Condition	trot barefoot footing	walk barefoot footing	0.5545	0.7185	43	0.77	0.4445	Tukey-Kramer	0.9709	0.05
Condition	trot barefoot footing	walk glue footing	1.5881	0.6805	47	2.33	0.0239	Tukey-Kramer	0.2022	0.05
Condition	trot glue footing	walk aluminum footing	-1.2400	0.6101	44	-2.03	0.0482	Tukey-Kramer	0.3409	0.05
Condition	trot glue footing	walk barefoot footing	-1.2274	0.6696	48.7	-1.83	0.0729	Tukey-Kramer	0.4557	0.05
Condition	trot glue footing	walk glue footing	-0.1937	0.6071	42.5	-0.32	0.7513	Tukey-Kramer	0.9995	0.05

Differences of Least Squares Means						
Effect	**Condition**	**Condition**	**Lower**	**Upper**	**Adj Lower**	**Adj Upper**
Condition	trot aluminum footing	trot barefoot footing	-2.3611	0.3261	-3.0040	0.9690
Condition	trot aluminum footing	trot glue footing	-0.4378	1.9664	-1.0100	2.5386
Condition	trot aluminum footing	walk aluminum footing	-1.6455	0.6942	-2.2015	1.2502
Condition	trot aluminum footing	walk barefoot footing	-1.7510	0.8250	-2.3682	1.4421
Condition	trot aluminum footing	walk glue footing	-0.5989	1.7402	-1.1548	2.2960
Condition	trot barefoot footing	trot glue footing	0.3822	3.1814	-0.2900	3.8536
Condition	trot barefoot footing	walk aluminum footing	-0.8279	1.9116	-1.4845	2.5682
Condition	trot barefoot footing	walk barefoot footing	-0.8946	2.0035	-1.5840	2.6929

Differences of Least Squares Means						
Effect	Condition	Condition	Lower	Upper	Adj Lower	Adj Upper
Condition	trot barefoot footing	walk glue footing	0.2192	2.9571	-0.4371	3.6133
Condition	trot glue footing	walk aluminum footing	-2.4695	-0.01042	-3.0557	0.5758
Condition	trot glue footing	walk barefoot footing	-2.5731	0.1184	-3.2200	0.7653
Condition	trot glue footing	walk glue footing	-1.4185	1.0311	-2.0006	1.6132
Condition	walk aluminum footing	walk barefoot footing	-1.3023	1.3276	-1.9334	1.9587
Condition	walk aluminum footing	walk glue footing	-0.1509	2.2435	-0.7208	2.8134
Condition	walk barefoot footing	walk glue footing	-0.2805	2.3479	-0.9113	2.9786

min: Overall Summary Statistics

Condition	SampleSize	Means	Medians	SD	SEM	Minimum	Maximum	FirstQuartile	ThirdQuartile	IQR
walk glue footing	11	15.7192	15.910	3.25918	0.98268	8.84013	19.3583	13.9720	18.8141	4.8421
trot glue footing	10	15.5831	15.464	3.08048	0.97413	8.87500	19.1790	14.4100	18.8250	4.4150
walk barefoot footing	8	17.0618	16.945	5.26061	1.85991	8.03700	25.2700	14.3838	20.2650	5.8812
trot barefoot footing	7	16.0771	15.530	4.76127	1.79959	8.63000	22.9600	12.6200	19.2300	6.6100

Condition	SampleSize	Means	Medians	SD	SEM	Minimum	Maximum	FirstQuartile	ThirdQuartile	IQR
walk aluminum footing	11	15.9309	15.280	4.06911	1.22688	7.92000	22.2500	13.0400	18.7500	5.7100
trot aluminum footing	12	16.2425	15.380	3.82171	1.10323	8.78000	24.7800	14.9400	18.5650	3.6250

min: Mixed Model Anova to assess the effects of Condition

The Mixed Procedure

Model Information	
Data Set	WORK.SDATA2
Dependent Variable	min
Covariance Structure	Variance Components
Estimation Method	REML
Residual Variance Method	Profile
Fixed Effects SE Method	Kenward-Roger
Degrees of Freedom Method	Kenward-Roger

Class Level Information		
Class	Levels	Values
HorseNo	15	Subject #1 Subject #10 Subject #11 Subject #12 Subject #13 Subject #14 Subject #15 Subject #2 Subject #3 Subject #4 Subject #5 Subject #6 Subject #7 Subject #8 Subject #9
Condition	6	trot aluminum footing trot barefoot footing trot glue footing walk aluminum footing walk barefoot footing walk glue footing

Covariance Parameter Estimates	
Cov Parm	**Estimate**
HorseNo	14.7197
Residual	3.9385

Type 3 Tests of Fixed Effects				
Effect	**Num DF**	**Den DF**	**F Value**	**Pr > F**
Condition	5	40.5	0.16	0.9743

Least Squares Means									
Effect	**Condition**	**Estimate**	**Standard Error**	**DF**	**t Value**	**Pr > |t|**	**Alpha**	**Lower**	**Upper**
Condition	trot aluminum footing	16.8166	1.2180	16	13.81	<.0001	0.05	14.2352	19.3980
Condition	trot barefoot footing	16.4627	1.3310	22.1	12.37	<.0001	0.05	13.7033	19.2222
Condition	trot glue footing	17.0629	1.2517	17.7	13.63	<.0001	0.05	14.4305	19.6953
Condition	walk aluminum footing	16.3878	1.2330	16.8	13.29	<.0001	0.05	13.7841	18.9915
Condition	walk barefoot footing	16.5381	1.2981	20.3	12.74	<.0001	0.05	13.8327	19.2436
Condition	walk glue footing	16.8866	1.2337	16.8	13.69	<.0001	0.05	14.2818	19.4915

Differences of Least Squares Means										
Effect	**Condition**	**Condition**	**Estimate**	**Standard Error**	**DF**	**t Value**	**Pr > |t|**	**Adjustment**	**Adj P**	**Alpha**
Condition	trot aluminum footing	trot barefoot footing	0.3538	0.9759	40.3	0.36	0.7188	Tukey-Kramer	0.9991	0.05
Condition	trot aluminum footing	trot glue footing	-0.2464	0.8588	40	-0.29	0.7757	Tukey-Kramer	0.9997	0.05
Condition	trot aluminum footing	walk aluminum footing	0.4288	0.8320	39.9	0.52	0.6092	Tukey-Kramer	0.9953	0.05
Condition	trot aluminum footing	walk barefoot footing	0.2784	0.9695	41.7	0.29	0.7754	Tukey-Kramer	0.9997	0.05
Condition	trot aluminum footing	walk glue footing	-0.07009	0.8330	39.9	-0.08	0.9334	Tukey-Kramer	1.0000	0.05
Condition	trot barefoot footing	trot glue footing	-0.6002	1.0315	40.5	-0.58	0.5639	Tukey-Kramer	0.9917	0.05
Condition	trot barefoot footing	walk aluminum footing	0.07494	1.0001	40.4	0.07	0.9406	Tukey-Kramer	1.0000	0.05
Condition	trot barefoot footing	walk barefoot footing	-0.07540	1.0560	40.9	-0.07	0.9434	Tukey-Kramer	1.0000	0.05
Condition	trot barefoot footing	walk glue footing	-0.4239	1.0026	40.4	-0.42	0.6747	Tukey-Kramer	0.9981	0.05
Condition	trot glue footing	walk aluminum footing	0.6751	0.8807	40	0.77	0.4478	Tukey-Kramer	0.9716	0.05
Condition	trot glue footing	walk barefoot footing	0.5248	1.0251	41.9	0.51	0.6114	Tukey-Kramer	0.9954	0.05
Condition	trot glue footing	walk glue footing	0.1763	0.8713	39.9	0.20	0.8407	Tukey-Kramer	0.9999	0.05
Condition	walk aluminum footing	walk barefoot footing	-0.1503	0.9937	41.8	-0.15	0.8805	Tukey-Kramer	1.0000	0.05
Condition	walk aluminum footing	walk glue footing	-0.4988	0.8549	40	-0.58	0.5628	Tukey-Kramer	0.9916	0.05
Condition	walk barefoot footing	walk glue footing	-0.3485	0.9962	41.8	-0.35	0.7282	Tukey-Kramer	0.9993	0.05

Differences of Least Squares Means						
Effect	Condition	Condition	Lower	Upper	Adj Lower	Adj Upper
Condition	trot aluminum footing	trot barefoot footing	-1.6182	2.3258	-2.5645	3.2722
Condition	trot aluminum footing	trot glue footing	-1.9822	1.4894	-2.8146	2.3219
Condition	trot aluminum footing	walk aluminum footing	-1.2530	2.1105	-2.0594	2.9169
Condition	trot aluminum footing	walk barefoot footing	-1.6784	2.2353	-2.6206	3.1774
Condition	trot aluminum footing	walk glue footing	-1.7537	1.6135	-2.5609	2.4207
Condition	trot barefoot footing	trot glue footing	-2.6841	1.4837	-3.6847	2.4843
Condition	trot barefoot footing	walk aluminum footing	-1.9457	2.0956	-2.9156	3.0655
Condition	trot barefoot footing	walk barefoot footing	-2.2082	2.0574	-3.2331	3.0823
Condition	trot barefoot footing	walk glue footing	-2.4497	1.6018	-3.4221	2.5743
Condition	trot glue footing	walk aluminum footing	-1.1048	2.4550	-1.9584	3.3086
Condition	trot glue footing	walk barefoot footing	-1.5441	2.5937	-2.5406	3.5902
Condition	trot glue footing	walk glue footing	-1.5849	1.9374	-2.4293	2.7818
Condition	walk aluminum footing	walk barefoot footing	-2.1560	1.8553	-3.1217	2.8210
Condition	walk aluminum footing	walk glue footing	-2.2266	1.2289	-3.0552	2.0575
Condition	walk barefoot footing	walk glue footing	-2.3592	1.6622	-3.3275	2.6304

max: Overall Summary Statistics

Condition	SampleSize	Means	Medians	SD	SEM	Minimum
walk glue footing	11	17.7307	17.910	3.57738	1.07862	9.5344
trot glue footing	10	17.3938	18.541	3.01471	0.95333	11.7746
walk barefoot footing	8	20.0971	19.545	5.88754	2.08156	10.9900
trot barefoot footing	7	19.6629	19.930	5.42703	2.05122	9.4800
walk aluminum footing	11	19.0000	18.580	3.86159	1.16431	11.7800
trot aluminum footing	12	18.8242	18.365	4.46092	1.28776	9.4500

Condition	Maximum	FirstQuartile	ThirdQuartile	IQR
walk glue footing	22.920	16.7800	19.4935	2.71350
trot glue footing	20.499	14.7520	19.8890	5.13700
walk barefoot footing	28.990	16.2485	24.6050	8.35655
trot barefoot footing	25.130	16.6600	23.9900	7.33000
walk aluminum footing	25.810	16.2800	21.1500	4.87000
trot aluminum footing	28.350	17.0150	20.7100	3.69500

max: Mixed Model Anova to assess the effects of Condition

The Mixed Procedure

Model Information	
Data Set	WORK.SDATA2
Dependent Variable	max
Covariance Structure	Variance Components
Estimation Method	REML
Residual Variance Method	Profile
Fixed Effects SE Method	Kenward-Roger
Degrees of Freedom Method	Kenward-Roger

Class Level Information		
Class	**Levels**	**Values**
HorseNo	15	Subject #1 Subject #10 Subject #11 Subject #12 Subject #13 Subject #14 Subject #15 Subject #2 Subject #3 Subject #4 Subject #5 Subject #6 Subject #7 Subject #8 Subject #9
Condition	6	trot aluminum footing trot barefoot footing trot glue footing walk aluminum footing walk barefoot footing walk glue footing

Covariance Parameter Estimates	
Cov Parm	**Estimate**
HorseNo	15.4947
Residual	5.7079

Type 3 Tests of Fixed Effects				
Effect	**Num DF**	**Den DF**	**F Value**	**Pr > F**
Condition	5	40.5	0.32	0.9009

Least Squares Means									
Effect	Condition	Estimate	Standard Error	DF	t Value	Pr > |t|	Alpha	Lower	Upper
Condition	trot aluminum footing	19.3895	1.3035	17.6	14.88	<.0001	0.05	16.6471	22.1319
Condition	trot barefoot footing	20.1867	1.4547	25.7	13.88	<.0001	0.05	17.1949	23.1784
Condition	trot glue footing	18.8901	1.3487	19.9	14.01	<.0001	0.05	16.0759	21.7043
Condition	walk aluminum footing	19.3523	1.3236	18.7	14.62	<.0001	0.05	16.5784	22.1261
Condition	walk barefoot footing	19.7075	1.4110	23.3	13.97	<.0001	0.05	16.7907	22.6243
Condition	walk glue footing	18.8674	1.3246	18.7	14.24	<.0001	0.05	16.0919	21.6428

Differences of Least Squares Means										
Effect	Condition	Condition	Estimate	Standard Error	DF	t Value	Pr > |t|	Adjustment	Adj P	Alpha
Condition	trot aluminum footing	trot barefoot footing	-0.7972	1.1744	40.2	-0.68	0.5011	Tukey-Kramer	0.9833	0.05
Condition	trot aluminum footing	trot glue footing	0.4994	1.0338	39.8	0.48	0.6317	Tukey-Kramer	0.9965	0.05
Condition	trot aluminum footing	walk aluminum footing	0.03719	1.0016	39.7	0.04	0.9706	Tukey-Kramer	1.0000	0.05
Condition	trot aluminum footing	walk barefoot footing	-0.3180	1.1640	42	-0.27	0.7860	Tukey-Kramer	0.9998	0.05
Condition	trot aluminum footing	walk glue footing	0.5221	1.0027	39.8	0.52	0.6055	Tukey-Kramer	0.9950	0.05
Condition	trot barefoot footing	trot glue footing	1.2966	1.2410	40.6	1.04	0.3023	Tukey-Kramer	0.8997	0.05
Condition	trot barefoot footing	walk aluminum footing	0.8344	1.2034	40.3	0.69	0.4920	Tukey-Kramer	0.9817	0.05

Differences of Least Squares Means										
Effect	**Condition**	**Condition**	**Estimate**	**Standard Error**	**DF**	**t Value**	**Pr > |t|**	**Adjustment**	**Adj P**	**Alpha**
Condition	trot barefoot footing	walk barefoot footing	0.4792	1.2693	40.9	0.38	0.7078	Tukey-Kramer	0.9989	0.05
Condition	trot barefoot footing	walk glue footing	1.3193	1.2064	40.4	1.09	0.2806	Tukey-Kramer	0.8811	0.05
Condition	trot glue footing	walk aluminum footing	-0.4622	1.0600	39.9	-0.44	0.6652	Tukey-Kramer	0.9979	0.05
Condition	trot glue footing	walk barefoot footing	-0.8174	1.2307	42.2	-0.66	0.5102	Tukey-Kramer	0.9849	0.05
Condition	trot glue footing	walk glue footing	0.02274	1.0489	39.7	0.02	0.9828	Tukey-Kramer	1.0000	0.05
Condition	walk aluminum footing	walk barefoot footing	-0.3552	1.1931	42	-0.30	0.7674	Tukey-Kramer	0.9997	0.05
Condition	walk aluminum footing	walk glue footing	0.4849	1.0290	39.8	0.47	0.6400	Tukey-Kramer	0.9969	0.05
Condition	walk barefoot footing	walk glue footing	0.8401	1.1960	42.1	0.70	0.4863	Tukey-Kramer	0.9806	0.05

Differences of Least Squares Means						
Effect	**Condition**	**Condition**	**Lower**	**Upper**	**Adj Lower**	**Adj Upper**
Condition	trot aluminum footing	trot barefoot footing	-3.1703	1.5759	-4.3091	2.7147
Condition	trot aluminum footing	trot glue footing	-1.5903	2.5890	-2.5921	3.5908
Condition	trot aluminum footing	walk aluminum footing	-1.9876	2.0620	-2.9581	3.0324
Condition	trot aluminum footing	walk barefoot footing	-2.6672	2.0311	-3.7990	3.1629
Condition	trot aluminum footing	walk glue footing	-1.5048	2.5490	-2.4763	3.5206

Differences of Least Squares Means						
Effect	**Condition**	**Condition**	**Lower**	**Upper**	**Adj Lower**	**Adj Upper**
Condition	trot barefoot footing	trot glue footing	-1.2104	3.8036	-2.4144	5.0075
Condition	trot barefoot footing	walk aluminum footing	-1.5971	3.2658	-2.7641	4.4329
Condition	trot barefoot footing	walk barefoot footing	-2.0845	3.0428	-3.3166	4.2750
Condition	trot barefoot footing	walk glue footing	-1.1181	3.7567	-2.2882	4.9268
Condition	trot glue footing	walk aluminum footing	-2.6048	1.6804	-3.6321	2.7078
Condition	trot glue footing	walk barefoot footing	-3.3007	1.6659	-4.4977	2.8629
Condition	trot glue footing	walk glue footing	-2.0976	2.1431	-3.1139	3.1594
Condition	walk aluminum footing	walk barefoot footing	-2.7629	2.0525	-3.9230	3.2125
Condition	walk aluminum footing	walk glue footing	-1.5951	2.5650	-2.5922	3.5621
Condition	walk barefoot footing	walk glue footing	-1.5734	3.2537	-2.7365	4.4168

5.4 Mixed model ANOVA for Ashalt vs footing

total_displacement: Overall Summary Statistics

asphalt_vs_footing	Condition1	SampleSize	Means	Medians	SD	SEM	Minimum	Maximur
asphalt	**walk glue**	15	2.23267	2.3900	0.57678	0.14892	0.8000	3.06
asphalt	**walk barefoot**	15	3.02667	2.9300	0.67256	0.17365	1.5800	4.41
asphalt	**walk aluminum**	15	1.96333	1.9700	0.48053	0.12407	1.1800	2.67

asphalt_vs_footing	Condition1	SampleSize	Means	Medians	SD	SEM	Minimum	Maximum
asphalt	**trot glue**	15	2.55667	2.5800	0.55118	0.14231	1.6100	3.45
asphalt	**trot barefoot**	15	3.28867	3.3700	0.61678	0.15925	2.1700	4.35
asphalt	**trot aluminum**	15	2.12467	2.0600	0.46563	0.12023	1.3300	3.01
footing	**walk glue**	11	2.01150	1.8647	1.51325	0.45626	0.1352	4.50
footing	**walk barefoot**	8	3.03529	2.8515	1.08533	0.38372	1.0899	4.35
footing	**walk aluminum**	11	3.06909	3.1100	0.92645	0.27934	1.4200	4.48
footing	**trot glue**	10	1.81067	1.3620	1.30280	0.41198	0.2630	3.87
footing	**trot barefoot**	7	3.58571	4.3900	2.06107	0.77901	0.5500	5.90
footing	**trot aluminum**	12	2.58167	2.9450	1.47731	0.42646	0.6700	4.85

asphalt_vs_footing	Condition1	FirstQuartile	ThirdQuartile	IQR
asphalt	**walk glue**	1.8500	2.6600	0.8100
asphalt	**walk barefoot**	2.6100	3.4100	0.8000
asphalt	**walk aluminum**	1.5500	2.3500	0.8000
asphalt	**trot glue**	2.2900	2.9600	0.6700
asphalt	**trot barefoot**	2.7400	3.7200	0.9800
asphalt	**trot aluminum**	1.9300	2.4100	0.4800
footing	**walk glue**	0.6466	3.2200	2.5734

asphalt_vs_footing	Condition1	FirstQuartile	ThirdQuartile	IQR
footing	walk barefoot	2.5447	4.0250	1.4803
footing	walk aluminum	2.3700	3.8600	1.4900
footing	trot glue	0.7070	2.8996	2.1926
footing	trot barefoot	0.8500	4.9700	4.1200
footing	trot aluminum	0.9150	3.6450	2.7300

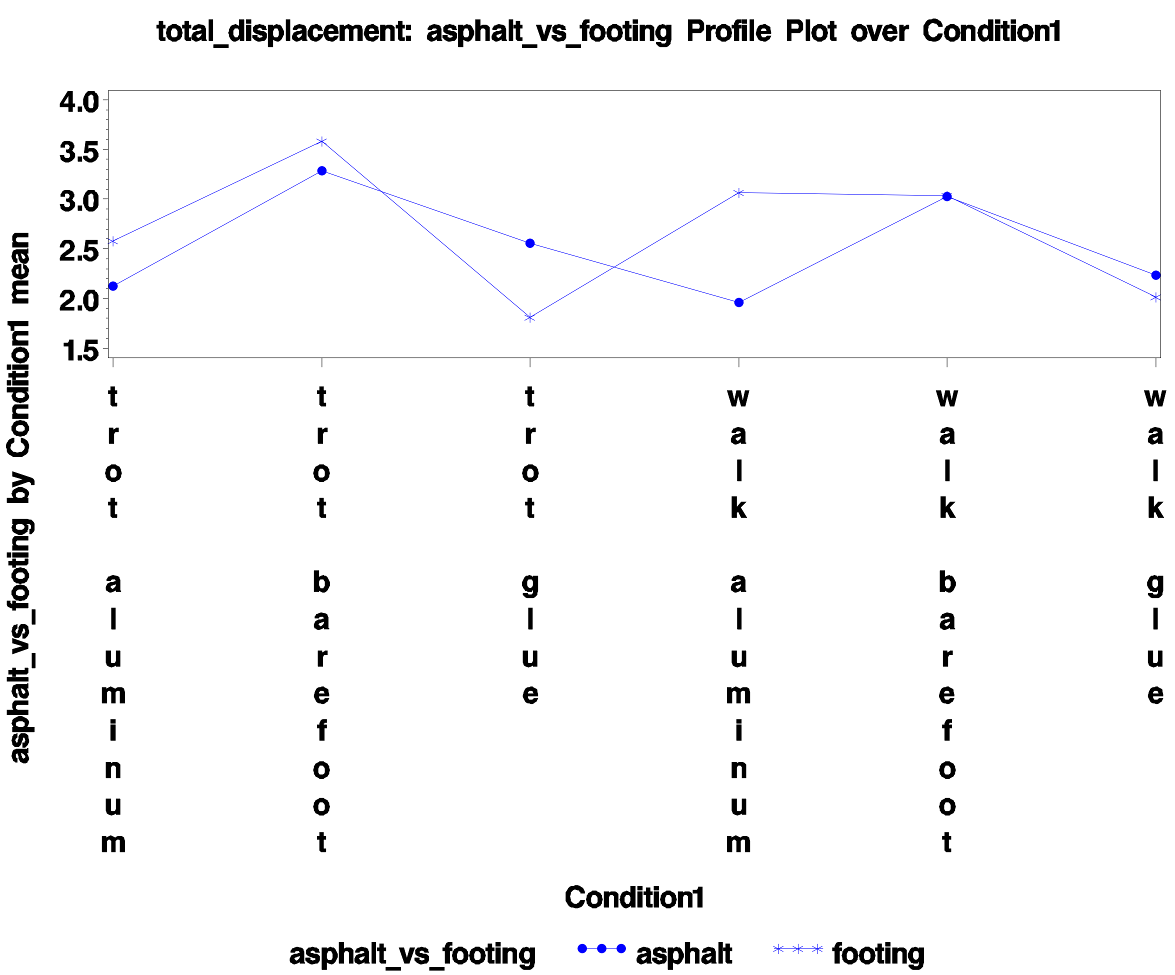

total_displacement: Mixed Model Anova to assess the effects of asphalt_vs_footing and Condition1

The GLIMMIX Procedure

Model Information	
Data Set	WORK.SDATA3
Response Variable	total_displacement
Response Distribution	Gaussian
Link Function	Identity
Variance Function	Default
Variance Matrix	Not blocked
Estimation Technique	Restricted Maximum Likelihood
Degrees of Freedom Method	Kenward-Roger
Fixed Effects SE Adjustment	Kenward-Roger

Class Level Information		
Class	**Levels**	**Values**
HorseNo	15	Subject #1 Subject #10 Subject #11 Subject #12 Subject #13 Subject #14 Subject #15 Subject #2 Subject #3 Subject #4 Subject #5 Subject #6 Subject #7 Subject #8 Subject #9
Condition1	6	trot aluminum trot barefoot trot glue walk aluminum walk barefoot walk glue
asphalt_vs_footing	2	asphalt footing

Covariance Parameter Estimates		
Cov Parm	**Estimate**	**Standard Error**
HorseNo	0.1607	0.09077
Residual	0.7936	0.1009

Type III Tests of Fixed Effects				
Effect	**Num DF**	**Den DF**	**F Value**	**Pr > F**
asphalt_vs_footing	1	130.3	1.49	0.2241
Condition1	5	124.7	7.64	<.0001
Condition*asphalt_vs	5	124.7	2.93	0.0156

total_displacement: Mixed Model Anova to assess the effects of asphalt_vs_footing and Condition1

The GLIMMIX Procedure
Condition*asphalt_vs
Least Squares Means

Condition1	asphalt_vs_footing	Estimate	Standard Error	DF	t Value	Pr > |t|
trot aluminum	asphalt	2.1247	0.2522	110	8.42	<.0001
trot aluminum	footing	2.5930	0.2797	120.1	9.27	<.0001
trot barefoot	asphalt	3.2887	0.2522	110	13.04	<.0001
trot barefoot	footing	3.7135	0.3593	134.4	10.33	<.0001
trot glue	asphalt	2.5567	0.2522	110	10.14	<.0001
trot glue	footing	1.8366	0.3041	126.8	6.04	<.0001
walk aluminum	asphalt	1.9633	0.2522	110	7.78	<.0001
walk aluminum	footing	3.0349	0.2910	123.6	10.43	<.0001
walk barefoot	asphalt	3.0267	0.2522	110	12.00	<.0001
walk barefoot	footing	3.1241	0.3374	132.3	9.26	<.0001

walk glue	asphalt	2.2327	0.2522	110	8.85	<.0001
walk glue	footing	2.0301	0.2910	123.5	6.98	<.0001

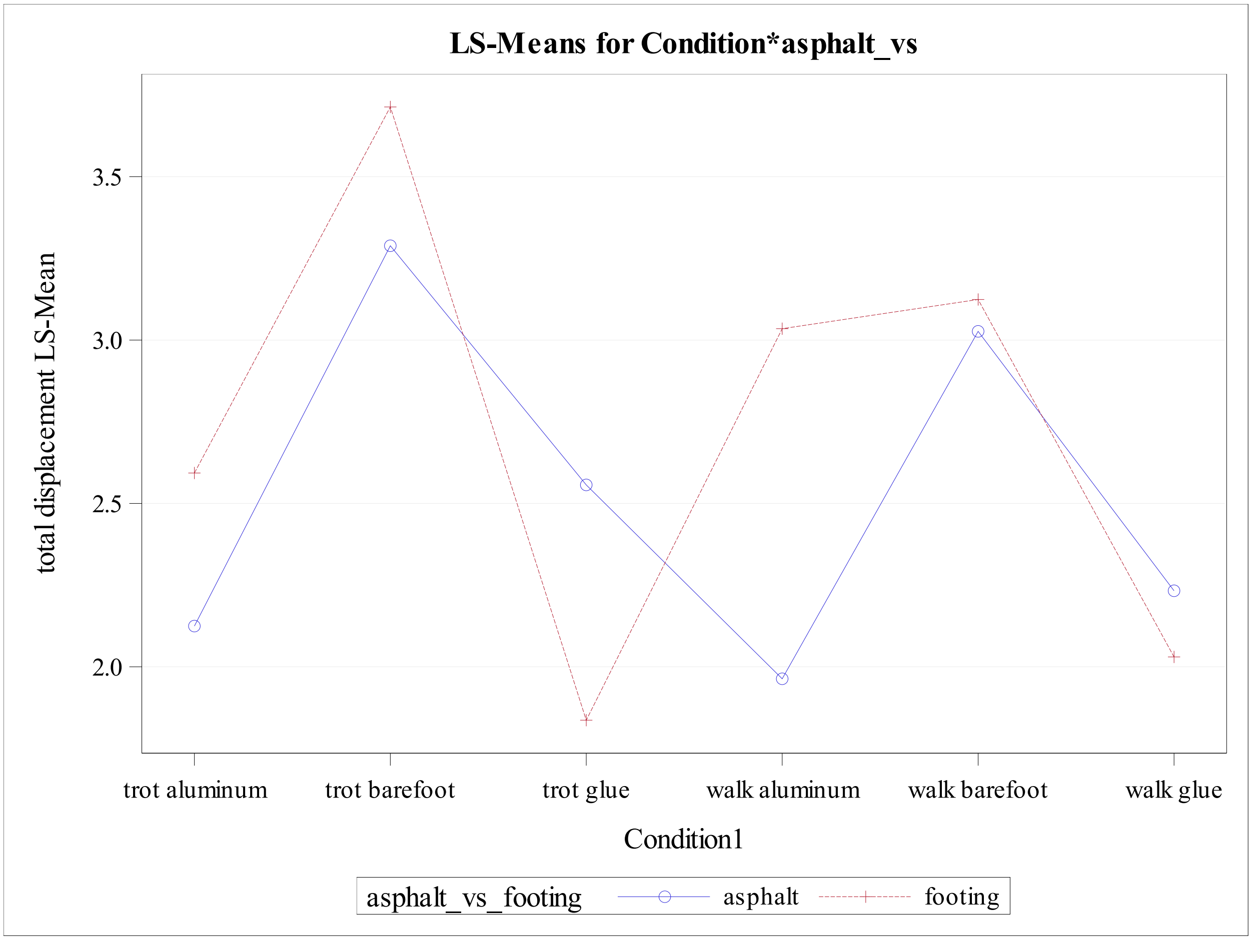

total_displacement: Mixed Model Anova to assess the effects of asphalt_vs_footing and Condition1

The GLIMMIX Procedure

Tests of Effect Slices for Condition*asphalt_vs Sliced By asphalt_vs_footing				
asphalt_vs_footing	Num DF	Den DF	F Value	Pr > F
asphalt	5	123.6	5.28	0.0002
footing	5	125.3	5.37	0.0002

Tests of Effect Slices for Condition*asphalt_vs Sliced By Condition1				
Condition1	Num DF	Den DF	F Value	Pr > F
trot aluminum	1	125.1	1.82	0.1795
trot barefoot	1	126.8	1.05	0.3066
trot glue	1	125.7	3.85	0.0519
walk aluminum	1	125.4	9.05	0.0032
walk barefoot	1	126.4	0.06	0.8055
walk glue	1	125.4	0.32	0.5707

Condition*asphalt_vs Least Squares Means									
Condition1	**asphalt_vs_footing**	**Estimate**	**Standard Error**	**DF**	**t Value**	**Pr > |t|**	**Alpha**	**Lower**	**Upper**
trot aluminum	asphalt	2.1247	0.2522	110	8.42	<.0001	0.05	1.6248	2.6245
trot aluminum	footing	2.5930	0.2797	120.1	9.27	<.0001	0.05	2.0393	3.1468
trot barefoot	asphalt	3.2887	0.2522	110	13.04	<.0001	0.05	2.7888	3.7885
trot barefoot	footing	3.7135	0.3593	134.4	10.33	<.0001	0.05	3.0028	4.4242
trot glue	asphalt	2.5567	0.2522	110	10.14	<.0001	0.05	2.0568	3.0565
trot glue	footing	1.8366	0.3041	126.8	6.04	<.0001	0.05	1.2349	2.4383
walk aluminum	asphalt	1.9633	0.2522	110	7.78	<.0001	0.05	1.4635	2.4632
walk aluminum	footing	3.0349	0.2910	123.6	10.43	<.0001	0.05	2.4589	3.6108
walk barefoot	asphalt	3.0267	0.2522	110	12.00	<.0001	0.05	2.5268	3.5265
walk barefoot	footing	3.1241	0.3374	132.3	9.26	<.0001	0.05	2.4567	3.7916
walk glue	asphalt	2.2327	0.2522	110	8.85	<.0001	0.05	1.7328	2.7325
walk glue	footing	2.0301	0.2910	123.5	6.98	<.0001	0.05	1.4541	2.6062

total_displacement: Mixed Model Anova to assess the effects of asphalt_vs_footing and Condition1

The GLIMMIX Procedure

Simple Effect Comparisons of Condition*asphalt_vs Least Squares Means By asphalt_vs_footing Adjustment for Multiple Comparisons: Tukey-Kramer									
Simple Effect Level	**Condition1**	**_Condition1**	**Estimate**	**Standard Error**	**DF**	**t Value**	**Pr > |t|**	**Adj P**	**Alpha**
asphalt_vs_footing asphalt	trot aluminum	trot barefoot	-1.1640	0.3253	123.6	-3.58	0.0005	0.0064	0.05
asphalt_vs_footing asphalt	trot aluminum	trot glue	-0.4320	0.3253	123.6	-1.33	0.1866	0.7689	0.05
asphalt_vs_footing asphalt	trot aluminum	walk aluminum	0.1613	0.3253	123.6	0.50	0.6208	0.9962	0.05
asphalt_vs_footing asphalt	trot aluminum	walk barefoot	-0.9020	0.3253	123.6	-2.77	0.0064	0.0687	0.05
asphalt_vs_footing asphalt	trot aluminum	walk glue	-0.1080	0.3253	123.6	-0.33	0.7404	0.9995	0.05
asphalt_vs_footing asphalt	trot barefoot	trot glue	0.7320	0.3253	123.6	2.25	0.0262	0.2227	0.05
asphalt_vs_footing asphalt	trot barefoot	walk aluminum	1.3253	0.3253	123.6	4.07	<.0001	0.0011	0.05
asphalt_vs_footing asphalt	trot barefoot	walk barefoot	0.2620	0.3253	123.6	0.81	0.4221	0.9661	0.05
asphalt_vs_footing asphalt	trot barefoot	walk glue	1.0560	0.3253	123.6	3.25	0.0015	0.0184	0.05
asphalt_vs_footing asphalt	trot glue	walk aluminum	0.5933	0.3253	123.6	1.82	0.0706	0.4542	0.05
asphalt_vs_footing asphalt	trot glue	walk barefoot	-0.4700	0.3253	123.6	-1.44	0.1510	0.6996	0.05
asphalt_vs_footing asphalt	trot glue	walk glue	0.3240	0.3253	123.6	1.00	0.3212	0.9184	0.05
asphalt_vs_footing asphalt	walk aluminum	walk barefoot	-1.0633	0.3253	123.6	-3.27	0.0014	0.0171	0.05
asphalt_vs_footing asphalt	walk aluminum	walk glue	-0.2693	0.3253	123.6	-0.83	0.4093	0.9618	0.05
asphalt_vs_footing asphalt	walk barefoot	walk glue	0.7940	0.3253	123.6	2.44	0.0161	0.1504	0.05
asphalt_vs_footing footing	trot aluminum	trot barefoot	-1.1205	0.4280	125.7	-2.62	0.0099	0.1006	0.05
asphalt_vs_footing footing	trot aluminum	trot glue	0.7565	0.3827	124.3	1.98	0.0503	0.3617	0.05
asphalt_vs_footing footing	trot aluminum	walk aluminum	-0.4418	0.3724	123.9	-1.19	0.2378	0.8427	0.05

Simple Effect Comparisons of Condition*asphalt_vs Least Squares Means By asphalt_vs_footing Adjustment for Multiple Comparisons: Tukey-Kramer									
Simple Effect Level	**Condition1**	**_Condition1**	**Estimate**	**Standard Error**	**DF**	**t Value**	**Pr > |t|**	**Adj P**	**Alpha**
asphalt_vs_footing footing	trot aluminum	walk barefoot	-0.5311	0.4118	126.4	-1.29	0.1995	0.7901	0.05
asphalt_vs_footing footing	trot aluminum	walk glue	0.5629	0.3725	124	1.51	0.1333	0.6577	0.05
asphalt_vs_footing footing	trot barefoot	trot glue	1.8769	0.4461	126.8	4.21	<.0001	0.0007	0.05
asphalt_vs_footing footing	trot barefoot	walk aluminum	0.6786	0.4363	126.2	1.56	0.1223	0.6292	0.05
asphalt_vs_footing footing	trot barefoot	walk barefoot	0.5894	0.4625	124.4	1.27	0.2050	0.7985	0.05
asphalt_vs_footing footing	trot barefoot	walk glue	1.6834	0.4364	126.3	3.86	0.0002	0.0025	0.05
asphalt_vs_footing footing	trot glue	walk aluminum	-1.1983	0.3913	124.7	-3.06	0.0027	0.0315	0.05
asphalt_vs_footing footing	trot glue	walk barefoot	-1.2875	0.4304	127.4	-2.99	0.0033	0.0384	0.05
asphalt_vs_footing footing	trot glue	walk glue	-0.1935	0.3899	124	-0.50	0.6205	0.9962	0.05
asphalt_vs_footing footing	walk aluminum	walk barefoot	-0.08927	0.4203	126.8	-0.21	0.8321	0.9999	0.05
asphalt_vs_footing footing	walk aluminum	walk glue	1.0047	0.3811	124.3	2.64	0.0095	0.0963	0.05
asphalt_vs_footing footing	walk barefoot	walk glue	1.0940	0.4204	126.9	2.60	0.0104	0.1043	0.05

total_displacement: Mixed Model Anova to assess the effects of asphalt_vs_footing and Condition1

The GLIMMIX Procedure

Simple Effect Comparisons of Condition*asphalt_vs Least Squares Means By asphalt_vs_footing Adjustment for Multiple Comparisons: Tukey-Kramer						
Simple Effect Level	**Condition1**	**_Condition1**	**Lower**	**Upper**	**Adj Lower**	**Adj Upper**
asphalt_vs_footing asphalt	trot aluminum	trot barefoot	-1.8078	-0.5202	-2.1055	-0.2225

Simple Effect Comparisons of Condition*asphalt_vs Least Squares Means By asphalt_vs_footing Adjustment for Multiple Comparisons: Tukey-Kramer						
Simple Effect Level	**Condition1**	**_Condition1**	**Lower**	**Upper**	**Adj Lower**	**Adj Upper**
asphalt_vs_footing asphalt	trot aluminum	trot glue	-1.0758	0.2118	-1.3735	0.5095
asphalt_vs_footing asphalt	trot aluminum	walk aluminum	-0.4825	0.8052	-0.7802	1.1029
asphalt_vs_footing asphalt	trot aluminum	walk barefoot	-1.5458	-0.2582	-1.8435	0.03953
asphalt_vs_footing asphalt	trot aluminum	walk glue	-0.7518	0.5358	-1.0495	0.8335
asphalt_vs_footing asphalt	trot barefoot	trot glue	0.08816	1.3758	-0.2095	1.6735
asphalt_vs_footing asphalt	trot barefoot	walk aluminum	0.6815	1.9692	0.3838	2.2669
asphalt_vs_footing asphalt	trot barefoot	walk barefoot	-0.3818	0.9058	-0.6795	1.2035
asphalt_vs_footing asphalt	trot barefoot	walk glue	0.4122	1.6998	0.1145	1.9975
asphalt_vs_footing asphalt	trot glue	walk aluminum	-0.05051	1.2372	-0.3482	1.5349
asphalt_vs_footing asphalt	trot glue	walk barefoot	-1.1138	0.1738	-1.4115	0.4715
asphalt_vs_footing asphalt	trot glue	walk glue	-0.3198	0.9678	-0.6175	1.2655
asphalt_vs_footing asphalt	walk aluminum	walk barefoot	-1.7072	-0.4195	-2.0049	-0.1218
asphalt_vs_footing asphalt	walk aluminum	walk glue	-0.9132	0.3745	-1.2109	0.6722
asphalt_vs_footing asphalt	walk barefoot	walk glue	0.1502	1.4378	-0.1475	1.7355
asphalt_vs_footing footing	trot aluminum	trot barefoot	-1.9675	-0.2734	-2.3594	0.1185
asphalt_vs_footing footing	trot aluminum	trot glue	-0.00108	1.5140	-0.3514	1.8643
asphalt_vs_footing footing	trot aluminum	walk aluminum	-1.1790	0.2953	-1.5198	0.6362
asphalt_vs_footing footing	trot aluminum	walk barefoot	-1.3460	0.2838	-1.7230	0.6608

Simple Effect Comparisons of Condition*asphalt_vs Least Squares Means By asphalt_vs_footing Adjustment for Multiple Comparisons: Tukey-Kramer						
Simple Effect Level	**Condition1**	**_Condition1**	**Lower**	**Upper**	**Adj Lower**	**Adj Upper**
asphalt_vs_footing footing	trot aluminum	walk glue	-0.1743	1.3002	-0.5152	1.6411
asphalt_vs_footing footing	trot barefoot	trot glue	0.9941	2.7598	0.5856	3.1683
asphalt_vs_footing footing	trot barefoot	walk aluminum	-0.1848	1.5420	-0.5842	1.9415
asphalt_vs_footing footing	trot barefoot	walk barefoot	-0.3261	1.5048	-0.7494	1.9281
asphalt_vs_footing footing	trot barefoot	walk glue	0.8198	2.5470	0.4202	2.9465
asphalt_vs_footing footing	trot glue	walk aluminum	-1.9727	-0.4238	-2.3309	-0.06565
asphalt_vs_footing footing	trot glue	walk barefoot	-2.1391	-0.4360	-2.5332	-0.04187
asphalt_vs_footing footing	trot glue	walk glue	-0.9653	0.5782	-1.3221	0.9350
asphalt_vs_footing footing	walk aluminum	walk barefoot	-0.9209	0.7424	-1.3057	1.1272
asphalt_vs_footing footing	walk aluminum	walk glue	0.2504	1.7591	-0.09850	2.1080
asphalt_vs_footing footing	walk barefoot	walk glue	0.2622	1.9258	-0.1228	2.3108

total_displacement: Mixed Model Anova to assess the effects of asphalt_vs_footing and Condition1

The GLIMMIX Procedure

Simple Effect Comparisons of Condition*asphalt_vs Least Squares Means By Condition1 Adjustment for Multiple Comparisons: Tukey-Kramer									
Simple Effect Level	asphalt_vs_footing	_asphalt_vs_footing	Estimate	Standard Error	DF	t Value	Pr > |t|	Adj P	Alpha
Condition1 trot aluminum	asphalt	footing	-0.4684	0.3470	125.1	-1.35	0.1795	0.1795	0.05
Condition1 trot barefoot	asphalt	footing	-0.4248	0.4139	126.8	-1.03	0.3066	0.3067	0.05
Condition1 trot glue	asphalt	footing	0.7201	0.3669	125.7	1.96	0.0519	0.0520	0.05
Condition1 walk aluminum	asphalt	footing	-1.0715	0.3562	125.4	-3.01	0.0032	0.0032	0.05
Condition1 walk barefoot	asphalt	footing	-0.09747	0.3950	126.4	-0.25	0.8055	0.8055	0.05
Condition1 walk glue	asphalt	footing	0.2025	0.3562	125.4	0.57	0.5707	0.5707	0.05

Simple Effect Comparisons of Condition*asphalt_vs Least Squares Means By Condition1 Adjustment for Multiple Comparisons: Tukey-Kramer						
Simple Effect Level	asphalt_vs_footing	_asphalt_vs_footing	Lower	Upper	Adj Lower	Adj Upper
Condition1 trot aluminum	asphalt	footing	-1.1551	0.2184	-1.1551	0.2184
Condition1 trot barefoot	asphalt	footing	-1.2439	0.3942	-1.2440	0.3943
Condition1 trot glue	asphalt	footing	-0.00612	1.4463	-0.00618	1.4463
Condition1 walk aluminum	asphalt	footing	-1.7764	-0.3666	-1.7765	-0.3666
Condition1 walk barefoot	asphalt	footing	-0.8792	0.6842	-0.8793	0.6843
Condition1 walk glue	asphalt	footing	-0.5025	0.9075	-0.5025	0.9075

total_displacement: Mixed Model Anova to assess the effects of asphalt_vs_footing and Condition1

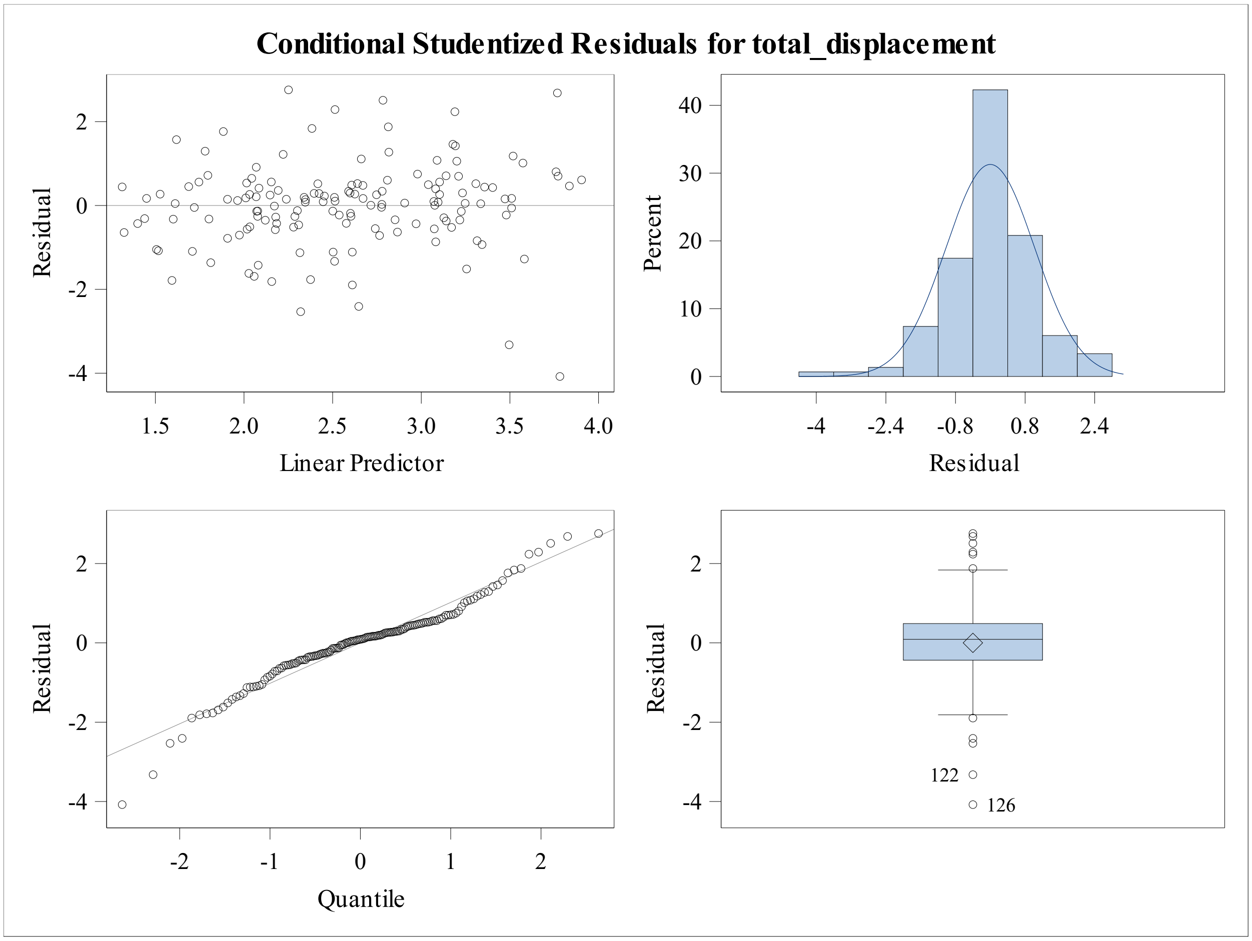

min: Overall Summary Statistics

asphalt_vs_footing	Condition1	SampleSize	Means	Medians	SD	SEM	Minimum	Maximum
asphalt	walk glue	15	16.9513	15.890	4.00580	1.03429	8.55000	25.4000
asphalt	walk barefoot	15	16.4640	14.960	4.13761	1.06833	8.33000	25.5200
asphalt	walk aluminum	15	16.7927	15.280	4.25558	1.09879	8.78000	25.8700
asphalt	trot glue	15	16.9640	16.060	4.15417	1.07260	8.55000	25.9400
asphalt	trot barefoot	15	16.7400	15.570	4.34951	1.12304	7.79000	26.1200

asphalt_vs_footing	Condition1	SampleSize	Means	Medians	SD	SEM	Minimum	Maximum
asphalt	**trot aluminum**	15	16.9627	15.510	4.35193	1.12366	7.90000	26.2200
footing	**walk glue**	11	15.7192	15.910	3.25918	0.98268	8.84013	19.3583
footing	**walk barefoot**	8	17.0618	16.945	5.26061	1.85991	8.03700	25.2700
footing	**walk aluminum**	11	15.9309	15.280	4.06911	1.22688	7.92000	22.2500
footing	**trot glue**	10	15.5831	15.464	3.08048	0.97413	8.87500	19.1790
footing	**trot barefoot**	7	16.0771	15.530	4.76127	1.79959	8.63000	22.9600
footing	**trot aluminum**	12	16.2425	15.380	3.82171	1.10323	8.78000	24.7800

asphalt_vs_footing	Condition1	FirstQuartile	ThirdQuartile	IQR
asphalt	**walk glue**	14.4800	19.1100	4.6300
asphalt	**walk barefoot**	14.2300	18.8500	4.6200
asphalt	**walk aluminum**	13.6300	19.3700	5.7400
asphalt	**trot glue**	14.1700	19.1200	4.9500
asphalt	**trot barefoot**	13.5000	19.2400	5.7400
asphalt	**trot aluminum**	14.3500	19.6900	5.3400
footing	**walk glue**	13.9720	18.8141	4.8421
footing	**walk barefoot**	14.3838	20.2650	5.8812
footing	**walk aluminum**	13.0400	18.7500	5.7100

asphalt_vs_footing	Condition1	FirstQuartile	ThirdQuartile	IQR
footing	trot glue	14.4100	18.8250	4.4150
footing	trot barefoot	12.6200	19.2300	6.6100
footing	trot aluminum	14.9400	18.5650	3.6250

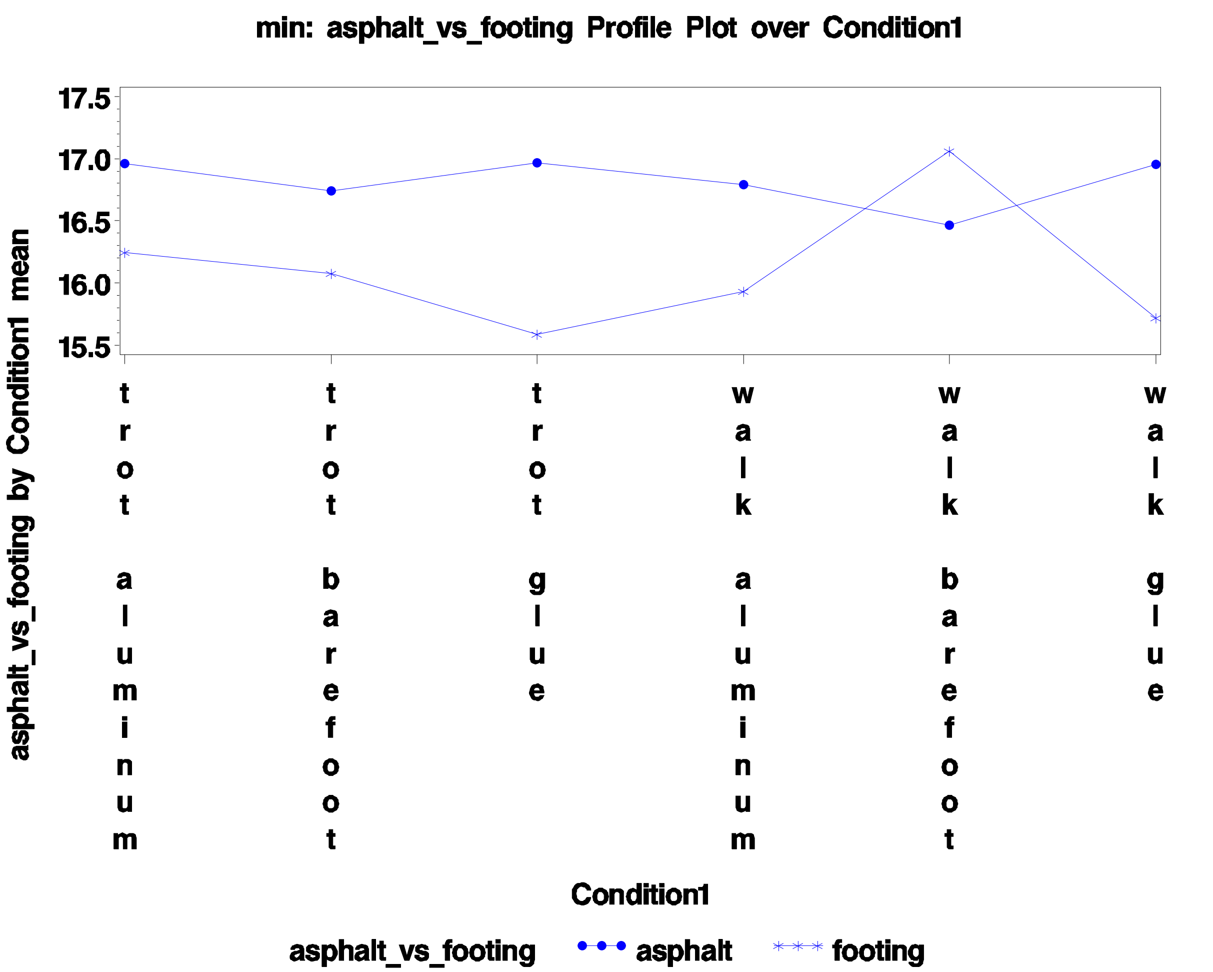

min: Mixed Model Anova to assess the effects of asphalt_vs_footing and Condition1

The GLIMMIX Procedure

Model Information	
Data Set	WORK.SDATA3
Response Variable	min
Response Distribution	Gaussian
Link Function	Identity
Variance Function	Default
Variance Matrix	Not blocked
Estimation Technique	Restricted Maximum Likelihood
Degrees of Freedom Method	Kenward-Roger
Fixed Effects SE Adjustment	Kenward-Roger

Class Level Information		
Class	**Levels**	**Values**
HorseNo	15	Subject #1 Subject #10 Subject #11 Subject #12 Subject #13 Subject #14 Subject #15 Subject #2 Subject #3 Subject #4 Subject #5 Subject #6 Subject #7 Subject #8 Subject #9
Condition1	6	trot aluminum trot barefoot trot glue walk aluminum walk barefoot walk glue
asphalt_vs_footing	2	asphalt footing

Covariance Parameter Estimates		
Cov Parm	**Estimate**	**Standard Error**
HorseNo	16.4440	6.2815
Residual	1.5267	0.1947

Type III Tests of Fixed Effects				
Effect	**Num DF**	**Den DF**	**F Value**	**Pr > F**
asphalt_vs_footing	1	123.3	0.23	0.6347
Condition1	5	123	0.82	0.5396
Condition*asphalt_vs	5	123	0.15	0.9801

min: Mixed Model Anova to assess the effects of asphalt_vs_footing and Condition1

The GLIMMIX Procedure

Condition*asphalt_vs Least Squares Means						
Condition1	**asphalt_vs_footing**	**Estimate**	**Standard Error**	**DF**	**t Value**	**Pr > |t|**
trot aluminum	asphalt	16.9627	1.0946	16.36	15.50	<.0001
trot aluminum	footing	17.0468	1.1079	17.16	15.39	<.0001
trot barefoot	asphalt	16.7400	1.0946	16.36	15.29	<.0001
trot barefoot	footing	16.8215	1.1521	20	14.60	<.0001
trot glue	asphalt	16.9640	1.0946	16.36	15.50	<.0001
trot glue	footing	17.3451	1.1205	17.94	15.48	<.0001
walk aluminum	asphalt	16.7927	1.0946	16.36	15.34	<.0001
walk aluminum	footing	16.5750	1.1136	17.51	14.88	<.0001
walk barefoot	asphalt	16.4640	1.0946	16.36	15.04	<.0001
walk barefoot	footing	16.6054	1.1390	19.13	14.58	<.0001
walk glue	asphalt	16.9513	1.0946	16.36	15.49	<.0001
walk glue	footing	17.1055	1.1137	17.51	15.36	<.0001

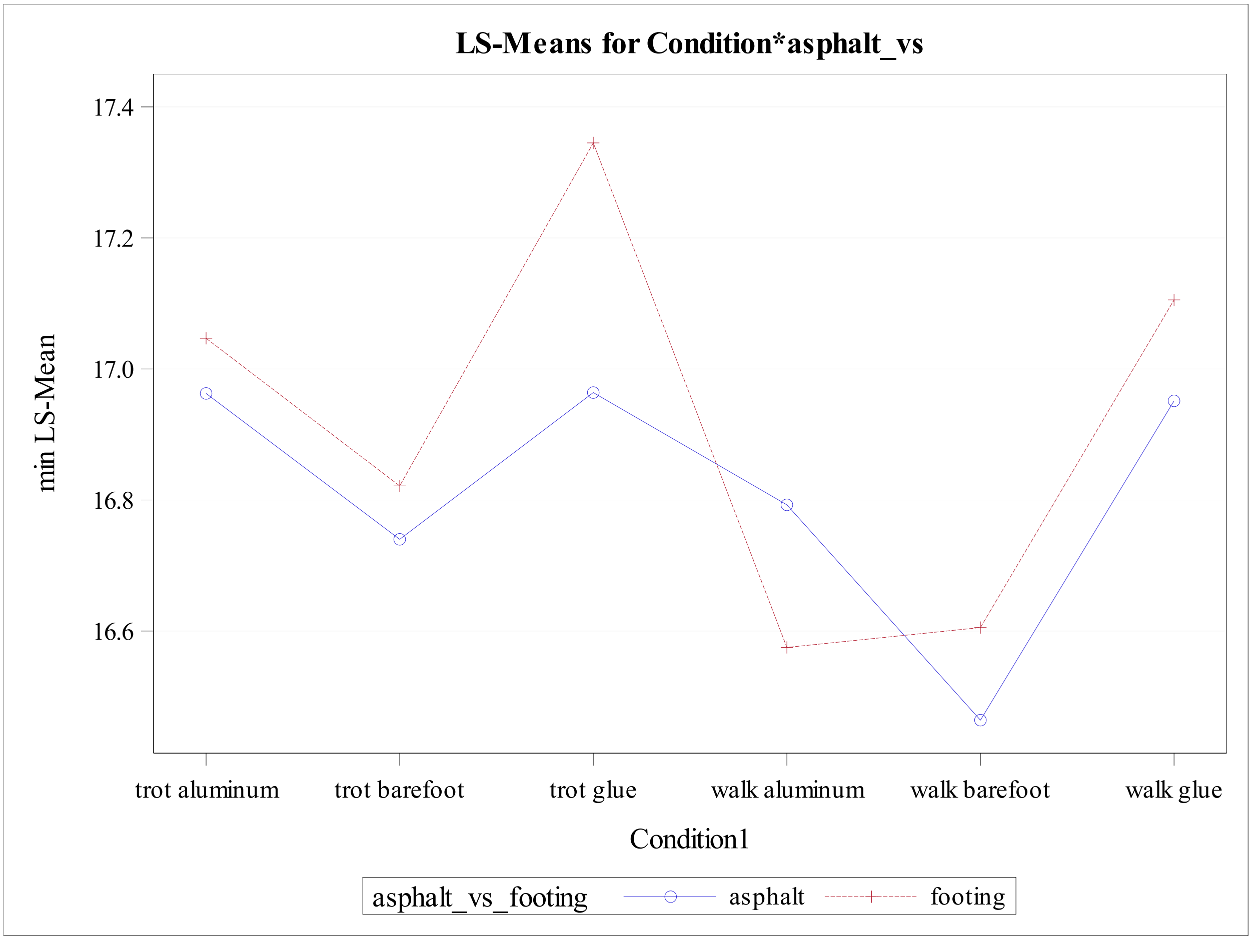

min: Mixed Model Anova to assess the effects of asphalt_vs_footing and Condition1

The GLIMMIX Procedure

Tests of Effect Slices for Condition*asphalt_vs Sliced By asphalt_vs_footing				
asphalt_vs_footing	**Num DF**	**Den DF**	**F Value**	**Pr > F**
asphalt	5	123	0.38	0.8637
footing	5	123	0.57	0.7196

Tests of Effect Slices for Condition*asphalt_vs Sliced By Condition1				
Condition1	Num DF	Den DF	F Value	Pr > F
trot aluminum	1	123	0.03	0.8619
trot barefoot	1	123.1	0.02	0.8878
trot glue	1	123.1	0.56	0.4571
walk aluminum	1	123.1	0.19	0.6613
walk barefoot	1	123.1	0.07	0.7977
walk glue	1	123.1	0.10	0.7564

Condition*asphalt_vs Least Squares Means									
Condition1	asphalt_vs_footing	Estimate	Standard Error	DF	t Value	Pr > |t|	Alpha	Lower	Upper
trot aluminum	asphalt	16.9627	1.0946	16.36	15.50	<.0001	0.05	14.6464	19.2789
trot aluminum	footing	17.0468	1.1079	17.16	15.39	<.0001	0.05	14.7110	19.3827
trot barefoot	asphalt	16.7400	1.0946	16.36	15.29	<.0001	0.05	14.4238	19.0562
trot barefoot	footing	16.8215	1.1521	20	14.60	<.0001	0.05	14.4182	19.2248
trot glue	asphalt	16.9640	1.0946	16.36	15.50	<.0001	0.05	14.6478	19.2802
trot glue	footing	17.3451	1.1205	17.94	15.48	<.0001	0.05	14.9905	19.6997

Condition*asphalt_vs Least Squares Means									
Condition1	asphalt_vs_footing	Estimate	Standard Error	DF	t Value	Pr > |t|	Alpha	Lower	Upper
walk aluminum	asphalt	16.7927	1.0946	16.36	15.34	<.0001	0.05	14.4764	19.1089
walk aluminum	footing	16.5750	1.1136	17.51	14.88	<.0001	0.05	14.2307	18.9193
walk barefoot	asphalt	16.4640	1.0946	16.36	15.04	<.0001	0.05	14.1478	18.7802
walk barefoot	footing	16.6054	1.1390	19.13	14.58	<.0001	0.05	14.2224	18.9883
walk glue	asphalt	16.9513	1.0946	16.36	15.49	<.0001	0.05	14.6351	19.2676
walk glue	footing	17.1055	1.1137	17.51	15.36	<.0001	0.05	14.7611	19.4499

min: Mixed Model Anova to assess the effects of asphalt_vs_footing and Condition1

The GLIMMIX Procedure

Simple Effect Comparisons of Condition*asphalt_vs Least Squares Means By asphalt_vs_footing Adjustment for Multiple Comparisons: Tukey-Kramer									
Simple Effect Level	Condition1	_Condition1	Estimate	Standard Error	DF	t Value	Pr > |t|	Adj P	Alpha
asphalt_vs_footing asphalt	trot aluminum	trot barefoot	0.2227	0.4512	123	0.49	0.6225	0.9963	0.05
asphalt_vs_footing asphalt	trot aluminum	trot glue	-0.00133	0.4512	123	-0.00	0.9976	1.0000	0.05
asphalt_vs_footing asphalt	trot aluminum	walk aluminum	0.1700	0.4512	123	0.38	0.7070	0.9990	0.05
asphalt_vs_footing asphalt	trot aluminum	walk barefoot	0.4987	0.4512	123	1.11	0.2712	0.8784	0.05
asphalt_vs_footing asphalt	trot aluminum	walk glue	0.01133	0.4512	123	0.03	0.9800	1.0000	0.05

Simple Effect Comparisons of Condition*asphalt_vs Least Squares Means By asphalt_vs_footing Adjustment for Multiple Comparisons: Tukey-Kramer									
Simple Effect Level	**Condition1**	**_Condition1**	**Estimate**	**Standard Error**	**DF**	**t Value**	**Pr > |t|**	**Adj P**	**Alpha**
asphalt_vs_footing asphalt	trot barefoot	trot glue	-0.2240	0.4512	123	-0.50	0.6204	0.9962	0.05
asphalt_vs_footing asphalt	trot barefoot	walk aluminum	-0.05267	0.4512	123	-0.12	0.9073	1.0000	0.05
asphalt_vs_footing asphalt	trot barefoot	walk barefoot	0.2760	0.4512	123	0.61	0.5418	0.9900	0.05
asphalt_vs_footing asphalt	trot barefoot	walk glue	-0.2113	0.4512	123	-0.47	0.6403	0.9971	0.05
asphalt_vs_footing asphalt	trot glue	walk aluminum	0.1713	0.4512	123	0.38	0.7048	0.9990	0.05
asphalt_vs_footing asphalt	trot glue	walk barefoot	0.5000	0.4512	123	1.11	0.2699	0.8772	0.05
asphalt_vs_footing asphalt	trot glue	walk glue	0.01267	0.4512	123	0.03	0.9776	1.0000	0.05
asphalt_vs_footing asphalt	walk aluminum	walk barefoot	0.3287	0.4512	123	0.73	0.4677	0.9781	0.05
asphalt_vs_footing asphalt	walk aluminum	walk glue	-0.1587	0.4512	123	-0.35	0.7257	0.9993	0.05
asphalt_vs_footing asphalt	walk barefoot	walk glue	-0.4873	0.4512	123	-1.08	0.2822	0.8884	0.05
asphalt_vs_footing footing	trot aluminum	trot barefoot	0.2253	0.5955	123	0.38	0.7058	0.9990	0.05
asphalt_vs_footing footing	trot aluminum	trot glue	-0.2982	0.5314	123	-0.56	0.5757	0.9933	0.05
asphalt_vs_footing footing	trot aluminum	walk aluminum	0.4718	0.5168	123	0.91	0.3630	0.9425	0.05
asphalt_vs_footing footing	trot aluminum	walk barefoot	0.4415	0.5737	123.1	0.77	0.4431	0.9721	0.05
asphalt_vs_footing footing	trot aluminum	walk glue	-0.05863	0.5169	123	-0.11	0.9099	1.0000	0.05
asphalt_vs_footing footing	trot barefoot	trot glue	-0.5235	0.6218	123.1	-0.84	0.4014	0.9590	0.05
asphalt_vs_footing footing	trot barefoot	walk aluminum	0.2465	0.6074	123.1	0.41	0.6855	0.9986	0.05
asphalt_vs_footing footing	trot barefoot	walk barefoot	0.2162	0.6424	123	0.34	0.7371	0.9994	0.05
asphalt_vs_footing footing	trot barefoot	walk glue	-0.2839	0.6077	123.1	-0.47	0.6412	0.9972	0.05
asphalt_vs_footing footing	trot glue	walk aluminum	0.7701	0.5435	123	1.42	0.1591	0.7168	0.05

Simple Effect Comparisons of Condition*asphalt_vs Least Squares Means By asphalt_vs_footing Adjustment for Multiple Comparisons: Tukey-Kramer									
Simple Effect Level	**Condition1**	**_Condition1**	**Estimate**	**Standard Error**	**DF**	**t Value**	**Pr > |t|**	**Adj P**	**Alpha**
asphalt_vs_footing footing	trot glue	walk barefoot	0.7397	0.6006	123.1	1.23	0.2204	0.8205	0.05
asphalt_vs_footing footing	trot glue	walk glue	0.2396	0.5411	123	0.44	0.6586	0.9978	0.05
asphalt_vs_footing footing	walk aluminum	walk barefoot	-0.03036	0.5859	123.1	-0.05	0.9588	1.0000	0.05
asphalt_vs_footing footing	walk aluminum	walk glue	-0.5305	0.5292	123	-1.00	0.3181	0.9163	0.05
asphalt_vs_footing footing	walk barefoot	walk glue	-0.5001	0.5862	123.1	-0.85	0.3952	0.9566	0.05

min: Mixed Model Anova to assess the effects of asphalt_vs_footing and Condition1

The GLIMMIX Procedure

Simple Effect Comparisons of Condition*asphalt_vs Least Squares Means By asphalt_vs_footing Adjustment for Multiple Comparisons: Tukey-Kramer						
Simple Effect Level	**Condition1**	**_Condition1**	**Lower**	**Upper**	**Adj Lower**	**Adj Upper**
asphalt_vs_footing asphalt	trot aluminum	trot barefoot	-0.6704	1.1157	-1.0836	1.5289
asphalt_vs_footing asphalt	trot aluminum	trot glue	-0.8944	0.8917	-1.3076	1.3049
asphalt_vs_footing asphalt	trot aluminum	walk aluminum	-0.7231	1.0631	-1.1362	1.4762
asphalt_vs_footing asphalt	trot aluminum	walk barefoot	-0.3944	1.3917	-0.8076	1.8049
asphalt_vs_footing asphalt	trot aluminum	walk glue	-0.8817	0.9044	-1.2949	1.3176
asphalt_vs_footing asphalt	trot barefoot	trot glue	-1.1171	0.6691	-1.5302	1.0822

Simple Effect Comparisons of Condition*asphalt_vs Least Squares Means By asphalt_vs_footing Adjustment for Multiple Comparisons: Tukey-Kramer						
Simple Effect Level	**Condition1**	**_Condition1**	**Lower**	**Upper**	**Adj Lower**	**Adj Upper**
asphalt_vs_footing asphalt	trot barefoot	walk aluminum	-0.9457	0.8404	-1.3589	1.2536
asphalt_vs_footing asphalt	trot barefoot	walk barefoot	-0.6171	1.1691	-1.0302	1.5822
asphalt_vs_footing asphalt	trot barefoot	walk glue	-1.1044	0.6817	-1.5176	1.0949
asphalt_vs_footing asphalt	trot glue	walk aluminum	-0.7217	1.0644	-1.1349	1.4776
asphalt_vs_footing asphalt	trot glue	walk barefoot	-0.3931	1.3931	-0.8062	1.8062
asphalt_vs_footing asphalt	trot glue	walk glue	-0.8804	0.9057	-1.2936	1.3189
asphalt_vs_footing asphalt	walk aluminum	walk barefoot	-0.5644	1.2217	-0.9776	1.6349
asphalt_vs_footing asphalt	walk aluminum	walk glue	-1.0517	0.7344	-1.4649	1.1476
asphalt_vs_footing asphalt	walk barefoot	walk glue	-1.3804	0.4057	-1.7936	0.8189
asphalt_vs_footing footing	trot aluminum	trot barefoot	-0.9534	1.4040	-1.4987	1.9493
asphalt_vs_footing footing	trot aluminum	trot glue	-1.3501	0.7536	-1.8367	1.2402
asphalt_vs_footing footing	trot aluminum	walk aluminum	-0.5511	1.4948	-1.0244	1.9680
asphalt_vs_footing footing	trot aluminum	walk barefoot	-0.6941	1.5770	-1.2194	2.1024
asphalt_vs_footing footing	trot aluminum	walk glue	-1.0818	0.9645	-1.5551	1.4379
asphalt_vs_footing footing	trot barefoot	trot glue	-1.7543	0.7072	-2.3237	1.2766

Simple Effect Comparisons of Condition*asphalt_vs Least Squares Means By asphalt_vs_footing Adjustment for Multiple Comparisons: Tukey-Kramer						
Simple Effect Level	**Condition1**	**_Condition1**	**Lower**	**Upper**	**Adj Lower**	**Adj Upper**
asphalt_vs_footing footing	trot barefoot	walk aluminum	-0.9558	1.4489	-1.5120	2.0051
asphalt_vs_footing footing	trot barefoot	walk barefoot	-1.0555	1.4878	-1.6438	2.0761
asphalt_vs_footing footing	trot barefoot	walk glue	-1.4868	0.9189	-2.0433	1.4754
asphalt_vs_footing footing	trot glue	walk aluminum	-0.3058	1.8459	-0.8035	2.3437
asphalt_vs_footing footing	trot glue	walk barefoot	-0.4491	1.9285	-0.9990	2.4785
asphalt_vs_footing footing	trot glue	walk glue	-0.8314	1.3106	-1.3268	1.8060
asphalt_vs_footing footing	walk aluminum	walk barefoot	-1.1901	1.1294	-1.7267	1.6660
asphalt_vs_footing footing	walk aluminum	walk glue	-1.5779	0.5170	-2.0625	1.0015
asphalt_vs_footing footing	walk barefoot	walk glue	-1.6604	0.6602	-2.1971	1.1969

min: Mixed Model Anova to assess the effects of asphalt_vs_footing and Condition1

The GLIMMIX Procedure

Simple Effect Comparisons of Condition*asphalt_vs Least Squares Means By Condition1 Adjustment for Multiple Comparisons: Tukey-Kramer									
Simple Effect Level	asphalt_vs_footing	_asphalt_vs_footing	Estimate	Standard Error	DF	t Value	Pr > |t|	Adj P	Alpha
Condition1 trot aluminum	asphalt	footing	-0.08417	0.4827	123	-0.17	0.8619	0.8619	0.05
Condition1 trot barefoot	asphalt	footing	-0.08154	0.5770	123.1	-0.14	0.8878	0.8878	0.05
Condition1 trot glue	asphalt	footing	-0.3811	0.5108	123.1	-0.75	0.4571	0.4571	0.05
Condition1 walk aluminum	asphalt	footing	0.2177	0.4956	123.1	0.44	0.6613	0.6613	0.05
Condition1 walk barefoot	asphalt	footing	-0.1414	0.5504	123.1	-0.26	0.7977	0.7977	0.05
Condition1 walk glue	asphalt	footing	-0.1541	0.4957	123.1	-0.31	0.7564	0.7564	0.05

Simple Effect Comparisons of Condition*asphalt_vs Least Squares Means By Condition1 Adjustment for Multiple Comparisons: Tukey-Kramer						
Simple Effect Level	asphalt_vs_footing	_asphalt_vs_footing	Lower	Upper	Adj Lower	Adj Upper
Condition1 trot aluminum	asphalt	footing	-1.0396	0.8713	-1.0396	0.8713
Condition1 trot barefoot	asphalt	footing	-1.2237	1.0606	-1.2237	1.0606
Condition1 trot glue	asphalt	footing	-1.3922	0.6301	-1.3922	0.6301
Condition1 walk aluminum	asphalt	footing	-0.7634	1.1987	-0.7634	1.1987
Condition1 walk barefoot	asphalt	footing	-1.2309	0.9481	-1.2309	0.9481
Condition1 walk glue	asphalt	footing	-1.1354	0.8271	-1.1354	0.8271

min: Mixed Model Anova to assess the effects of asphalt_vs_footing and Condition1

The GLIMMIX Procedure

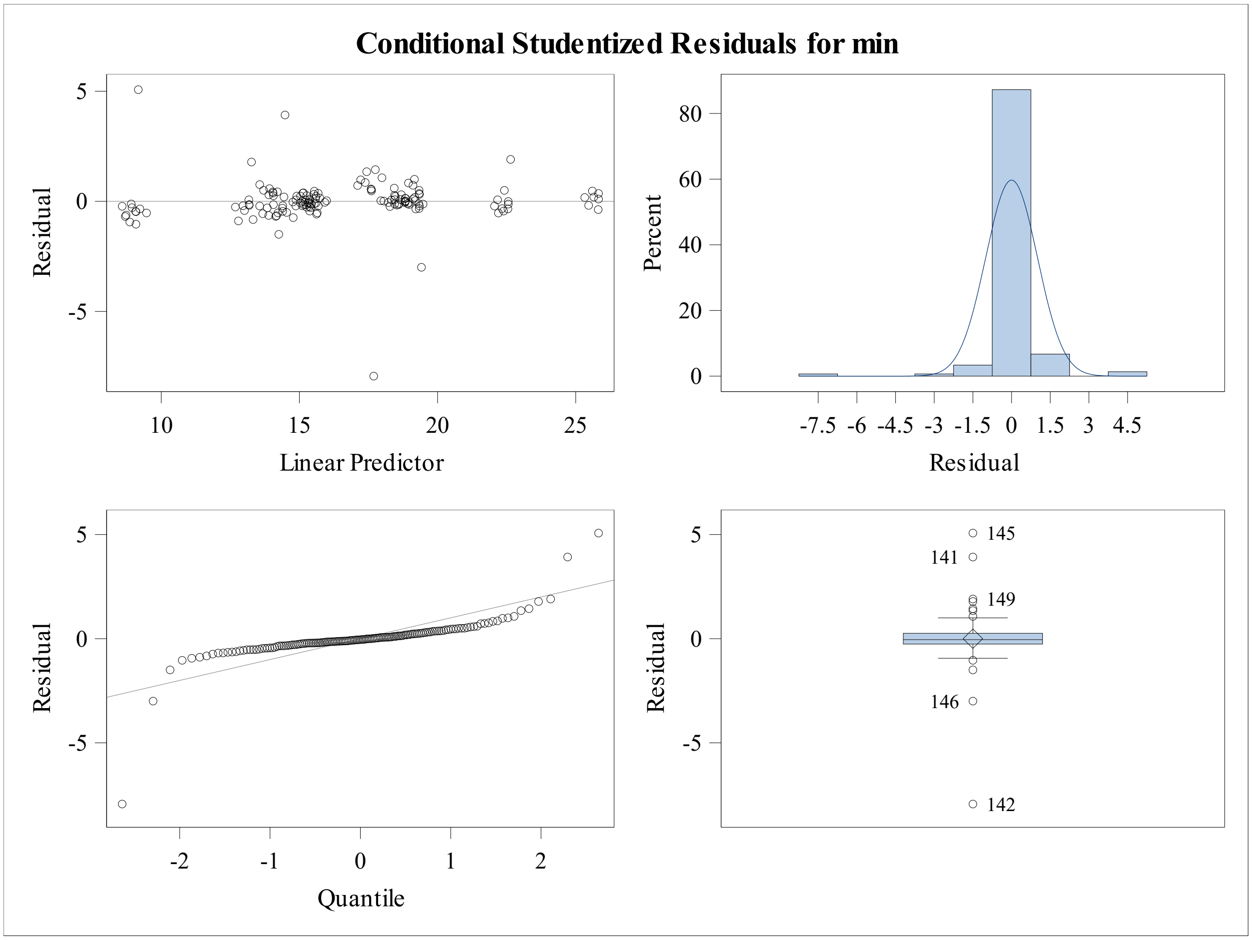

max: Overall Summary Statistics

asphalt_vs_footing	Condition1	SampleSize	Means	Medians	SD	SEM	Minimum	Maximur
asphalt	walk glue	15	19.1840	18.800	4.03494	1.04182	11.0100	28.24
asphalt	walk barefoot	15	19.4907	19.290	4.19232	1.08245	11.6400	29.30
asphalt	walk aluminum	15	18.7560	17.950	4.18989	1.08182	10.9900	28.22

asphalt_vs_footing	Condition1	SampleSize	Means	Medians	SD	SEM	Minimum	Maximur
asphalt	**trot glue**	15	19.5207	19.180	3.99469	1.03142	11.0500	28.23
asphalt	**trot barefoot**	15	20.0287	19.500	4.31917	1.11521	10.9400	29.72
asphalt	**trot aluminum**	15	19.0873	18.320	4.33783	1.12002	9.9300	28.15
footing	**walk glue**	11	17.7307	17.910	3.57738	1.07862	9.5344	22.92
footing	**walk barefoot**	8	20.0971	19.545	5.88754	2.08156	10.9900	28.99
footing	**walk aluminum**	11	19.0000	18.580	3.86159	1.16431	11.7800	25.81
footing	**trot glue**	10	17.3938	18.541	3.01471	0.95333	11.7746	20.49
footing	**trot barefoot**	7	19.6629	19.930	5.42703	2.05122	9.4800	25.13
footing	**trot aluminum**	12	18.8242	18.365	4.46092	1.28776	9.4500	28.35

asphalt_vs_footing	Condition1	FirstQuartile	ThirdQuartile	IQR
asphalt	**walk glue**	16.9200	21.2700	4.35000
asphalt	**walk barefoot**	16.8300	21.3400	4.51000
asphalt	**walk aluminum**	15.7800	20.9100	5.13000
asphalt	**trot glue**	16.8500	21.4300	4.58000
asphalt	**trot barefoot**	17.0800	22.1300	5.05000
asphalt	**trot aluminum**	16.0300	21.7500	5.72000
footing	**walk glue**	16.7800	19.4935	2.71350

asphalt_vs_footing	Condition1	FirstQuartile	ThirdQuartile	IQR
footing	walk barefoot	16.2485	24.6050	8.35655
footing	walk aluminum	16.2800	21.1500	4.87000
footing	trot glue	14.7520	19.8890	5.13700
footing	trot barefoot	16.6600	23.9900	7.33000
footing	trot aluminum	17.0150	20.7100	3.69500

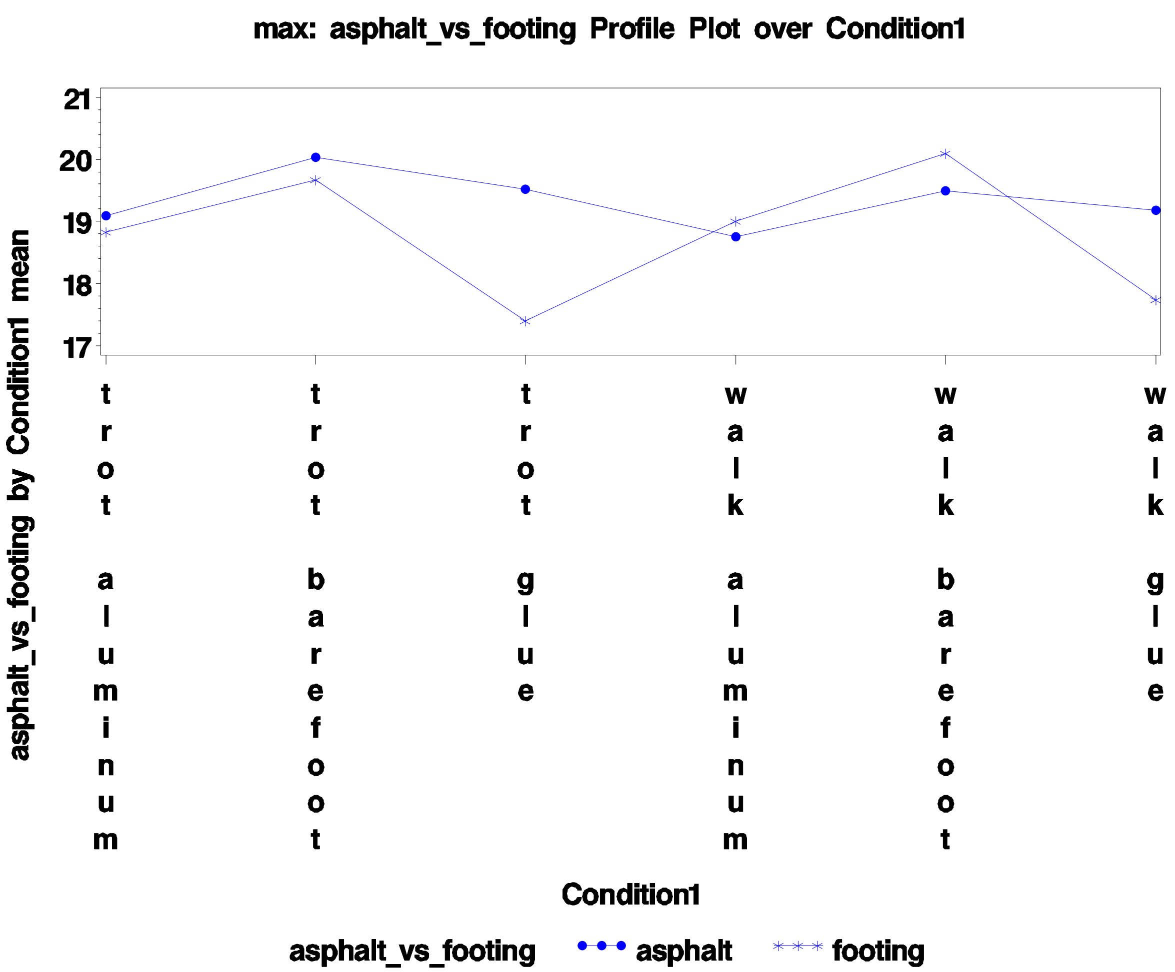

max: Mixed Model Anova to assess the effects of asphalt_vs_footing and Condition1

The GLIMMIX Procedure

Model Information	
Data Set	WORK.SDATA3
Response Variable	max
Response Distribution	Gaussian
Link Function	Identity
Variance Function	Default
Variance Matrix	Not blocked
Estimation Technique	Restricted Maximum Likelihood
Degrees of Freedom Method	Kenward-Roger
Fixed Effects SE Adjustment	Kenward-Roger

Class Level Information		
Class	**Levels**	**Values**
HorseNo	15	Subject #1 Subject #10 Subject #11 Subject #12 Subject #13 Subject #14 Subject #15 Subject #2 Subject #3 Subject #4 Subject #5 Subject #6 Subject #7 Subject #8 Subject #9
Condition1	6	trot aluminum trot barefoot trot glue walk aluminum walk barefoot walk glue
asphalt_vs_footing	2	asphalt footing

Covariance Parameter Estimates		
Cov Parm	**Estimate**	**Standard Error**
HorseNo	16.7302	6.4183
Residual	2.1904	0.2793

Type III Tests of Fixed Effects				
Effect	Num DF	Den DF	F Value	Pr > F
asphalt_vs_footing	1	123.4	1.40	0.2395
Condition1	5	123	1.70	0.1398
Condition*asphalt_vs	5	123	0.52	0.7603

max: Mixed Model Anova to assess the effects of asphalt_vs_footing and Condition1

The GLIMMIX Procedure
Condition*asphalt_vs
Least Squares Means

Condition1	asphalt_vs_footing	Estimate	Standard Error	DF	t Value	Pr > |t|
trot aluminum	asphalt	19.0873	1.1231	17.36	17.00	<.0001
trot aluminum	footing	19.6423	1.1417	18.51	17.20	<.0001
trot barefoot	asphalt	20.0287	1.1231	17.36	17.83	<.0001
trot barefoot	footing	20.5935	1.2029	22.66	17.12	<.0001
trot glue	asphalt	19.5207	1.1231	17.36	17.38	<.0001
trot glue	footing	19.1856	1.1592	19.64	16.55	<.0001
walk aluminum	asphalt	18.7560	1.1231	17.36	16.70	<.0001
walk aluminum	footing	19.5922	1.1497	19.02	17.04	<.0001
walk barefoot	asphalt	19.4907	1.1231	17.36	17.35	<.0001

walk barefoot	footing	19.7718	1.1849	21.38	16.69	<.0001
walk glue	asphalt	19.1840	1.1231	17.36	17.08	<.0001
walk glue	footing	19.1385	1.1497	19.02	16.65	<.0001

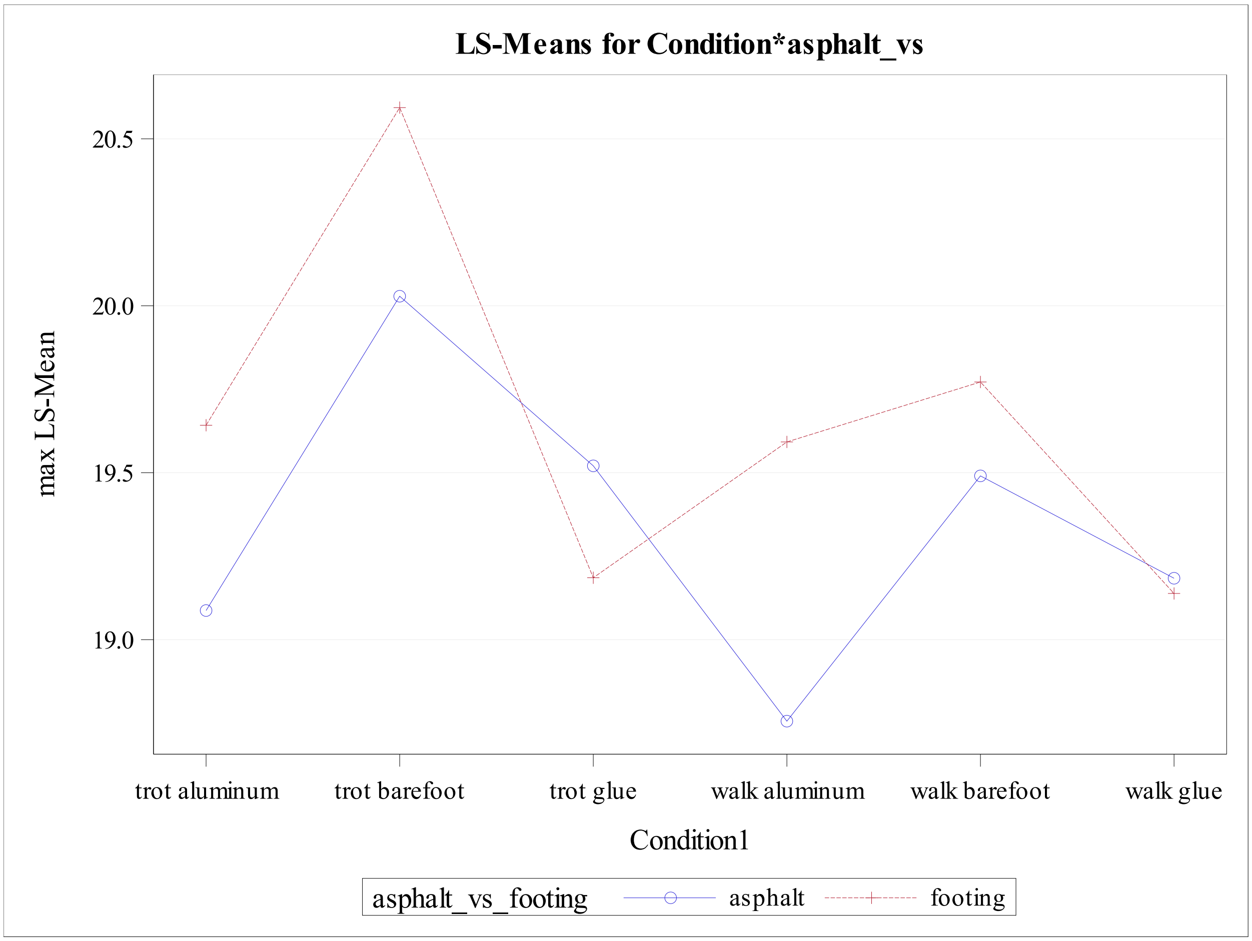

max: Mixed Model Anova to assess the effects of asphalt_vs_footing and Condition1

The GLIMMIX Procedure

Tests of Effect Slices for Condition*asphalt_vs Sliced By asphalt_vs_footing				
asphalt_vs_footing	**Num DF**	**Den DF**	**F Value**	**Pr > F**
asphalt	5	123	1.31	0.2628
footing	5	123.1	0.97	0.4385

Tests of Effect Slices for Condition*asphalt_vs Sliced By Condition1				
Condition1	**Num DF**	**Den DF**	**F Value**	**Pr > F**
trot aluminum	1	123.1	0.92	0.3390
trot barefoot	1	123.1	0.67	0.4153
trot glue	1	123.1	0.30	0.5849
walk aluminum	1	123.1	1.98	0.1614
walk barefoot	1	123.1	0.18	0.6705
walk glue	1	123.1	0.01	0.9390

Condition*asphalt_vs Least Squares Means									
Condition1	asphalt_vs_footing	Estimate	Standard Error	DF	t Value	Pr > |t|	Alpha	Lower	Upper
trot aluminum	asphalt	19.0873	1.1231	17.36	17.00	<.0001	0.05	16.7215	21.4532
trot aluminum	footing	19.6423	1.1417	18.51	17.20	<.0001	0.05	17.2483	22.0363
trot barefoot	asphalt	20.0287	1.1231	17.36	17.83	<.0001	0.05	17.6628	22.3945
trot barefoot	footing	20.5935	1.2029	22.66	17.12	<.0001	0.05	18.1031	23.0840
trot glue	asphalt	19.5207	1.1231	17.36	17.38	<.0001	0.05	17.1548	21.8865
trot glue	footing	19.1856	1.1592	19.64	16.55	<.0001	0.05	16.7647	21.6064
walk aluminum	asphalt	18.7560	1.1231	17.36	16.70	<.0001	0.05	16.3901	21.1219
walk aluminum	footing	19.5922	1.1497	19.02	17.04	<.0001	0.05	17.1861	21.9984
walk barefoot	asphalt	19.4907	1.1231	17.36	17.35	<.0001	0.05	17.1248	21.8565
walk barefoot	footing	19.7718	1.1849	21.38	16.69	<.0001	0.05	17.3104	22.2333
walk glue	asphalt	19.1840	1.1231	17.36	17.08	<.0001	0.05	16.8181	21.5499
walk glue	footing	19.1385	1.1497	19.02	16.65	<.0001	0.05	16.7323	21.5447

max: Mixed Model Anova to assess the effects of asphalt_vs_footing and Condition1

The GLIMMIX Procedure

Simple Effect Comparisons of Condition*asphalt_vs Least Squares Means By asphalt_vs_footing Adjustment for Multiple Comparisons: Tukey-Kramer									
Simple Effect Level	**Condition1**	**_Condition1**	**Estimate**	**Standard Error**	**DF**	**t Value**	**Pr > |t|**	**Adj P**	**Alpha**
asphalt_vs_footing asphalt	trot aluminum	trot barefoot	-0.9413	0.5404	123	-1.74	0.0840	0.5071	0.05
asphalt_vs_footing asphalt	trot aluminum	trot glue	-0.4333	0.5404	123	-0.80	0.4242	0.9667	0.05
asphalt_vs_footing asphalt	trot aluminum	walk aluminum	0.3313	0.5404	123	0.61	0.5409	0.9899	0.05
asphalt_vs_footing asphalt	trot aluminum	walk barefoot	-0.4033	0.5404	123	-0.75	0.4569	0.9756	0.05
asphalt_vs_footing asphalt	trot aluminum	walk glue	-0.09667	0.5404	123	-0.18	0.8583	1.0000	0.05
asphalt_vs_footing asphalt	trot barefoot	trot glue	0.5080	0.5404	123	0.94	0.3491	0.9353	0.05
asphalt_vs_footing asphalt	trot barefoot	walk aluminum	1.2727	0.5404	123	2.35	0.0201	0.1806	0.05
asphalt_vs_footing asphalt	trot barefoot	walk barefoot	0.5380	0.5404	123	1.00	0.3214	0.9186	0.05
asphalt_vs_footing asphalt	trot barefoot	walk glue	0.8447	0.5404	123	1.56	0.1206	0.6243	0.05
asphalt_vs_footing asphalt	trot glue	walk aluminum	0.7647	0.5404	123	1.41	0.1596	0.7179	0.05
asphalt_vs_footing asphalt	trot glue	walk barefoot	0.03000	0.5404	123	0.06	0.9558	1.0000	0.05
asphalt_vs_footing asphalt	trot glue	walk glue	0.3367	0.5404	123	0.62	0.5345	0.9891	0.05
asphalt_vs_footing asphalt	walk aluminum	walk barefoot	-0.7347	0.5404	123	-1.36	0.1765	0.7510	0.05
asphalt_vs_footing asphalt	walk aluminum	walk glue	-0.4280	0.5404	123	-0.79	0.4299	0.9684	0.05
asphalt_vs_footing asphalt	walk barefoot	walk glue	0.3067	0.5404	123	0.57	0.5714	0.9929	0.05
asphalt_vs_footing footing	trot aluminum	trot barefoot	-0.9512	0.7132	123.1	-1.33	0.1848	0.7658	0.05
asphalt_vs_footing footing	trot aluminum	trot glue	0.4567	0.6365	123	0.72	0.4744	0.9795	0.05
asphalt_vs_footing footing	trot aluminum	walk aluminum	0.05004	0.6190	123	0.08	0.9357	1.0000	0.05

Simple Effect Comparisons of Condition*asphalt_vs Least Squares Means By asphalt_vs_footing Adjustment for Multiple Comparisons: Tukey-Kramer									
Simple Effect Level	**Condition1**	**_Condition1**	**Estimate**	**Standard Error**	**DF**	**t Value**	**Pr > |t|**	**Adj P**	**Alpha**
asphalt_vs_footing footing	trot aluminum	walk barefoot	-0.1296	0.6871	123.1	-0.19	0.8507	1.0000	0.05
asphalt_vs_footing footing	trot aluminum	walk glue	0.5038	0.6191	123	0.81	0.4174	0.9645	0.05
asphalt_vs_footing footing	trot barefoot	trot glue	1.4079	0.7447	123.1	1.89	0.0610	0.4129	0.05
asphalt_vs_footing footing	trot barefoot	walk aluminum	1.0013	0.7275	123.1	1.38	0.1712	0.7411	0.05
asphalt_vs_footing footing	trot barefoot	walk barefoot	0.8217	0.7695	123	1.07	0.2877	0.8932	0.05
asphalt_vs_footing footing	trot barefoot	walk glue	1.4550	0.7279	123.1	2.00	0.0478	0.3489	0.05
asphalt_vs_footing footing	trot glue	walk aluminum	-0.4067	0.6510	123	-0.62	0.5334	0.9890	0.05
asphalt_vs_footing footing	trot glue	walk barefoot	-0.5863	0.7193	123.2	-0.82	0.4166	0.9643	0.05
asphalt_vs_footing footing	trot glue	walk glue	0.04709	0.6481	123	0.07	0.9422	1.0000	0.05
asphalt_vs_footing footing	walk aluminum	walk barefoot	-0.1796	0.7018	123.1	-0.26	0.7984	0.9998	0.05
asphalt_vs_footing footing	walk aluminum	walk glue	0.4538	0.6338	123	0.72	0.4754	0.9797	0.05
asphalt_vs_footing footing	walk barefoot	walk glue	0.6334	0.7021	123.1	0.90	0.3688	0.9453	0.05

max: Mixed Model Anova to assess the effects of asphalt_vs_footing and Condition1

The GLIMMIX Procedure

Simple Effect Comparisons of Condition*asphalt_vs Least Squares Means By asphalt_vs_footing Adjustment for Multiple Comparisons: Tukey-Kramer						
Simple Effect Level	**Condition1**	**_Condition1**	**Lower**	**Upper**	**Adj Lower**	**Adj Upper**
asphalt_vs_footing asphalt	trot aluminum	trot barefoot	-2.0111	0.1284	-2.5059	0.6233
asphalt_vs_footing asphalt	trot aluminum	trot glue	-1.5031	0.6364	-1.9979	1.1313
asphalt_vs_footing asphalt	trot aluminum	walk aluminum	-0.7384	1.4011	-1.2333	1.8959
asphalt_vs_footing asphalt	trot aluminum	walk barefoot	-1.4731	0.6664	-1.9679	1.1613
asphalt_vs_footing asphalt	trot aluminum	walk glue	-1.1664	0.9731	-1.6613	1.4679
asphalt_vs_footing asphalt	trot barefoot	trot glue	-0.5617	1.5777	-1.0566	2.0726
asphalt_vs_footing asphalt	trot barefoot	walk aluminum	0.2029	2.3424	-0.2919	2.8373
asphalt_vs_footing asphalt	trot barefoot	walk barefoot	-0.5317	1.6077	-1.0266	2.1026
asphalt_vs_footing asphalt	trot barefoot	walk glue	-0.2251	1.9144	-0.7199	2.4093
asphalt_vs_footing asphalt	trot glue	walk aluminum	-0.3051	1.8344	-0.7999	2.3293
asphalt_vs_footing asphalt	trot glue	walk barefoot	-1.0397	1.0997	-1.5346	1.5946
asphalt_vs_footing asphalt	trot glue	walk glue	-0.7331	1.4064	-1.2279	1.9013
asphalt_vs_footing asphalt	walk aluminum	walk barefoot	-1.8044	0.3351	-2.2993	0.8299
asphalt_vs_footing asphalt	walk aluminum	walk glue	-1.4977	0.6417	-1.9926	1.1366
asphalt_vs_footing asphalt	walk barefoot	walk glue	-0.7631	1.3764	-1.2579	1.8713

Simple Effect Comparisons of Condition*asphalt_vs Least Squares Means By asphalt_vs_footing Adjustment for Multiple Comparisons: Tukey-Kramer						
Simple Effect Level	**Condition1**	**_Condition1**	**Lower**	**Upper**	**Adj Lower**	**Adj Upper**
asphalt_vs_footing footing	trot aluminum	trot barefoot	-2.3630	0.4606	-3.0162	1.1137
asphalt_vs_footing footing	trot aluminum	trot glue	-0.8032	1.7166	-1.3861	2.2995
asphalt_vs_footing footing	trot aluminum	walk aluminum	-1.1753	1.2754	-1.7421	1.8422
asphalt_vs_footing footing	trot aluminum	walk barefoot	-1.4897	1.2306	-2.1189	1.8598
asphalt_vs_footing footing	trot aluminum	walk glue	-0.7218	1.7293	-1.2887	2.2963
asphalt_vs_footing footing	trot barefoot	trot glue	-0.06619	2.8821	-0.7482	3.5640
asphalt_vs_footing footing	trot barefoot	walk aluminum	-0.4388	2.4414	-1.1051	3.1076
asphalt_vs_footing footing	trot barefoot	walk barefoot	-0.7015	2.3449	-1.4062	3.0495
asphalt_vs_footing footing	trot barefoot	walk glue	0.01429	2.8958	-0.6522	3.5623
asphalt_vs_footing footing	trot glue	walk aluminum	-1.6953	0.8820	-2.2915	1.4782
asphalt_vs_footing footing	trot glue	walk barefoot	-2.0101	0.8376	-2.6688	1.4963
asphalt_vs_footing footing	trot glue	walk glue	-1.2357	1.3299	-1.8292	1.9234
asphalt_vs_footing footing	walk aluminum	walk barefoot	-1.5687	1.2095	-2.2113	1.8521
asphalt_vs_footing footing	walk aluminum	walk glue	-0.8009	1.7084	-1.3813	2.2888
asphalt_vs_footing footing	walk barefoot	walk glue	-0.7563	2.0231	-1.3993	2.6660

max: Mixed Model Anova to assess the effects of asphalt_vs_footing and Condition1

The GLIMMIX Procedure

Simple Effect Comparisons of Condition*asphalt_vs Least Squares Means By Condition1 Adjustment for Multiple Comparisons: Tukey-Kramer									
Simple Effect Level	**asphalt_vs_footing**	**_asphalt_vs_footing**	**Estimate**	**Standard Error**	**DF**	**t Value**	**Pr > |t|**	**Adj P**	**Alpha**
Condition1 trot aluminum	asphalt	footing	-0.5549	0.5781	123.1	-0.96	0.3390	0.3390	0.05
Condition1 trot barefoot	asphalt	footing	-0.5648	0.6911	123.1	-0.82	0.4153	0.4153	0.05
Condition1 trot glue	asphalt	footing	0.3351	0.6119	123.1	0.55	0.5849	0.5849	0.05
Condition1 walk aluminum	asphalt	footing	-0.8362	0.5936	123.1	-1.41	0.1614	0.1614	0.05
Condition1 walk barefoot	asphalt	footing	-0.2812	0.6592	123.1	-0.43	0.6705	0.6705	0.05
Condition1 walk glue	asphalt	footing	0.04551	0.5938	123.1	0.08	0.9390	0.9390	0.05

Simple Effect Comparisons of Condition*asphalt_vs Least Squares Means By Condition1 Adjustment for Multiple Comparisons: Tukey-Kramer						
Simple Effect Level	**asphalt_vs_footing**	**_asphalt_vs_footing**	**Lower**	**Upper**	**Adj Lower**	**Adj Upper**
Condition1 trot aluminum	asphalt	footing	-1.6993	0.5895	-1.6993	0.5895
Condition1 trot barefoot	asphalt	footing	-1.9328	0.8031	-1.9328	0.8031
Condition1 trot glue	asphalt	footing	-0.8760	1.5462	-0.8760	1.5462
Condition1 walk aluminum	asphalt	footing	-2.0113	0.3388	-2.0113	0.3388

Simple Effect Comparisons of Condition*asphalt_vs Least Squares Means By Condition1 Adjustment for Multiple Comparisons: Tukey-Kramer						
Simple Effect Level	asphalt_vs_footing	_asphalt_vs_footing	Lower	Upper	Adj Lower	Adj Upper
Condition1 walk barefoot	asphalt	footing	-1.5861	1.0237	-1.5861	1.0238
Condition1 walk glue	asphalt	footing	-1.1298	1.2208	-1.1298	1.2208

max: Mixed Model Anova to assess the effects of asphalt_vs_footing and Condition1

The GLIMMIX Procedure